Development of Non-Proprietary Ultra-High Performance Concrete (UHPC) for Iowa Bridges

Final Report
September 2021

BRIDGE ENGINEERING C E N T E R

IOWA STATE UNIVERSITY
Institute for Transportation

About the Bridge Engineering Center

The mission of the Bridge Engineering Center (BEC) is to conduct research on bridge technologies to help bridge designers/owners design, build, and maintain long-lasting bridges.

About the Institute for Transportation

The mission of the Institute for Transportation (InTrans) at Iowa State University is to save lives and improve economic vitality through discovery, research innovation, outreach, and the implementation of bold ideas.

Iowa State University Nondiscrimination Statement

Iowa State University does not discriminate on the basis of race, color, age, ethnicity, religion, national origin, pregnancy, sexual orientation, gender identity, genetic information, sex, marital status, disability, or status as a US veteran. Inquiries regarding nondiscrimination policies may be directed to the Office of Equal Opportunity, 3410 Beardshear Hall, 515 Morrill Road, Ames, Iowa 50011, telephone: 515-294-7612, hotline: 515-294-1222, email: eooffice@iastate.edu.

Disclaimer Notice

The contents of this report reflect the views of the authors, who are responsible for the facts and the accuracy of the information presented herein. The opinions, findings and conclusions expressed in this publication are those of the authors and not necessarily those of the sponsors.

The sponsors assume no liability for the contents or use of the information contained in this document. This report does not constitute a standard, specification, or regulation.

The sponsors do not endorse products or manufacturers. Trademarks or manufacturers' names appear in this report only because they are considered essential to the objective of the document.

Iowa DOT Statements

Federal and state laws prohibit employment and/or public accommodation discrimination on the basis of age, color, creed, disability, gender identity, national origin, pregnancy, race, religion, sex, sexual orientation or veteran's status. If you believe you have been discriminated against, please contact the Iowa Civil Rights Commission at 800-457-4416 or Iowa Department of Transportation's affirmative action officer. If you need accommodations because of a disability to access the Iowa Department of Transportation's services, contact the agency's affirmative action officer at 800-262-0003.

The preparation of this report was financed in part through funds provided by the Iowa Department of Transportation through its "Second Revised Agreement for the Management of Research Conducted by Iowa State University for the Iowa Department of Transportation" and its amendments.

The opinions, findings, and conclusions expressed in this publication are those of the authors and not necessarily those of the Iowa Department of Transportation.

Technical Report Documentation Page

1. Report No. IHRB Project TR-773	2. Government Accession No.	3. Recipient's Catalog No.	
4. Title and Subtitle Development of Non-Proprietary Ultra-High Performance Concrete (UHPC) for Iowa Bridges		**5. Report Date** September 2021	
		6. Performing Organization Code	
7. Author(s) Behrouz Shafei (orcid.org/0000-0001-5677-6324) and Rizwan Karim (orcid.org/0000-0003-4130-568X)		**8. Performing Organization Report No.** InTrans Project 19-693	
9. Performing Organization Name and Address Bridge Engineering Center Iowa State University 2711 South Loop Drive, Suite 4700 Ames, IA 50010-8664		**10. Work Unit No. (TRAIS)**	
		11. Contract or Grant No.	
12. Sponsoring Organization Name and Address Iowa Highway Research Board Iowa Department of Transportation 800 Lincoln Way Ames, IA 50010	Accelerated Bridge Construction University Transportation Center Florida International University 10555 W. Flagler Street Miami, FL 33174	**13. Type of Report and Period Covered** Final Report	
		14. Sponsoring Agency Code IHRB Project TR-773	

15. Supplementary Notes
Visit https://bec.iastate.edu for color pdfs of this and other research reports.

16. Abstract

Ultra-high performance concrete (UHPC) provides superior properties in strength and durability for the long-term performance of bridges. Despite these desirable properties and the potential to be applicable in the majority of projects, UHPC is still not widely used, mainly because of the cost associated with it.

This report details a study performed on the design of non-proprietary UHPC mixes that provide comparable strength properties to that of commercially available mixtures. A set of base mixtures were explored by varying the ratios for various constituents and investigating their durability, strength, and transport properties, including volume stability and freeze-thaw resistance.

In the later stage of the project, the selected non-proprietary mixes were evaluated for their flexural strength. The flexural strength in UHPC comes mainly from the fibers used in the mix. Bearing in mind the role of fibers, the effects of various types of steel fibers (i.e., variation in shape, size, and dosage) were evaluated. The role of fibers on strength and post-cracking behavior was carefully examined using laboratory testing and image analysis utilizing digital image correlation techniques. The efforts found that an optimal combination of micro- and macrofibers can enhance the flexural strength of UHPC mixtures.

Steel fibers contribute to more than a third of the cost of UHPC mixtures, so the possibility of utilizing less expensive and more environmentally friendly synthetic fibers—polypropylene, polyvinyl alcohol, nylon, alkali resistant glass, or carbon—to partially replace the steel fibers could reduce the cost of UHPC. The steel fibers were partially replaced by the different synthetic fibers to see their effect on the UHPC's fresh properties and flexural strength. Utilizing digital image correlation, the synthetic fiber contribution to post-cracking behavior was evaluated, especially from the crack width control and crack propagation aspects. The replacement of steel fibers with synthetic fibers showed promise for flexural strength and post-cracking behavior.

This report provides recommendations for the preparation of cost-effective, non-proprietary UHPC mixtures that could be used for various transportation infrastructure applications. Further recommendations are also made for the optimal combination of different types of steel micro- and macrofibers to get the best flexural response. Recommendations are then extended for the use of different types of synthetic fibers and the optimum percentage of dosage replacement for steel fibers.

17. Key Words digital image correlation—freeze-thaw cycles—macrofibers—microfibers—strength—transport properties—ultra-high performance concrete—workability		**18. Distribution Statement** No restrictions.	
19. Security Classification (of this report) Unclassified.	**20. Security Classification (of this page)** Unclassified.	**21. No. of Pages** 94	**22. Price** NA

Form DOT F 1700.7 (8-72)　　　　　　　　　　　　　　**Reproduction of completed page authorized**

DEVELOPMENT OF NON-PROPRIETARY ULTRA-HIGH PERFORMANCE CONCRETE (UHPC) FOR IOWA BRIDGES

Final Report
September 2021

Principal Investigator
Behrouz Shafei, Associate Professor
Bridge Engineering Center, Iowa State University

Co-Principal Investigators
Brent Phares, Research Structural Engineer
Bridge Engineering Center, Iowa State University

Peter Taylor, Director
National Concrete Pavement Technology Center, Iowa State University

Research Assistant
Rizwan Karim

Authors
Behrouz Shafei and Rizwan Karim

A report from
Bridge Engineering Center
Iowa State University
2711 South Loop Drive, Suite 4700
Ames, IA 50010-8664
Phone: 515-294-8103 / Fax: 515-294-0467
https://bec.iastate.edu

TABLE OF CONTENTS

LIST OF FIGURES

LIST OF TABLES

ACKNOWLEDGMENTS

EXECUTIVE SUMMARY

This report details the holistic study performed for designing non-proprietary ultra-high performance concrete (UHPC) mixes. The initial part of the report details the investigations performed on the development of non-proprietary UHPC by other researchers around the world.

A set of base mixes were decided based on the available literature review and the existing theoretical particle packing models. The UHPC base mixtures were explored further by varying the ratios of various constituents of the UHPC mixes. A set of mixtures were identified to provide comparable strength properties for commercially available UHPC mixtures. These base mixtures were further investigated for their strength and transport properties.

A set of cost-effective base mixes were prepared based on these investigations. A more detailed set of experiments were performed on selected mixes to evaluate their transport properties, volume stability, and freeze-thaw resistance. The mixtures' properties were compared to two commercially available UHPC mixes. The test results showed that the developed non-proprietary mixes had comparable properties to those of the proprietary mixes.

In the later stage of the project, the selected non-proprietary mixes were evaluated for their flexural strength. The flexural strength in UHPC comes mainly from the fibers used in the mix. Bearing in mind the role of fibers, the effect of various types of steel fibers (i.e., variation in shape, size, and dosage) were evaluated on the flexural strength of the UHPC. The role of fibers on strength and post-cracking behavior was carefully examined using laboratory testing and image analysis utilizing digital image correlation techniques. The efforts found that an optimal combination of micro- and macrofibers can enhance the flexural strength of UHPC mixtures.

The steel fibers contribute to more than a third of the cost of UHPC mixtures. The possibility of utilizing less expensive and more environmentally friendly synthetic fibers to partially replace the steel fibers could reduce the cost of UHPC. The steel fibers were partially replaced by different types of synthetic fibers to understand their effect on the UHPC's fresh properties and flexural strength. Five types of synthetic fibers—polypropylene, polyvinyl alcohol, nylon, alkali resistant glass, and carbon—were selected. The effect of these fibers on flexural strength and the post-cracking behavior was carefully analyzed utilizing digital image correlation. The synthetic fiber contribution to post-cracking behavior resulted in detailed observations from the crack width control and crack propagation aspects.

This report provides a set of cost-effective, non-proprietary UHPC mixtures that could be prepared with straight steel fibers. Further recommendations are also made for the optimal combination of different types of steel micro- and macrofibers to get the best flexural response. The replacement of steel fibers with synthetic fibers showed promise for flexural strength and post-cracking behavior. Recommendations are made for the use of different types of synthetic fibers and the optimum percentage dosage replacement for steel fibers.

This report provides a comprehensive understanding of how non-proprietary UHPC mixes can be designed, along with their properties and the results obtained from the non-proprietary UHPC mixes that were developed. The report provides recommendations for the preparation of cost-effective, non-proprietary UHPC mixtures that could be used effectively for various transportation infrastructure applications.

1. DEVELOPMENT OF COST-EFFECTIVE, NON-PROPRIETARY UHPC BASE MIX

1.1. Introduction

Disruption in the functionality of highway transportation infrastructure as a result of deterioration of concrete structures has been a growing concern for various transportation agencies. This has required the identification of strategies to enhance the performance of concrete under the penetration of destructive agents to reduce the deterioration of concrete structures and increase their service lives.

The initial attempts in this regard came in the form of reactive powder concrete and research on the strength of cementitious material pastes, which resulted in the development of pastes with compressive strengths as high as 22 ksi (150 MPa). De Larrard and Sedran (1994) used Mooney's suspension models to predict the particle packing of materials.

With the use of superplasticizer, silica fume, and a very low water-to-cement (w/c) ratio of 0.14, De Larrard and Sedran developed a special type of concrete, called ultra-high performance concrete (UHPC), with a compressive strength of 22 ksi (150 MPa). Later on, UHPC was modified as a fiber-reinforced, portland cement based product with advantageous fresh and hardened properties.

UHPC commonly provides a compressive strength greater than 20 ksi (138 MPa), a post-cracking tensile strength of at least 0.72 ksi (5 MPa), and high durability because of the discontinuous pore structure and, thus, reduced permeability. UHPC is now considered the material of choice for many bridge components, (e.g., connections, overlays, and bridge girders and piers) especially when superior strength and durability characteristics are critical (Chen et al. 2018, Zou and Wang 2018, Dong 2018, Yoo and Yoon 2015, Graybeal 2014, and Gu et al. 2015).

The exceptional properties of UHPC are achieved through the following: (1) low w/c ratio, (2) aggregate gradations optimized for high particle packing density, (3) high quality aggregates and cements, (4) excessive amount of cement and supplementary cementitious materials (SCMs), (5) high particle dispersion during mixing, and (6) incorporation of fibers. The aggregates used for UHPC are considerably finer than the aggregates used for conventional concrete.

Due to cost considerations, use of proprietary UHPC in conventional projects has been limited. Therefore, recent studies have focused on making UHPC cost effective by optimizing cement content, replacing a portion of cement with other less expensive cementitious materials, and using less expensive granular materials. El-Tawil et al. (2016) attempted to replace cement with silica powder, Ghafari et al. (2015) developed a statistical model for optimizing cement content, Yu et al. (2014) studied the effect of replacing cement with filler materials like limestone and quartz powder, Shi et al. (2015) suggested replacing cement with fly ash or slag, Soliman and Tagnit-Hamou (2017a, 2017b) worked on replacing quartz sand with glass powder and silica fume with fine glass powder, and Wille and Boisvert-Cotulio (2015) used a range of readily

available materials to find the least expensive combination for UHPC preparation. The most recent study on the development of non-proprietary UHPC was completed by Berry et al. (2017), in which the use of masonry sand was optimized based on the Andreasen-Andersen model.

This project report details the effort to develop and characterize economic, non-proprietary UHPC mixtures made with the readily available materials in Iowa. For this purpose, non-proprietary UHPC mixtures were developed by using ordinary portland cement, regular sand, widely available masonry sand, silica fume, and steel fibers.

The non-proprietary UHPC mixtures that were developed were tested for transport properties, since they can be considered an accelerated tool for evaluating the concrete durability, and, as a result, service life of concrete structures. The base mixtures were then evaluated for the effect of individual constituents on the properties of the UHPC.

1.2. Mixture Design of UHPC

Among the factors that influence the properties of UHPC, particle packing is known to play an important role to obtain a densely-packed mixture with proper workability (Chen et al. 2018). Different packing models can be employed for the particle packing of UHPC. Initially, the linear particle density model was introduced in the literature to predict the optimal ratio between cement and mortar. This was based on the concept of virtual density, which was defined as the maximum density that can be achieved if the particles are placed by hand one by one. Due to the limitations of this model, the compaction density model was later introduced. This model took into consideration the difference between the virtual and actual particle packing densities through a compaction index.

With further advances, the most recent particle packing model, which was used in this study, employs the concept of continuous gradation. This model is based on Fuller and Thompson (1907), which indicated that the packing of aggregates can affect the overall properties of concrete mixtures. This concept formed the foundation of the particle packing model proposed by Andreasen and Andersen (1930). The latest model highlights that an optimal particle size density can result in minimum porosity, and, thus, maximum strength. The percentage of particles smaller than size D, i.e., $P(D)$, for a particle-packed concrete mixture can be calculated as follows:

$$P(D) = \left(\frac{D}{D_{max}}\right)^q \tag{1}$$

where D_{max} is the maximum particle size, and q is the distribution modulus, which determines the proportion of fine and coarse particles in the mixture. As the original model was unable to consider the effect of the smallest particles, it was further modified by Funk and Dinger (1994).

The modified Andreasen and Andersen particle packing model is based on the following equation, as reported by Yu et al. 2014:

$$P(D) = \frac{D^q - D_{min}^q}{D^q - D_{max}^q} \qquad (2)$$

where D_{min} and D_{max} represent the smallest and largest particle size, respectively. The distribution modulus, q, varies based on the type of concrete. A q value greater than 0.50 results in a coarse mixture, while a q value less than 0.25 provides a mixture of fine content. According to Brouwers (2005) and Brouwers and Radix (2006), a q value under 0.28 results in an optimal packing density.

For self-compacting concrete, Hunger (2010) suggested a q value in the range of 0.22 to 0.25. Borges et al. (2014) suggested that a q value of 0.37 provides high particle density for self-compacting concrete. This was confirmed by El-Tawil et al. (2016) for UHPC mixtures.

The preliminary results on different q values of 0.23, 0.30, and 0.37 supported the use of 0.37, which produced the highest packing density and strength. Therefore, for this study, the modified Andreasen and Andersen packing model with a q value of 0.37 was used as the target curve, and the proportions of individual concrete ingredients were selected such that the obtained curve closely fits the target curve. A curve fit was considered an optimum fit when the sum of squares of residuals (RSS) was minimized. The RSS was calculated by the least squares method, as follows:

$$RSS = \sum_{i=1}^{n}(P_{mix}(D_i) - P_{tar}(D_i))^2 \qquad (3)$$

where $P_{tar}(D_i)$ is the target passing percentage at particle size D_i, and $P_{mix}(D_i)$ is the passing percentage of the combined solid materials for particle size D_i in the designed mixture.

1.3. Details of Material

The materials used for the production of the non-proprietary UHPC included cement, silica fume, regular sand, masonry sand, steel fiber, high-range water reducer (HRWR), and water. ASTM Type I cement was used in this study. The specific density of cement was 3.10. The list of this cement's chemical oxides is shown in Table 1.

Table 1. Chemical oxides of cement and silica fume

Type of Binder	CaO	SiO$_2$	SO$_3$	Fe$_2$O$_3$	Al$_2$O$_3$	MgO	K$_2$O	Na$_2$O	TiO$_2$
Portland cement	62.94	20.10	3.18	3.09	4.44	2.88	0.61	0.10	0.24
Silica fume	0.3	94.3	-	0.1	0.09	0.43	0.83	0.27	–

The regular laboratory fine aggregate (≤ 4.75 mm (0.1850 in.)) was used. This was modified in such a way that the maximum size remaining is 2.38 mm (0.0937 in). The specific density of fine aggregate was 2.72. The masonry sand used was 15% of the total sand to obtain the maximum particle packing in accordance with Andreasen and Andersen particle packing. The particle size distribution of laboratory sand, masonry sand, cement, and silica fume is shown in Figure 1(a).

(a)

(b)
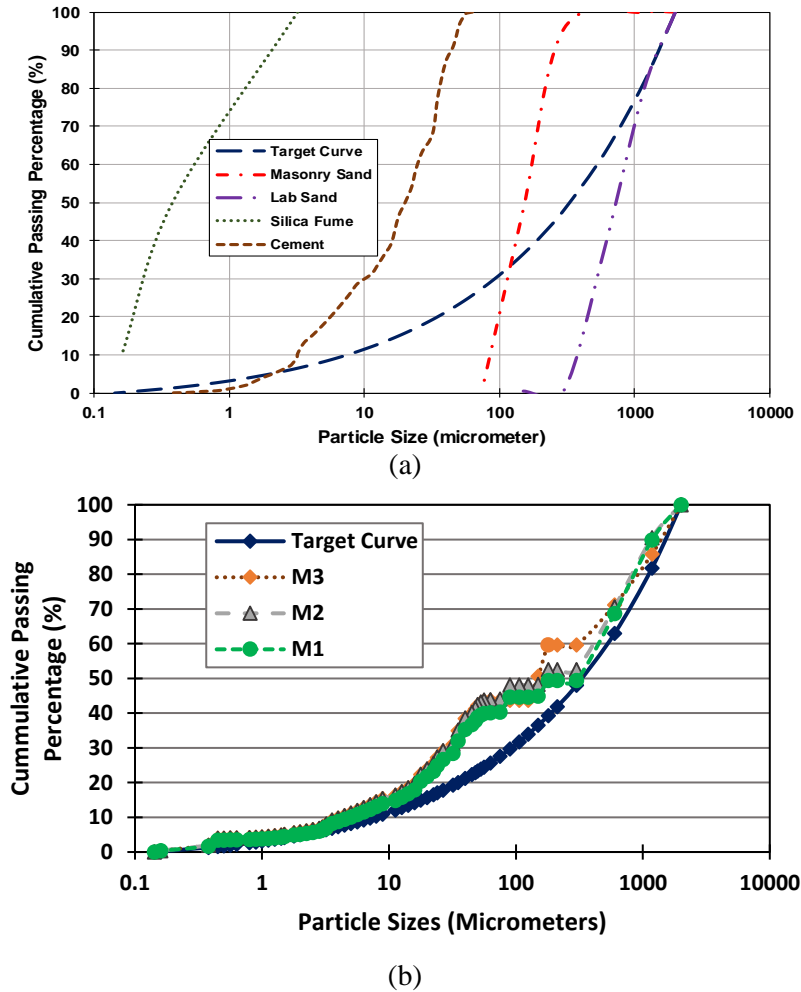
Figure 1. (a) Particle size distribution of materials used in non-proprietary UHPC mixtures and (b) Andreasen-Andersen curves for mixtures M1, M2, and M3

The steel fibers had a diameter of 0.2 mm (0.00788 in.) and a length of 13 mm (0.5120 in.).

1.4. Mix Proportions

The mixture proportioning of non-proprietary UHPC was developed by using the modified Andreasen-Andersen curve to ensure maximum particle packing. The mixtures were made by selecting a range of 1.2 to 1.4 for the sand-to-cement ratio. Using this range, three non-proprietary mixtures were prepared (see Table 2).

Table 2. Mixture proportions

Mix	Cement	Sand	Masonry sand	Silica fume	Water/ Cement	HRWR
M1	1	1.20	0.20	0.07	0.20	0.09
M2	1	1.02	0.18	0.07	0.20	0.11
M3	1	1.02	0.18	0.07	0.20	0.06

The mix designs previously shown in Figure 1(b) were developed by fixing the sand-to-cement ratio at 1.2 for mix M2 and 1.4 for mix M1. For these two mixtures, sands passing the 0.0937 in. (2.38 mm) sieve, #8 sieve in ASTM E-11 standard test sieve specification, were used. On the other hand, mix M3 was prepared with a special procedure for the preparation of sand. For this mixture, sand was sieved and separated. Then, the exact amount of sand fitting the target curve was used.

1.5. Testing Procedure

The samples of the prepared mixtures were tested for flow, compressive strength, and surface resistivity. The flow was measured using the flow table modified by ASTM C143 for testing the flow of mortars. This was measured in accordance with the standard, except that dropping the flow table 25 times was removed given the developed UHPCs were self-consolidating. The compressive test was done in accordance with ASTM C39 on three 100×200 mm (4×8 in.) cylinders. The ends of the cylinders were ground before compressive testing, as the strength of UHPC samples is usually higher than the capping materials used for normal concrete sample testing. The surface resistivity was measured using the 100×200 mm (4×8 in.) cylinders at the age of 28 days, in accordance with ASTM WK37880.

1.6. Results and Discussions

The flow of UHPC mixtures were measured similar to mortars by using a flow table, except that dropping the flow table 25 times was removed. The mix was allowed to spread and the flow was measured after the mix stopped. The results of the flow test are shown in Table 3.

Table 3. Flow, compressive strength, and resistivity of UHPC mixes

Mix	P-UHPC	M1	M2	M3
Flow (mm (in.))	216 (8.5)	216 (8.5)	216 (8.5)	203 (8.0)
Compressive strength (MPa (ksi))	100.7 (14.6)	97.2 (14.1)	97.9 (14.2)	101.4 (14.7)
Resistivity (kohm-cm)	23.5	8.0	8.5	20.2

As shown, all the mixtures had a similar flow of 203 mm (8.0 in) to 216 mm (8.5 in). This confirms that they can all be properly consolidated.

The compression test was also conducted on three cylinders of each mixture, at the age of 7 days, and their average values are shown in Table 3. Among the developed non-proprietary mixtures, the compressive strengths for mix M3, i.e., the mix with modified sand, showed the highest strength, followed by mixtures M2 and M1. The compressive strength of these mixtures were almost in the same range of the compressive strength of the proprietary mix P-UHPC. The compressive strength of all mixtures were sufficient to be used as UHPC. It should be noted that there have been debates on the strength required for a concrete to be considered UHPC, whether considerably high strength is needed when an exceptional durability performance is provided, or if strength is the critical aspect for a UHPC mixture.

The surface resistivity was also measured on three cylinders of each mixture, and their average values are provided in Table 3. Surface resistivity was a measure employed to evaluate the electrical resistivity of the UHPC samples investigated in this project. This measure is quantified by using non-destructive Wenner probes on 4×8 in. cylinders. The electrical resistivity is correlated in general to the risk of chloride ion penetration. The qualitative indicators reported in the literature provide ranges for surface resistivity and chloride penetration. Specifically, for a surface resistivity lower than 20 kohm-cm, the chloride penetration risk is deemed high. The risk becomes moderate for 20–40, low for 40–60, very low for 60–200, and negligible for a surface resistivity higher than 200. Although the reported ranges in Table 3 may make it appear that at least two of the mixtures (Mix 1 and Mix2) have a high chloride penetration risk, advanced chloride penetration tests, i.e., rapid chloride penetration and migration tests, confirm the negligible penetration of chloride ions in the developed mixtures. The surface resistivity for Mix 3 was almost equal to that of the proprietary mix P-UHPC, while mixes M1 and M2 showed lower values for surface resistivity.

1.7. Optimization of Base Mix

The base mix M2 developed in the results presented above was further modified by changing the maximum particle size, the sand-to-cement ratio, and the silica fume-to-cement ratio in the UHPC mixtures. The modified Andreasen-Andersen curve depends on two major aspects: the distribution modulus and the maximum particle size. To explore the effect of these two factors on the strength development of the UHPC, six mixes were developed using the proportioning of mix M2.

The maximum particle size of sand was reduced from 2.38 mm (0.0937 in.) to 0.6 mm (0.0234 in.). The distribution modulus was also varied from the initial selection of 0.37. Two further values, i.e., 0.23 and 0.30, were evaluated for the distribution modulus. Three additional sand-to-cement ratios 0.80, 0.90, and 1.0 were evaluated. The change in the particle sizes resulted in an increase in the compressive strength, as smaller particle sizes result in reduced pore volumes. The compressive strength increased to 15.2 ksi for the maximum particle size of 0.60 mm (0.0234 in.), from 14.10 ksi for the maximum particle size of 2.38 mm (0.0937 in.). The results for the change in the distribution modulus are shown in Figure 2.

(a)

(b)
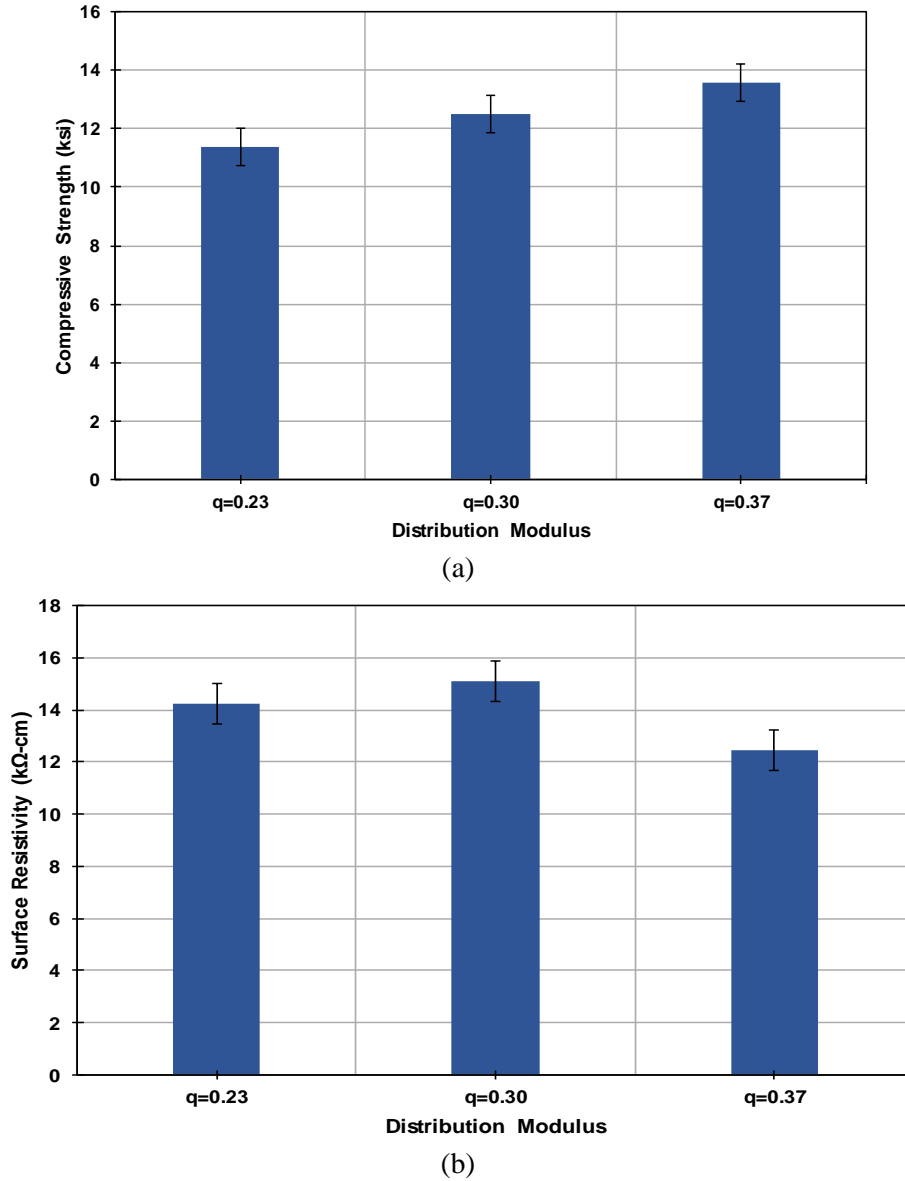
Figure 2. Effect of distribution modulus on (a) compressive strength and (b) surface resistivity

The distribution modulus of 0.37 resulted in the highest compressive strength, confirming the findings of Brouwers and Radix (2005).

1.7.1. Effect of Sand-to-Cement Ratio

The sand-to-cement ratio plays an important role in the strength gain of UHPC, as more cement is available for hydration and filling the voids produced between coarser sand particles. To further understand this effect, three additional sand-to-cement ratios were evaluated in addition to the base mix of M1. The results presented in Table 4 show that the mix with the sand-to-cement ratio of 1 resulted in the highest compressive strength.

Table 4. Compressive strength, resistivity, and absorption for varying sand to cement ratios

S/C ratio	7-Day Compressive Strength (ksi)		Resistivity (kΩ-cm)	Absorption (%)
	Cylinders	Cubes		
0.8	78.3	96.7	13.6	6.4
0.9	87.4	95.8	13.3	5.11
1.0	85.2	104.5	9.4	5.58
1.2	76.7	98.6	9.6	6.04

The surface resistivity increased with a lower sand-to-cement ratio; however, the same trend was not observed in the absorption values of the samples.

1.7.2. Effect of Silica Fume-to-Cement Ratio

The amount of silica fume in a UHPC mixture helps in two ways: accelerates the hydration process and acts as filler between larger particles, as it has smaller particle sizes. Two silica fume percentages were tested: 7% and 14% of the cement. The two ratios were tested for two different sand-to-cement ratios: 0.9 and 1.0. The obtained mixes were then tested for compressive strength and surface resistivity of the mixture. The results presented in Figure 3 show that the mixture with 14% silica fume showed the highest compressive strength and better surface resistivity.

(a)

(b)
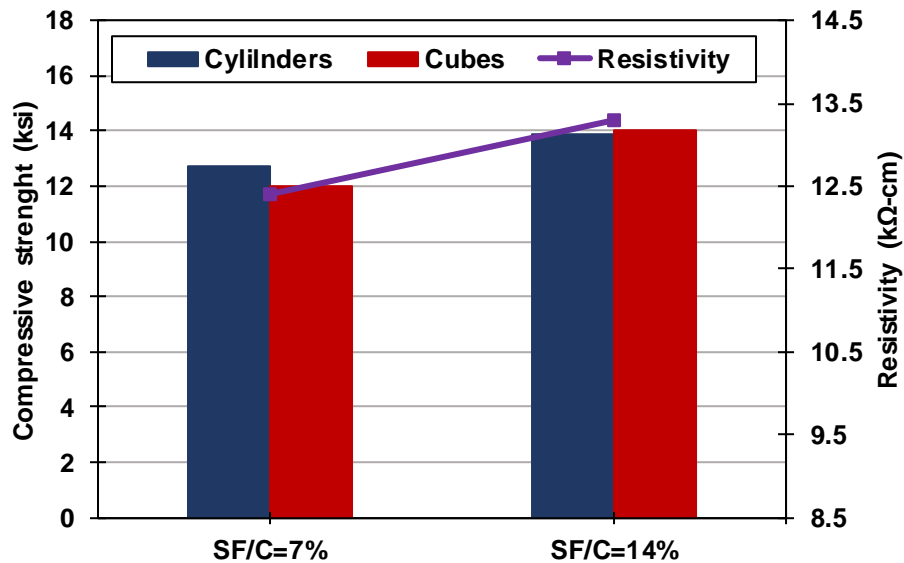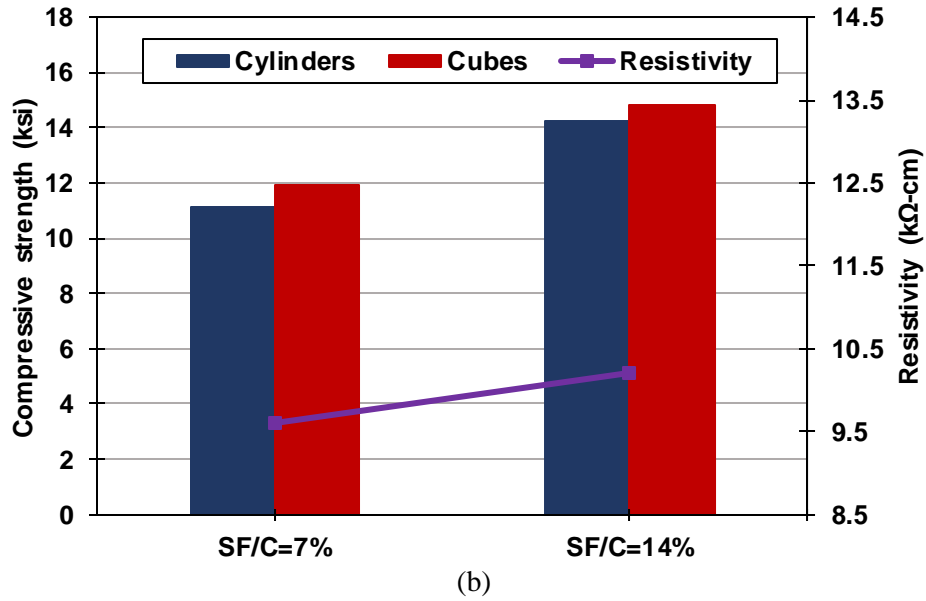
Figure 3. Effect of the silica fume-to-cement ratio in (a) a mixture with a sand-to-cement ratio of 1.0 and (b) sand-to-cement ratio of 0.9

1.7.3. Effect of Type of Silica Fume

To further explore the effect of the type of silica fume, two different types, densified and undensified, were tested (see Figure 4).

(a)

9

(b)
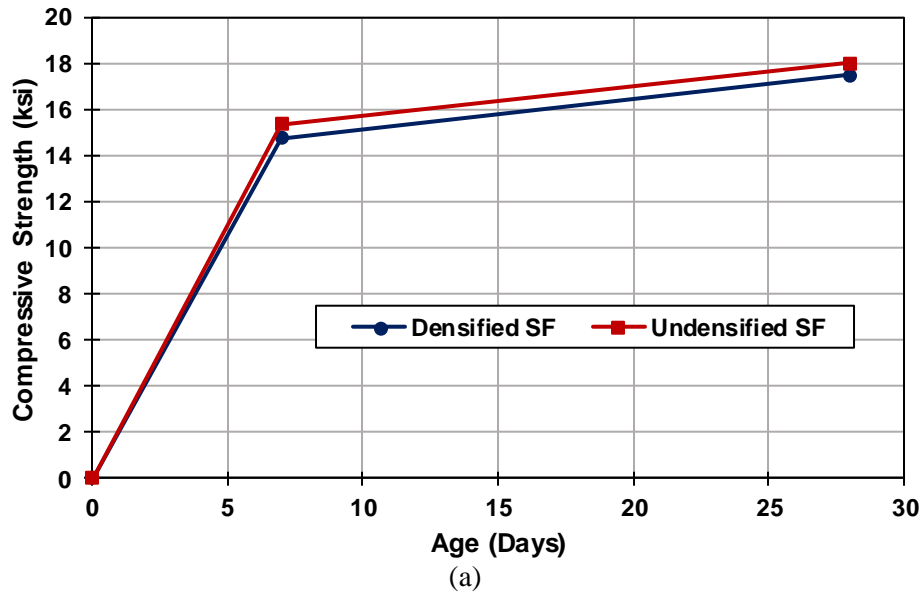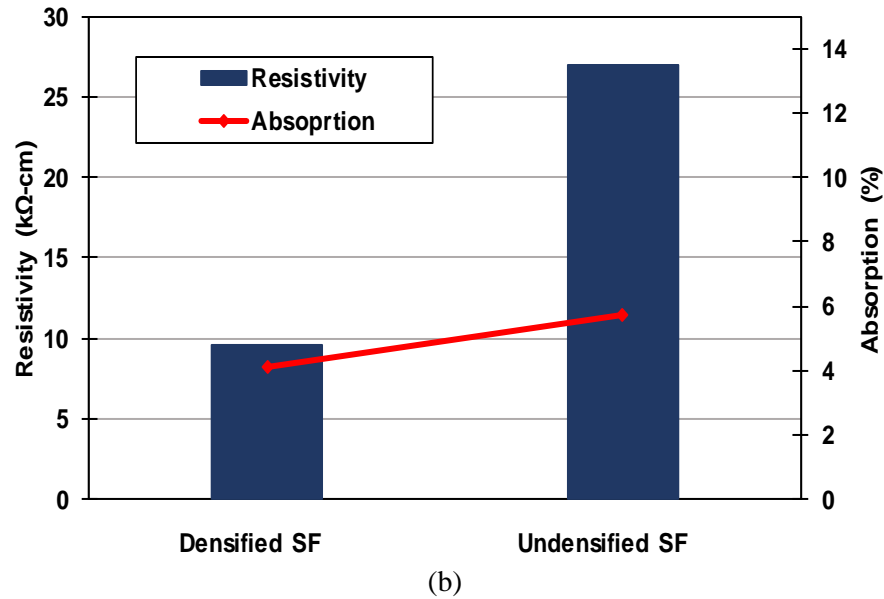
Figure 4. Effect of the type of silica fume on (a) compressive strength and (b) surface resistivity and absorption

The undensified silica fume has more surface area and is thus supposed to help more with hydration than the densified silica fume. The results from this test showed a marginal difference in the compressive strengths obtained for the two mixes; however, the undensified silica fume resulted in surface resistivity three times that of the mixture with densified silica fume.

1.8. Main Findings

A set of non-proprietary UHPC mixes were developed based on the theoretical model for particle packing (the Andreasen-Andersen packing model) and the available literature. The obtained mixes were further improved by optimizing the parameters of the theoretical model, i.e., maximum particle size and the distribution modulus. A set of further investigations were performed to evaluate the effect of the sand-to-cement ratio, silica fume-to-cement ratio, and types of silica fume. The following conclusions can be drawn from these explorations:

- The theoretical model proposed by Andreasen and Andersen is helpful in deciding the maximum particle size and the distribution of materials required for a UHPC mix. The model needs to be used carefully, however, as the preliminary mixture obtained from the optimized Andreasen-Andersen model resulted in a mixture with a sand-to-cement ratio of 2.3, and the compressive strength results were very low. The sand-to-cement ratio needs to be fixed in a range of 1.0–1.7, as suggested by previous researchers. The Andreasen-Andersen curve can then be optimized for all other ingredients.

- The two parameters, maximum particle size and distribution modulus, in the Andreasen-Andersen model were further optimized. The particle size of 0.6 mm (0.0234 in.) and the

10

distribution modulus of 0.37 resulted in the highest compressive strength. Smaller particle sizes result in smaller pores, which result in a denser and stronger UHPC mix.

- The mixtures with the sand-to-cement ratio fixed as 1.2 and 1.4 and optimized for the Andreasen-Andersen model resulted in compressive strengths and transport properties comparable to that of the proprietary mixtures. The sand-to-cement ratio was further explored by making three more mixes with varying ratios. The sand-to-cement ratios of 0.8, 0.9, and 1.0 were further investigated. The sand-to-cement ratio of 1.0 resulted in the highest compressive strength.

- The silica fume-to-cement ratio was also further investigated. The percentage of silica fume was increased from 7% to 14%. The results showed that the higher silica fume percentages showed higher compressive strength and surface resistivity values. Two types of silica fume were also further investigated: densified and undensified. The undensified silica fume showed a very small increase in compressive strength while the increase in surface resistivity was about three times that of the densified silica fume.

- The material cost of non-proprietary mixes was in the range of $519/yd^3 to $584yd^3, less than a third of the commercially available proprietary UHPC. The majority of the cost of non-proprietary UHPC comes from the cost of steel fibers and the cement content (33% each). As a baseline, the material cost of conventional concrete often lies in the range of $80–$100/yd^3.

Non-proprietary UHPC mixtures can be obtained by utilizing widely available materials. A sand-to-cement ratio in the range of 1.0–1.4, w/c ratio in the range of 0.2–0.25, and silica fume-to-cement ratio of 0.7–0.14 can result in a cost-effective non-proprietary mixture with comparable results to that of proprietary mixtures.

2. ASSESSMENT OF TRANSPORT PROPERTIES, VOLUME STABILITY, AND FROST RESISTANCE OF NON-PROPRIETARY UHPC MIXES

2.1. Introduction

The efforts to develop non-proprietary UHPC have mainly concentrated on two major aspects: strength and cost. While central to the applicability of UHPC, these two aspects need further complementary data to make UHPC a widely used material, especially for transportation structures like bridges.

Strength, while desirable, may not be the main aspect when it comes to concrete for bridges; other properties such as transport properties, volume stability, and frost resistance may hold equal or more significance. The reason for this is the exposure of bridge structures to environmental weathering agents, deicing salts, and temperature changes that make durability indispensable for bridges.

Studies on the durability aspects of non-proprietary UHPC mixtures are limited. Among the existing studies, El-Tawil et al. (2016), investigated non-proprietary UHPC mixtures made with different types of cement, silica fume contents, and volume percentages of steel fiber. The UHPC mixtures showed no significant variation in relative dynamic modulus, the mass loss was less than 3% for all of the tested specimens, and the passing electric charge was negligible in the rapid chloride penetration test.

Berry et al. (2017) developed a non-proprietary UHPC mixture, for which the drying shrinkage strain was recorded to be in the range of 130 microstrain after 120 days, the passing electric charge was very low, a negligible mass loss was observed after 300 cycles of freeze and thaw, and no scaling was reported when the specimens were subjected to deicing chemicals for 50 cycles.

In a separate effort, Bao et al. (2017) developed a non-proprietary UHPC mixture and tested it for resistivity, shrinkage, and frost resistance. The autogenous and drying shrinkage results for the non-proprietary mixture that contained only cement as the binder were high. This issue was addressed by replacing 50% of the cement with ground granulated blast furnace slag (GGBFS). The electrical resistivity measured for the mixtures was in the range of 30 to 45 kΩ-cm. The durability factor reduced only 0.03% after 300 freeze-thaw cycles, highlighting the superior frost resistance of the developed mixture.

Despite the contributions of past studies to shed light on some of the durability aspects of non-proprietary UHPC mixtures, the transport properties and volume stability of such mixtures were not investigated in detail. In particular, the conducted experimental tests were only focused on rapid chloride penetration or resistivity tests, which cannot be sufficient considering the drawbacks identified for each of these two tests. On the other hand, shrinkage, and especially autogenous shrinkage, which is known to be a critical issue for UHPC, was either not explored in depth or rarely considered for non-proprietary UHPC mixtures.

2.2. Experimental Program

To address the current research gaps, the objective covered in this chapter was to assess the performance of the developed non-proprietary UHPC mixtures under the penetration of chloride ions, moisture variations, and freeze-thaw cycles. For this purpose, a set of six non-proprietary UHPC mixtures were designed by using ordinary portland cement, regular sand, masonry sand, silica fume, and steel fiber. Upon ensuring that the expected strength was achieved, a set of experimental tests were performed to (1) evaluate transport properties using the rapid chloride penetration test (RCPT), the surface resistivity test, and the rapid chloride migration test (RCMT); (2) assess volume stability by measuring shrinkage properties (both autogenous and drying shrinkage); and (3) examine frost resistance through freeze-thaw cycles. For comparison purposes, two proprietary UHPC mixtures were also produced and subjected to similar tests.

2.2.1. Mixture Proportions

The proportioning of the non-proprietary UHPC mixtures was developed by using the modified Andreasen and Andersen curve to ensure that the maximum particle packing was achieved. The initial approach was to optimize the cumulative passing percentage curve by bringing it as close as possible to the target curve. Noting that the sand-to-cement ratio plays a significant role in strength development, this ratio was kept constant to be in the range of 1.2 to 1.4 (by weight). Using this range and a w/c ratio of 0.20 and 0.25, six non-proprietary mixtures were developed (see Table 5).

Table 5. Mixture proportions developed for the six non-proprietary UHPC mixtures

Mixture	Cement	Sand	Masonry Sand	Silica Fume	w/c	HRWR
NP1	1	1.20	0.20	0.07	0.20	0.090
NP2	1	1.02	0.18	0.07	0.20	0.110
NP3	1	1.02	0.18	0.07	0.25	0.047
NP4	1	1.20	0.20	0.07	0.25	0.034
NP-HSF	1	1.20	0.20	0.25	0.25	0.060
NP-GMS*	1	1.02	0.18	0.07	0.20	0.060

* Gradation-modified sand
All ratios are given by weight

The mixture designs were obtained by fixing the sand-to-cement ratio at 1.4 for the NP1 mixture and 1.2 for the NP2 mixture, both with a w/c ratio of 0.2. The NP3 and NP4 mixtures were made with similar sand-to-cement ratios of 1.4 and 1.2, respectively, but with a w/c ratio of 0.25 to investigate the effect of the w/c ratio on the main properties of the non-proprietary UHPCs.

The NP-HSF mixture was designed similar to the NP1 mixture, but with the silica fume content increased to 25% of the cement weight. This percentage was decided based on the other studies

available in the literature. In particular, the maximum silica fume content recommended by Richard and Cheyrezy (1995) was 25% of the cement weight. In a separate investigation, Chan and Chu (2004) suggested a silica fume dosage in the range of 20% to 30% of the cement weight.

For all of the mixtures, sand that passed the 2.38 mm (0.0937 in.) sieve was used, except that the NP-GMS mixture was designed with gradation modified sand. For this mixture, after the sand was sieved and separated, the exact amount of sand fitting the target curve was used. This was to evaluate the effect of the particle size of granular materials. Again, two proprietary UHPC mixtures were also prepared for comparison purposes.

2.2.2 Mixing and Curing

Upon completing a set of preliminary tests, a step-by-step mixing procedure was developed similar to the previous study on the development of non-proprietary UHPC from Berry et al. (2017). The sand and silica fume were first mixed for 5 minutes, followed by the addition of the cement. After mixing the dry materials for 5 additional minutes, the water and HRWR admixture were added. The mixing process was continued until each mixture became fluid (usually within 5 to 10 minutes). The steel fibers were then added by 2% of the concrete's volume and mixed until they fully dispersed (usually within 5 minutes). Upon finishing the mixing process, the flow was measured and samples were cast. The samples were left in the mixing room for a day. They were then demolded and stored in the curing room until the time of the planned tests.

2.2.3 Test Plan

The samples of the developed non-proprietary and proprietary UHPC mixtures were tested for flow, compressive strength, tensile strength, rapid chloride penetration, rapid chloride migration, surface resistivity, autogenous shrinkage, drying shrinkage, and frost resistance.

- Flow was measured using the flow table modified following ASTM C143 for testing mortars. The flow test was in accordance with the standard, except that dropping the flow table 25 times was skipped, given the developed UHPC mixtures were self-consolidating.

- The compressive test was performed on three 100×200 mm (4×8 in.) cylinders of each mixture at the age of 7 days according to ASTM C39.

- Split tensile strength test was conducted using three 100×200 mm (4×8 in.) cylinders after 7 days following ASTM C469.

- The RCPT was carried out on three 50×100 mm (2×4 in.) disks in accordance with ASTM C1202.

- Similar sized disks (3 for each test) were used for the RCMT based on NordTest (NT) BUILD 492 (https://ebaengineering.com/nt-build-492-an-option-for-concrete-durability-testing-youve-never-heard-of/).

- Surface resistivity was measured using 100×200 mm (4×8 in.) cylinders at the age of 28 days in accordance with ASTM WK37880.

- Autogenous shrinkage was measured from the sealed corrugated plastic tubes of 420 mm (16.53 in.) long with a diameter of 29 mm (1.14 in.) according to ASTM C1698. In this test, the samples were stored at a room temperature of $23 \pm 2°C$, and their initial lengths were measured at the time of final setting. After that, the readings were taken at the ages of 1, 3, 7, 14, and 28 days. The test was continued for 140 days with weekly readings after the 28th day.

- Drying shrinkage was measured on 25×25×258 mm (1×1×10 in.) prisms following ASTM C596. The first reading was taken at the 72-hour age after removing the specimens from the curing chamber. The specimens were then placed in the shrinkage room (with a room temperature of $23°C \pm 2°C$ and relative humidity of $50 \pm 4\%$), and specimen lengths were measured at the ages of 4, 7, 14, 21, and 28 days. The length measurements were continued for 140 days with weekly readings.

- Resistance to freeze-thaw cycles was evaluated for each mixture on three beam samples of 75×100×279 mm (3×4×11 in.) in accordance with ASTM C666.

2.3. Assessment of Flow and Strength Properties

2.3.1. Flow

The mixture designs were optimized in such a way that an adequate flow (i.e., for self-consolidating) was achieved without bleeding or segregation. The flow of UHPC mixtures was evaluated similar to that for mortars by using a flow table. Each mixture was allowed to spread, and the flow was measured after the mixture stopped spreading. The results of the flow tests are provided in Table 6.

Table 6. Results of fresh, strength, and transport properties

Mixture	NP1	NP2	NP3	NP4	NP-HSF	NP-GMS	P1	P2
Flow (mm (in.))	216 (8.5)	216 (8.5)	203 (8.0)	229 (9.0)	216 (8.5)	203 (8.0)	216 (8.5)	216 (8.5)
7-Day Compressive Strength (MPa (ksi))	97.2 (14.0)	97.9 (14.2)	86.9 (12.6)	77.2 (11.2)	71.7 (10.3)	101.4 (14.7)	117.2 (16.9)	100.7 (14.6)
Split Tensile Strength (MPa (ksi))	10.1 (1.5)	10.6 (1.5)	10.6 (1.5)	10.3 (1.5)	11.0 (1.6)	11.8 (1.7)	14.5 (2.1)	12.0 (1.7)
Resistivity (kΩ-cm)	8.0	8.5	9.7	6.1	25.7	20.2	60.0	23.5
Ultimate Autogenous Shrinkage ($\times 10^{-6}$ m/m (in/in))	280	240	400	260	980	370	477	322
Ultimate Drying Shrinkage (%)	0.110	0.135	0.124	0.110	0.148	0.125	0.110	0.124

It can be seen that all of the mixtures had a consistent flow of 203 mm (8 in.) to 228 mm (9 in.). This confirmed that all the developed mixtures were self-consolidating and can be properly cast without external vibration.

2.3.2. Compressive and Split Tensile Strength

The compressive strength test was conducted on three cylinders of each mixture at the age of 7 days. Their average values are also included in the previous Table 6.

Among the developed non-proprietary mixtures, the compressive strength of the NP-GMS mixture was the highest, followed by the NP2, NP1, NP3, NP4, and NP-HSF mixtures. The compressive strengths of the non-proprietary mixtures were in the same range as the compressive strength of the P2 proprietary mixture, while the P1 proprietary mixture provided the highest 7-day compressive strength.

The change in the w/c ratio from 0.20 to 0.25 (for NP1 and NP2 compared to NP3 and NP4, respectively) was found to decrease the compressive strength of the mixtures by up to 20%. The increase of the silica fume content also resulted in a reduction of compressive strength, proving that an excessive amount of silica fume can have an adverse effect on the strength properties. The increase in the sand-to-cement ratio (in the studied range of 1.2 to 1.4) resulted in a negligible reduction of compressive strength. As further supported by the results reported in Wille et al. (2012), this can be explained with the fact that UHPC contains a high amount of cement, a great portion of which remains unhydrated. Therefore, a change of the cement content

in the studied range did not influence the hydration or strength development in any significant way.

Table 6 also summarizes the results of the split tensile tests performed on the developed mixtures. The tensile strength for the NP-GMS mixture was the highest among the developed non-proprietary UHPC mixtures because of the modified sand gradation and improved packing. The obtained tensile strengths showed similar trends with changes in the w/c ratio, sand-to-cement ratio, and silica fume content. Although the tensile strengths of the developed mixtures were weaker than their proprietary counterparts, they can be considered sufficient for non-proprietary UHPC.

2.4. Assessment of Transport Properties

2.4.1. Electrical Resistivity

Considering the advantages of electrical resistivity tests, including low cost and ease of use in practice, there has been growing attention to this test for evaluating the concrete's transport and permeability properties. In this study, surface resistivity was measured using three cylinders of each mixture, and their average values are also included in the previous Table 6.

The surface resistivity of the non-proprietary UHPC mixtures varied in the low range of 6.1 to 9.7 kΩ-cm for the mixtures with low silica fume content and increased to 25.7 kΩ-cm for the mixture with high silica fume content (NP-HSF). The superior resistivity of the NP-HSF mixture highlights that the increase of silica fume can result in a considerable increase in resistivity.

The surface resistivity of the proprietary mixtures, and particularly for P1, was high. This indicates that, although the mixture proportions for the proprietary UHPC mixtures were not available, they should have contained a significant amount of silica fume. This observation raises the important question regarding whether the developed non-proprietary mixtures can provide the expected resistance against chloride penetration. The answer to this question was sought in additional tests.

2.4.2. Chloride Penetration

The developed UHPC mixtures were tested for chloride penetration with both the RCPT and RCMT. The results from the RCPTs followed the trend observed from the surface resistivity test results, showing a significantly high passing charge in the range of 3,000 to 10,000 Coulombs in the various non-proprietary mixtures.

To understand if the mixtures are truly vulnerable to chloride attack and if the surface resistivity test and RCPT are proper tests for such an evaluation, a RCMT was devised. While the RCPT measured the charge passed through the concrete sample and related it to chloride ion penetration, the RCMT measurement was based on observing the penetrated depth of chloride ions through the formation of white silver chloride, where the sprayed silver nitrate reaches to

and reacts with the penetrated chloride (Najimi et al. 2018). The RCMT results are presented in Figure 5 for all of the non-proprietary and proprietary mixtures.
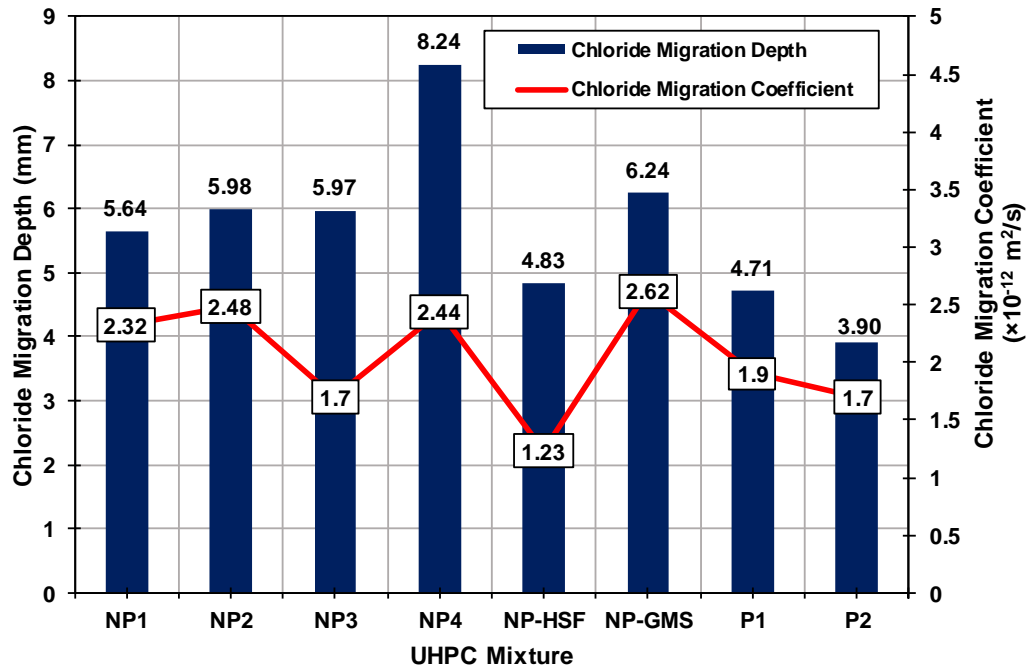
Figure 5. Chloride migration depth and chloride migration coefficient of the UHPC mixtures tested

It can be seen in this figure that the depth of chloride penetration into the non-proprietary mixtures (and the associated chloride migration coefficients) was very low to negligible, and similar to that for the proprietary mixtures. In the developed mixtures, increasing the w/c ratio was found to result in a slight increase in the depth of chloride penetration. This can be explained by the presence of water (along with chloride ions) in the pores, making the concrete electrically conductive. Increasing the sand-to-cement ratio also increased the depth of chloride penetration, which is consistent with the results of compressive strength and resistivity tests. Increasing the silica fume content, however, decreased the depth of chloride penetration. This can be directly related to the effect of silica fume on the volume and connectivity of the pores in the mixture (Shihada and Arafa 2010). Figure 6 highlights the low penetration depth of chloride ions in a sample of the NP1 mixture after the RCMT.

Figure 6. Chloride migration observed in a sample of the NP1 mixture under rapid chloride migration test

To evaluate the common perception that steel fibers do not corrode in UHPC (or only corrode on the surfaces), the samples were carefully examined to understand if there were any signs of steel fiber corrosion. Figure 7(a) shows that there was corrosion of steel fibers in the non-proprietary mixtures, but this corrosion was only on the exposed surfaces of the samples.

(a)

(b)

Figure 7. Corrosion of steel fibers at (a) surface of the NP2 and (b) depth of the P1 mixture

On the other hand, there were signs of steel fiber corrosion farther deep into the samples for the P1 proprietary mixtures, as shown in Figure 7(b). Based on the results collectively obtained from the resistivity test, RCPT, and RCMT, as well as the corrosion observed in the steel fibers of the proprietary mixtures (with considerably high resistivity), the capability of existing accelerated test methods for determining the susceptibility of UHPC mixtures to chloride penetration was found to be in need of further investigation. This, however, fell beyond the scope of this study.

2.5. Assessment of Volume Stability

2.5.1. Autogenous Shrinkage

Figure 8 shows the results of the autogenous shrinkage tests performed during the 140-day period.
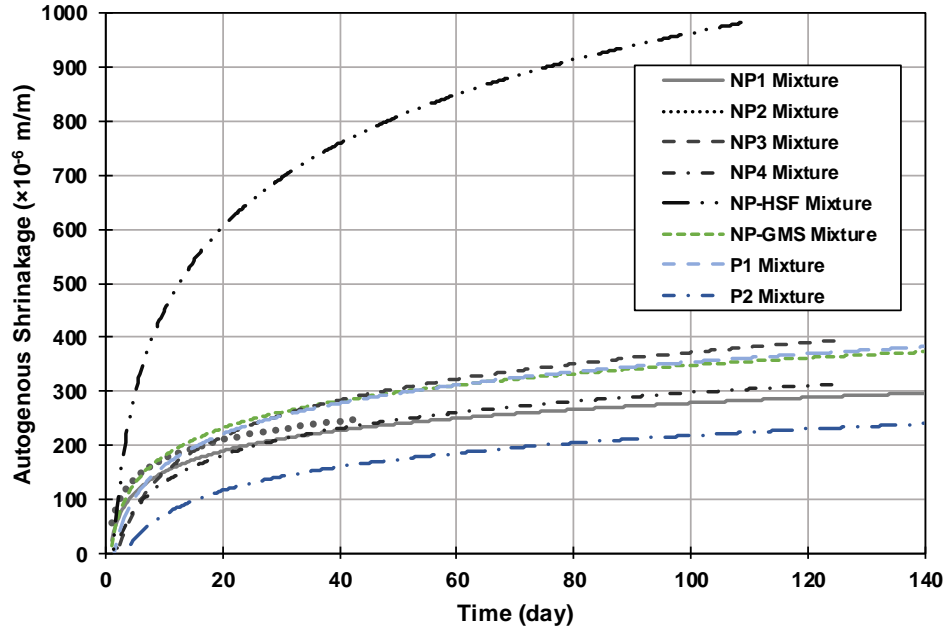
Figure 8. Results of autogenous shrinkage tests performed on the UHPC mixtures

It can be seen in Figure 8 that, except for the NP-HSF mixture, which consistently showed the greatest shrinkage, the autogenous shrinkage of the developed non-proprietry mixtures were in the same range as that of the proprietary mixtures. The high autogenous shrinkage results for the NP-HSF mixture can be related to its high silica fume content. This is consistent with the literature, as the use of mineral additives that contain fine capillary pores (e.g., silica fume) is proven to increase the susceptibility of a mixture to self-desiccation and autogenous shrinkage (Meng and Khayat 2017, Mazloom et al. 2004, Zhang et al. 2003).

The reduction of the w/c ratio in the mixtures that had a similar sand-to-cement ratio resulted in increased initial autogenous shrinkage (at early ages) and reduced ultimate shrinkage (when comparing the NP4 mix with the NP1 mixture for the sand-to-cement ratio of 1.4 and the NP3 mix with the NP2 mixture for the sand-to-cement ratio of 1.2). In reducing the w/c ratio, self-desiccation increases the capillary tension in the pore fluid, resulting in greater autogenous shrinkage (Meng and Khayat 2017). This is commonly observed in the early age of UHPC (Mechterine et al. 2009, Koh et al. 2011, Yoo et al. 2014). The mixtures with a lower sand-to-cement ratio were found to experience greater autogenous shrinkage. This can be attributed to the lower content of fine aggregates in their mixtures, which in turn, can reduce their restraining effect to prevent the autogenous shrinkage.

2.5.2. Drying Shrinkage

The drying shrinkage readings were taken for four samples of each mixture, and their average values were plotted in Figure 9.

21
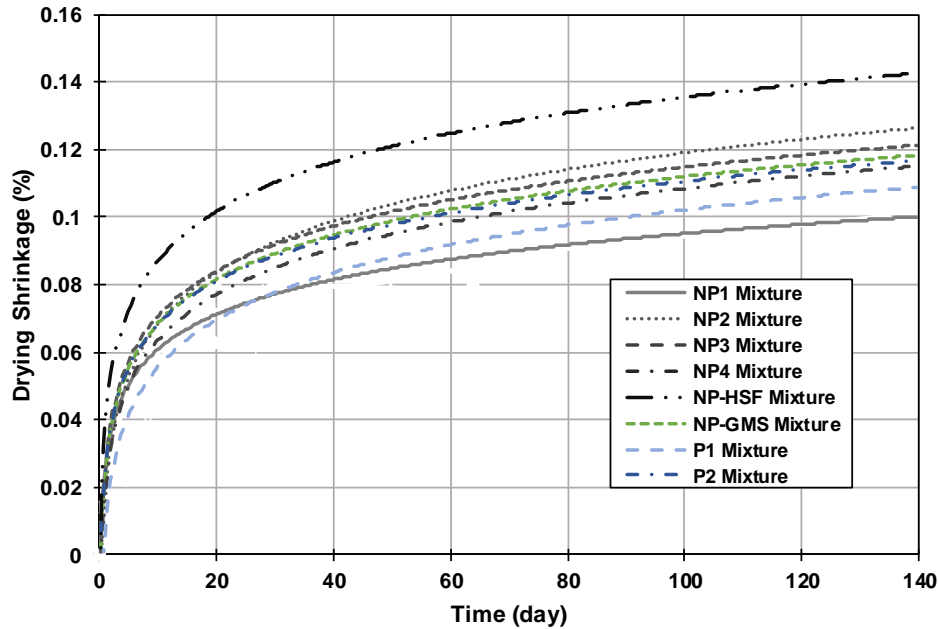
Figure 9. Results of drying shrinkage tests performed on the UHPC mixtures

Except for the NP-HSF mixture, which contained a high amount of silica fume, the drying shrinkage of all the developed non-proprietary UHPC mixtures were close to each other. As discussed for autogenous shrinkage, the inclusion of silica fume can be the cause of this increased shrinkage. Increases in the w/c ratio for the mixtures with a similar sand-to-cement ratio resulted in greater drying shrinkage. This can be explained with the weakened microstructure of the paste and the availability of evaporable moisture, which is responsible for volume instability. An increase in the sand-to-cement ratio for the mixtures with a similar w/c ratio led to the reduction of drying shrinkage. This can be attributed to the restraining effect of fine aggregates, which was improved by increasing the sand-to-cement ratio.

While the drying shrinkage results for the non-proprietary and proprietary UHPC mixtures were close (except for the NP-HSF mixture), most of the non-proprietary mixtures showed a slightly greater drying shrinkage than the P1 proprietary mixture. Based on this observation and the fact that the P1 mixture most likely contains high silica fume, it was inferred that the P1 mixture may also have some type of shrinkage-reducing admixture (in the form of powder) included in the premix binder. The NP-HSF mixture, which had a 25% silica fume content, showed the greatest drying shrinkage. This confirmed the direct relationship between the silica fume content and drying shrinkage in UHPC mixtures.

2.6. Main Findings

With the ultimate goal of developing economically viable, non-proprietary UHPC mixtures with desired performance characteristics, the goal of this chapter was primarily focused on the transport properties, volume stability, and frost resistance of the six non-proprietary UHPC mixtures in comparison to the two proprietary UHPC mixtures. The following conclusions can

be drawn based on the results and observations obtained from this rigorous set of testing, including flow, compressive strength, tensile strength, rapid chloride penetration, rapid chloride migration, surface resistivity, autogenous shrinkage, drying shrinkage, and freeze-thaw.

- Use of the modified particle packing density curve and the optimization of the cumulative passing percentage may not result in the expected performance without a proper selection of w/c and sand-to-cement ratios. This highlights the importance of taking into consideration all the main contributing factors when designing non-proprietary UHPC mixtures.

- While the surface resistivity of the non-proprietary mixtures was lower than that of the proprietary mixtures, the depth of chloride penetration and the chloride migration coefficient were almost the same for all of the non-proprietary and proprietary mixtures. On the other hand, traces of steel fiber corrosion were observed in the proprietary mixtures with a high surface resistivity and low RCPT passing charge. Such findings suggested that the surface resistivity test and RCPT may not be the most proper experiments for assessing the performance of UHPC against chloride penetration. Thus, further investigations involving chloride diffusion and chloride-induced corrosion of the UHPC mixtures could be helpful.

- The average autogenous shrinkage of the non-proprietary mixtures was 22.5% lower than that of the proprietary mixtures. However, the autogenous shrinkages of the developed non-proprietary mixtures increased when increasing the silica fume content (up to twice the average for all of the tested non-proprietary mixtures). An increase of 26% and 36% was recorded by changing the w/c ratio from 0.20 to 0.25 and the sand-to-cement ratio from 1.2 to 1.4, respectively. The drying shrinkage results for the non-proprietary and proprietary mixtures were close to each other with a variation less than 3%.

- The developed non-proprietary mixtures performed very well under the freeze-thaw tests, which continued up to 300 cycles. All the mixtures were found to have a mass loss of less than 2% and drops in their relative dynamic modulus of elasticity results of less than 7%. This indicated the capability of the developed UHPC mixtures for applications that involve extreme exposure conditions.

3. EFFECTS OF STEEL FIBER DOSAGE AND TYPE ON THE FLEXURAL STRENGTH OF UHPC MIXES

3.1. Introduction

The most common type of fiber used in UHPC to date is steel fiber. A variety of fresh and hardened properties of UHPC, and those related to tensile response in particular, are known to be largely dependent on the dosage, shape, and size of the steel fibers included in the UHPC mixtures (Russell and Graybeal 2013, Hannawi et al. 2016, Larsen and Thorstensen 2020).

The effect of steel fiber dosage on the performance characteristics of UHPC has been a subject of a few research studies. Such studies have been motivated by the significant contribution of steel fibers to the flow and flexural capacity of UHPC, in addition to the total material cost, which is greatly influenced by the dosage of the steel fibers recommended (Meng and Khayat 2018).

In the current literature, the role of the steel fiber dosage has been mainly investigated for straight microfibers, which commonly have a length of 13 to 30 mm (0.51 to 1.18 in.). Among the studies available, Abbas et al. (2015) investigated the effects of straight steel fibers with various dosages and lengths on the mechanical and durability properties of UHPC. The study explored three different dosages (1.0%, 3.0%, and 6.0% by volume) and three different lengths (8, 12, and 16 mm (0.31, 0.47, and 0.63 in.)). The test results indicated that an increase in the steel fiber dosage results in improvements to both splitting tensile strength and flexural strength. In particular, the maximum load under a three-point loading setup showed a 64% increase after changing the steel fiber dosage from 1.0% to 3.0% (by volume). The study also reported that UHPC mixtures with shorter steel fibers provide a higher strength and strain hardening than those with longer steel fibers. A 42% increase in the load carrying capacity was noted after transitioning from shorter to longer steel fibers at the fiber dosage of 6.0%. The UHPC mixtures with shorter fibers, however, showed a steep drop in their load carrying capacity after the peak load was reached.

In a separate study, Shehab El-Din et al. (2016) investigated various dosages and aspect ratios of steel fibers. The study found that an increase in the fiber dosage from 1.0% to 3.0% results in an increase in the range of 15% to 40% in the flexural strength of UHPC. Similarly, the flexural strength increased when transitioning to high aspect ratio fibers for all of the fiber dosages tested.

In a study conducted for the Colorado DOT, Kim et al. (2011) reported that, while the compressive strength of UHPC increases by 6% after the addition of 2.0% straight steel fibers to a plain UHPC mixture, the flexural capacity shows a significantly more pronounced increase, which can be up to 60%. The addition of steel fibers was also found to change the failure mode of the UHPC from brittle to ductile, introducing a notable post-crack resistance.

Milan et al. (2016) studied the effects of straight steel fibers on the compressive and flexural strengths of UHPC. The study determined that the strength properties consistently improve when

increasing the fiber dosage from 0.0% to 3.5%. It was, however, noted that a fiber dosage beyond 2.5% creates difficulties in achieving desired workability.

Arora et al. (2019) investigated the effects of steel fiber dosage on the flexural behavior of UHPC beams under third point tests and found a 45% increase in the recorded peak load after the steel fiber dosage was increased from 1.0% to 3.0%. The mixtures with higher dosages also provided higher ductility and toughness.

In a study conducted for the Arizona DOT, Mobasher et al. (2019) developed a non-proprietary UHPC mixture. The reference mixture that had no fibers showed brittle behavior, while the mixture with 1.0% steel fiber provided ductile behavior with a 20% increase in the flexural load carrying capacity under the four-point bending test. The absorbed energy measured for the UHPC mixture with 1.0% steel fiber was also observed to be two to three times greater than that recorded for the UHPC with no fibers. An increase in the fiber dosage also improved the pre-peak response and the flexural load carrying capacity. The average maximum load carrying capacity obtained from the third point tests was 68% higher in the mixtures with 3.0% steel fiber than those with 1.0% steel fiber. Consistent with the other studies, however, the high dosage of steel fibers introduced workability issues. This led to recommending an upper limit for the steel fiber dosage, which in turn set a limit for the tensile strength and ductility that could be achieved.

A potential solution to overcome the issues caused by a high dosage of steel microfiber is to utilize a combination of micro- and macrofibers, where the microfibers strengthen the concrete matrix and control shrinkage, while the macrofibers improve the tensile strength and the crack bridging capacity. The type of macrofibers, however, has a notable influence on both pre- and post-cracking behavior of UHPC.

Kim et al. (2011) investigated the performance of UHPC mixtures with micro- and macrofibers under flexure. Two different fiber lengths (13 mm and 30 mm [0.51 to 1.18 in.]) were tested for straight fibers and two different fiber lengths (30 mm and 60 mm [1.18 and 2.36 in.]) were tested for hooked fibers. The microfibers were blended with macrofibers in the ratios of 0.5%, 1.0%, and 1.5%. Among the results, the toughness of the UHPC mixtures with 1.0% hooked fiber and 1.0% microfiber was found to be up to 60% higher than that of the mixtures made with only microfibers. In particular, the mixtures with the long hooked fibers were noted to perform best.

Meng and Khayat (2018) investigated the use of straight steel, hooked steel, and polyvinyl alcohol (PVA) fibers to enhance the mechanical properties of UHPC. The compressive strength was reported to improve by increasing the dosage of straight steel fibers until 3.0%, beyond which the strength started to drop. This could be because of the use of a high dosage of superplasticizer, resulting in a high volume of entrapped air. It was also observed that the flexural strength did not have a linear increase with increasing the fiber dosage. The combination of fibers with a target fiber content of 2.0% resulted in the best flexural properties for the mixtures investigated. In particular, the combination of 1.0% hooked fiber and 1.0% microfiber provided the maximum post-crack strength.

Ma et al. (2019) investigated the effects of a combination of straight steel fibers with hooked steel and cellulose fibers. The total fiber content was maintained constant at 2.0% by volume. The UHPC mixtures made with only cellulose fibers provided the lowest strength. Upon the addition of steel fibers, hooked fibers were found more effective than straight fibers in improving the flexural strength of the UHPC mixtures including the cellulose fibers. The ratio of straight to hooked steel fibers was also varied from 0.0% to 5.0%. This, however, did not lead to a significant variation in the flexural test results.

Wu et al. (2016) studied the use of straight, hooked, and twisted steel fibers with the dosages varying from 0.0% to 3.0%. The UHPC mixtures made with the hooked fibers resisted the highest peak load, followed by the mixtures made with twisted and straight steel fibers.

Zhang et al. (2018) also investigated a hybrid use of straight and hooked steel fibers. The total steel fiber dosage was maintained at a constant 2.0%. The hooked fibers used for the study had the same length but two different diameters (0.25 mm and 0.35 mm [0.0098 and 0.0137 in.]). The UHPC mixtures also included coarse aggregates (with a maximum particle size of 10 mm [0.393 in.]). The mixtures with a hybrid of steel and hooked fibers provided the maximum peak and post-crack capacities compared to those with either straight or hooked fibers.

Ragalwar et al. (2019) studied steel wool as a secondary fiber, along with hooked steel fibers, in UHPC. The study used a constant 2.0% hooked fiber dosage, while the steel wool dosage was varied between 0.0% and 2.0% in 0.5% increments. The addition of steel wool up to 1.5% resulted in a more than 20% improvement in maximum compressive strength and a more than 65% improvement in flexural strength. However, a drop in the strength properties was noted after increasing the steel wool content from 1.5% to 2.0%. This was attributed to high viscosity and poor workability. The study recommended a combined use of steel fiber and steel wool, as steel wool can cost up to 50% less than steel fiber.

Further to the dosage and shape of steel fibers, their lengths have been an important contributing factor to the performance of UHPC mixtures. The effects of variation in the steel fiber length was investigated by Yoo and Banthia (2016). The study tested three different lengths of 13.0 mm (0.51 in.), 16.3 mm (0.64 in.), and 19.5 mm (0.77 in.) for straight steel fibers. The outcome reflected that the fiber length had no major effect on the flexural response of the tested mixtures in the elastic range. However, the longer fibers were found more effective in the post-cracking behavior of the UHPC, leading to an improved toughness and load carrying capacity.

In a separate effort, Yoo et al. (2017) investigated the effects of using two lengths of straight steel fibers, (19.5 mm and 30.0 mm [0.77 in. and 1.81 in.]) and two types of steel fibers (twisted long fibers and hooked long fibers that were 30.0 mm [1.81 in.] long). The study reported low toughness and flexural strength properties for the mixtures made with the long hooked fibers when the fiber dosage was above 1.0%. The twisted long fibers were similarly most effective in low fiber dosages (below 1.5%).

Park et al. (2017) also studied the effects of the length and dosage of steel fibers on the flexural strength of UHPC. That study found that longer straight fibers have a more pronounced

contribution to flexural performance than shorter steel fibers at low fiber dosages. At high fiber dosages, however, the positive effects of longer steel fibers started diminishing.

Despite the wealth of information available regarding the role of steel fibers in UHPC, there have been standing questions on how a combination of micro- and macrofibers can contribute to delivering the desired fresh and hardened properties. This motivated the current study to focus on a hybrid of micro- and macrofibers in the forms of twisted wire and hooked fibers.

Building on the findings and observations reported in the literature, a holistic matrix of non-proprietary UHPC mixtures was developed and investigated in this study. The matrix included 13 UHPC mixtures, focusing on the pre- and post-cracking response of UHPC mixtures in flexure. Five of these mixtures were made by changing the dosage of steel microfibers from 1.0% to 3.0% in 0.5% increments, two mixtures were prepared with a 2.0% dosage of each of the twisted wire and hooked fibers, three mixtures were prepared with a hybrid of microfibers and twisted wire fibers, and three mixtures were prepared using a combination of microfibers and hooked fibers.

The researchers performed a set of flow tests to evaluate workability, as well as compressive and flexural strength tests to determine the mechanical properties of the developed mixtures. In particular, the toughness and residual strength properties of a set of UHPC beam specimens were investigated under the standardized vertical deflections of L/600 and L/150, in addition to L/100, where L refers to the beam's clear span length between the two supports. The results were then paired with robust digital image correlation (DIC) analyses to understand the patterns of cracking, as a function of the applied load. For this purpose, the crack width along the depth of the tested UHPC beam specimens was monitored to evaluate the contribution of each type of fiber to limiting crack propagation. The outcome of this part of the study provides original information that can be directly used in the process of fiber selection for the UHPC mixtures that can deliver the desired fresh and hardened properties.

3.2. Mixture Proportions and Test Plans

The materials used for the non-proprietary UHPC mixtures in the current study included portland cement Type I, densified silica fume, regular sand, masonry sand, and superplasticizer. The regular sand was modified to reduce the maximum size from 2.38 mm (0.0937 in.) to 0.60 mm (0.0236 in.). The sand to cement, silica fume to cement, and w/c ratios were fixed at 1.00, 014, and 0.21, respectively. The fibers considered for the developed UHPC mixtures were straight microfibers (S), twisted wire macrofibers (T), and hooked macrofibers (H) (see Figure 10).

(a)

(b)

(c)

Figure 10. (a) Straight microfibers, (b) twisted wire fibers, and (c) hooked macrofibers

The geometric properties and tensile strength of the selected fibers are listed in Table 7.

Table 7. Properties of steel fibers

Steel Fiber Type	Length	Diameter	Tensile Strength
Straight microfibers (S)	0.5 in. (13 mm)	0.008 in. (0.20 mm)	290 ksi (2,000 MPa)
Twisted wire fibers (W)	1 in. (25 mm)	0.02 in. (0.5 mm)	246.5 ksi (1,700 MPa)
Hooked macrofibers (H)	1.37 in. (34 mm)	0.021 in. (0.54 mm)	159.5 ksi (1,100 MPa)

The dosages of straight microfibers were varied from 1.0% to 3.0% by volume of the UHPC mixture in 0.5% increments. This introduced five different mixtures labeled as S1.0, S1.5, S2.0, S2.5, and S3.0. Two separate mixtures were also prepared using 2.0% twisted wire fiber and 2.0% hooked fiber. Upon a thorough investigation of the mixtures made with only one type of steel fibers, the study was expanded to investigate six more mixtures that utilized a combination of straight microfibers and twisted wire fibers (labeled as S0.5T1.5, S1.0T1.0, and S0.5T1.5) and straight microfibers and hooked fibers (labeled as S0.5H1.5, S1.0H1.0, and S0.5H1.5). The entire matrix of the developed UHPC mixtures is listed in Table 8.

Table 8. Testing matrix for evaluating effects of variation in type of steel fibers

UHPC Mixture	Cement	Sand	Masonry sand	Silica Fume	Water	HRWR	Micro Fiber (%)	Twisted Fiber (%)	Hooked Fiber (%)
S1.0	1	0.53	0.47	0.14	0.21	0.045	1.0	-	
S1.5	1	0.53	0.47	0.14	0.21	0.045	1.5	-	-
S2.0	1	0.53	0.47	0.14	0.21	0.050	2.0	-	-
S2.5	1	0.53	0.47	0.14	0.21	0.052	2.5	-	-
S3.0	1	0.53	0.47	0.14	0.21	0.055	3.0	-	-
T2.0	1	0.53	0.47	0.14	0.21	0.051	-	2.0	-
S0.5T1.5	1	0.53	0.47	0.14	0.21	0.051	0.5	1.5	-
S1.0T1.0	1	0.53	0.47	0.14	0.21	0.050	1.0	1.0	-
S1.5T0.5	1	0.53	0.47	0.14	0.21	0.051	1.5	0.5	-
H2.0	1	0.53	0.47	0.14	0.21	0.066	-	-	2.0
S0.5H1.5	1	0.53	0.47	0.14	0.21	0.061	0.5	-	1.5
S1.0H1.0	1	0.53	0.47	0.14	0.21	0.059	1.0	-	1.0
S1.5H0.5	1	0.53	0.47	0.14	0.21	0.053	1.5	-	0.1

This table also provides the mixture proportions used for each of the mixtures.

The developed mixtures were tested for flow, compressive strength, and flexural strength. The flow was measured using a flow table modified according to ASTM C143. The flow test was in accordance with the standard, except for skipping the 25 drops of the table, which were not necessary given the developed mixtures were self-consolidating. The compressive strength was measured using 50 mm (2 in.) cubes in accordance with ASTM C109. The choice of cubes sized 50 mm (2 in.) (or smaller) over cylinders has been supported by past studies that are available in the literature (Gesoglu et al. 2016, Ibrahim et al. 2017, Meng and Khayat 2017, Wang and Gao 2016, Wu et al. 2016 and 2017).

The four-point bending test was performed on 100×100×350 mm (4×4×13.8 in.) UHPC beam specimens with a loading span of 300 mm (11.81 in.) in accordance with ASTM C1609. The test was carried out using a loading frame with the maximum capacity of 890 kN and a loading rate of 1.83 mm/min (0.072 in/min). For each mixture, three samples were tested.

3.3. Flow and Compressive Strength

Flow characteristics were measured for all of the developed mixtures, particularly with respect to the dosage and type of fibers used. The target was to achieve a flow of 200 mm (7.87 in.). As reflected in Figure 11(a), this target flow was exceeded by all of the tested mixtures.

(a)

(b)
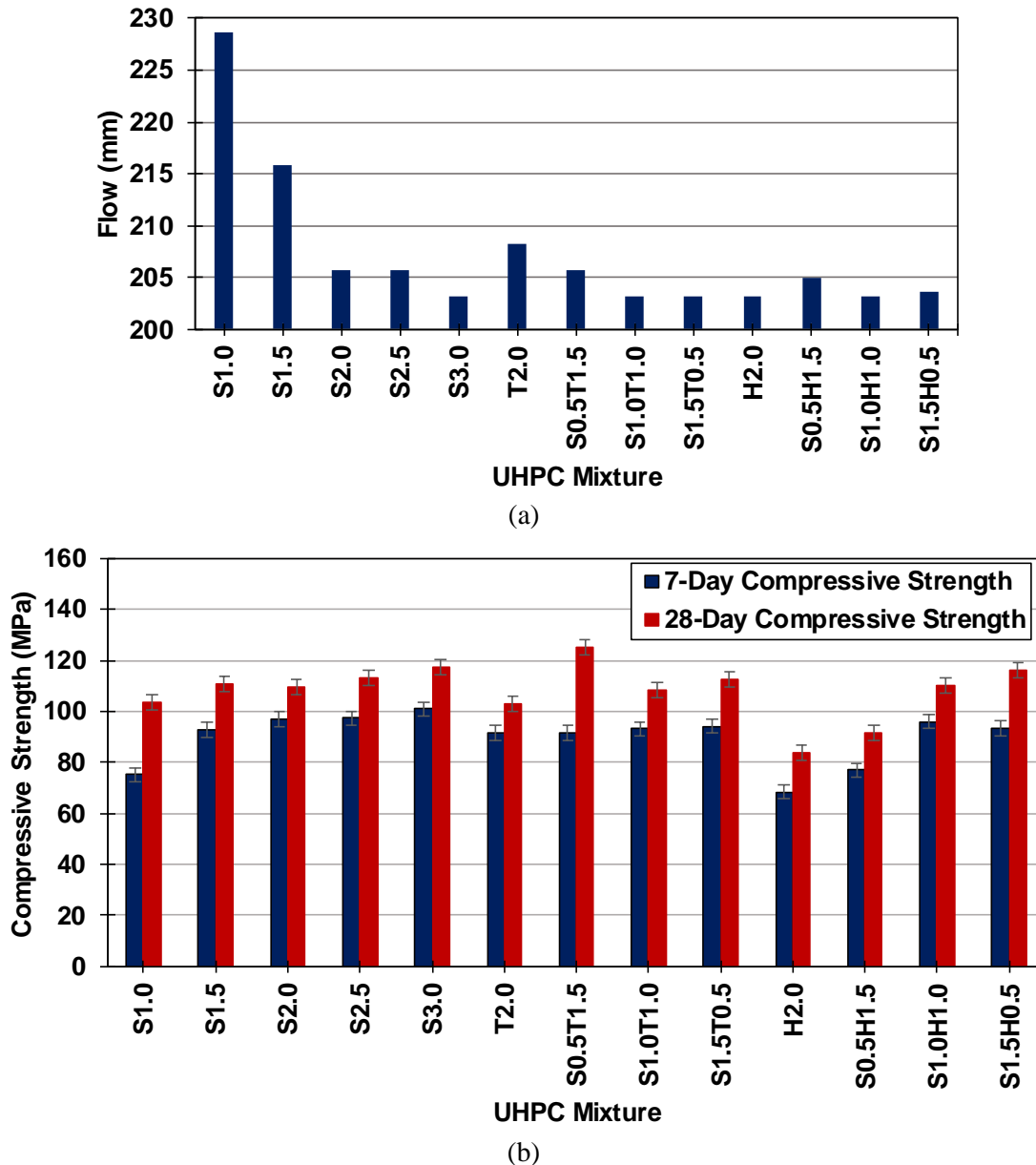
Figure 11. Comparison of (a) flow and (b) compressive strength (after 7 and 28 days) measured for the developed UHPC mixtures

This, however, resulted in a variation in the amount of superplasticizer required for each mixture. Consistent with the findings provided in Meng and Khayat (2018), the required amount of superplasticizer increased when increasing the dosage of fibers. The flow and required amount of

superplasticizer also changed when switching the type of fiber from straight to twisted wire and hooked fiber. This change remained marginal for the twisted wire fibers, mainly because of the similarity of the overall shape of the twisted wire fibers to the steel microfibers. The UHPC mixtures with the hooked fibers, however, needed a significantly greater amount of superplasticizer than the mixtures with the steel microfibers for the same dosage. This was further verified during the mixing process in the shear mixer. The hooked fibers agglomerated around the fins of the mixer, and their hooked ends entangled with each other.

Meng and Khayat (2018) reported a 60% increase in the need for superplasticizer after replacing steel microfibers with hooked fibers in the mixtures with a 2.0% fiber content. Consistent with that observation, the mixtures developed for this study were in need of 32% more superplasticizer (on average) when the hooked fibers were used.

Compressive strengths were measured after 7 and 28 days of curing. The average compressive strengths are shown in the previous Figure 11(b) for all of the tested mixtures. For the mixtures with microfibers, the compressive strength was consistently higher with increased fiber dosage. This result was in good agreement with the trends reported in the past studies, including Milan et al. (2016). The 7-day compressive strength for the mixtures with the steel microfibers and twisted wire fibers did not significantly vary. However, the 28-day compressive strength showed notable differences, with the S0.5T1.5 mixture providing the highest strength and the T2.0 mixture providing the lowest strength.

In the mixtures that contained both microfibers and hooked fibers, compressive strength was found to increase when increasing the ratio of microfibers to hooked fibers. The H2.0 mixture, which had no microfibers, showed the lowest compressive strength, while the S1.5H0.5 mixture showed the greatest compressive strength after both 7 and 28 days. Comparing the contribution of the two macrofibers, the mixtures that included twisted wire fibers consistently demonstrated a greater compressive strength than those with hooked fibers.

From a fundamental perspective, this can be attributed to the size of the fibers. The inclusion of fibers results in discontinuity in the homogeneous concrete mixture, leading to the formation of microcracks at the interface of the cementitious matrix and individual fibers. The size of such microcracks has been reported to be proportional to the size of the fibers (Hung et al. 2020).

The relatively low compressive strengths obtained for the T2.0 and H2.0 mixtures highlights the fact that the use of macrofibers alone does not provide a reliable alternative. A comparison of compressive strength changes from S1.0H1.0 to H2.0 indicates a reduction of 23% in the 28-day compressive strength. This compares well with Hung et al. (2020), which reported a 15% reduction in the 28-day compressive strength after adding 1.0% hooked macrofibers to the UHPC mixture.

3.4. Flexural Properties

3.4.1. Effects of Fiber Dosage on Flexural Strength and Toughness

The flexural responses of the developed mixtures were evaluated through a third-point bending test. The obtained load-deflection curves show an initial cracking point where the load-deflection relationship becomes nonlinear. After the first cracking point, strain hardening is noted, in which microcracks come together to form a macrocrack. This continues until the applied load reaches the peak load. In addition to the points associated with the first cracking strength and maximum flexural strength, ASTM 1609 recommends that flexural strength be evaluated at two additional points, deflections equal to L/600 and to L/150. These additional points help define the post-crack response.

Given the use of fiber-reinforced mixtures that are known to have superior flexural strength and post-crack response, an additional point at the deflection equal to L/100 was also considered, following the recommendation made by Kim et al. (2008 and 2011). This contributed to further evaluating the performance of the mixtures, and especially those with substantial ductility.

The maximum stresses at the points of first cracking, peak load, and vertical deflection equal to L/600, L/150, and L/100 are calculated using Equation 4:

$$f = \frac{PL}{bd^2} \qquad\qquad (4)$$

where P is the applied vertical load; L is the clear span length; and b and d are the width and depth of the beam's cross section, respectively. For the UHPC mixtures with steel microfibers, all of the mixtures showed a (relatively) ductile behavior with a deflection capacity beyond L/100 (3 mm [0.118 in.]), as reflected in Figure 12(a).

(a)

32

(b)
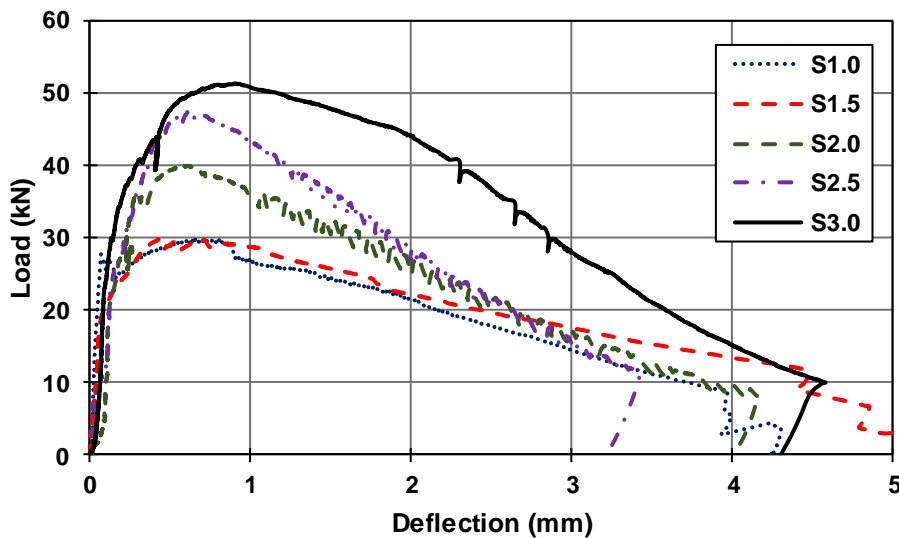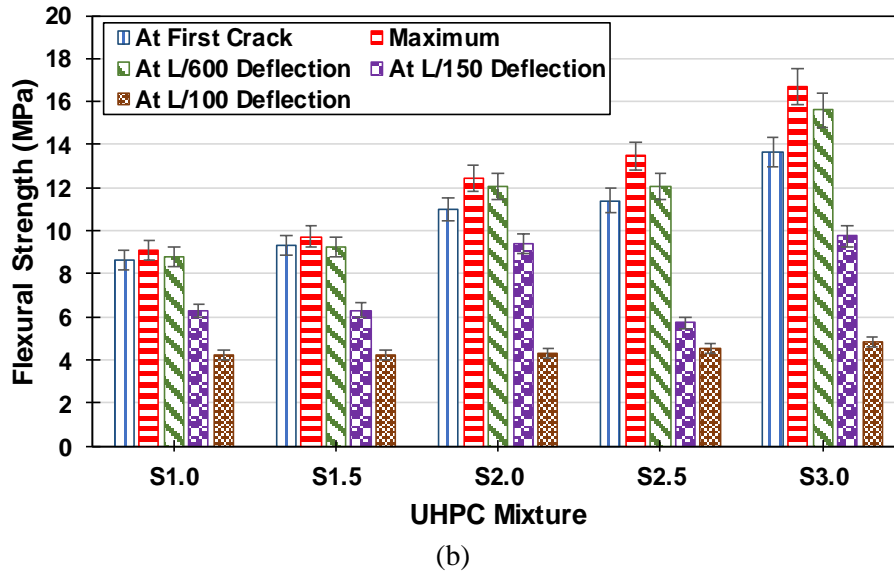
Figure 12. (a) Load-deflection curves and (b) flexural strengths of the UHPC mixtures made with various dosages of straight microfibers

The load-deflection curves show that, for the mixtures with a low steel fiber dosage (the S1.0 and S1.5 mixtures), a small sudden drop occurs as soon as the first crack is initiated, while the load-deflection curves for the other mixtures (S2.0, S2.5, and S3.0) exhibit a smooth transition from the linear to the nonlinear range. This observation can be attributed to the presence of fibers in the mixtures with a relatively high dosages of steel fibers, in which the microcracks were effectively bridged, and, thus, the onset of the macrocracks was delayed, as shown in the previous Figure 12(a). In particular, it was noted that, as the steel fiber dosage increased, the deflection recorded between the first cracking point and the point of peak load consistently increased.

The increased fiber dosage was also observed to result in an increase in the load associated with the first crack and the peak load. Specifically, the first cracking strength increased by 8%, 27%, 31%, and 58% for the steel dosages of 1.5%, 2.0%, 2.5%, and 3.0%, respectively, compared to the first cracking strength of the mixture with 1.0% steel microfiber. On the other hand, the maximum flexural strength increased by 7%, 37%, 48%, and 83% for the steel dosages of 1.5%, 2.0%, 2.5%, and 3.0%, respectively, compared to the maximum flexural strength of the mixture with 1.0% steel microfiber.

Following the procedure outlined in ASTM C1609, the residual strength was calculated at the beam deflections of L/600 (0.5 mm [0.020 in.]), L/150 (2.0 mm [0.079 in.]), and L/100 (3.0 mm [0.118 in.]). The residual strength at the L/600 deflection was almost equal to that obtained at the peak load for the S1.0 mixture, but the difference between the maximum flexural strength and the residual strength at the L/600 deflection started to emerge as the steel fiber dosage was increased (previous Figure 12(b)).

The increase in the residual strength by increasing the fiber dosage was further pronounced at the L/150 deflection, i.e., by 49% from the S1.0 to the S2.0 mixture and by 71% from the S2.0 to the S3.0 mixture. The sensitivity of the residual strength to the fiber dosage, however, decreased at the L/100 deflection, in which the percentage of increase remained under 5% by changing the fiber dosage from 1.0% to 2.0% and from 2.0% to 3.0%.

The energy absorption capacity was also obtained by finding the area under each load-deflection curve. This area, which is often referred to as toughness, was evaluated at three deflection points: L/600, L/150, and L/100. The first two points were recommended by ASTM C1609, while the third point was added to obtain a holistic perspective. As summarized in Figure 13, the toughness at the L/600 deflection increased by up to 46% when increasing the steel fiber dosage.
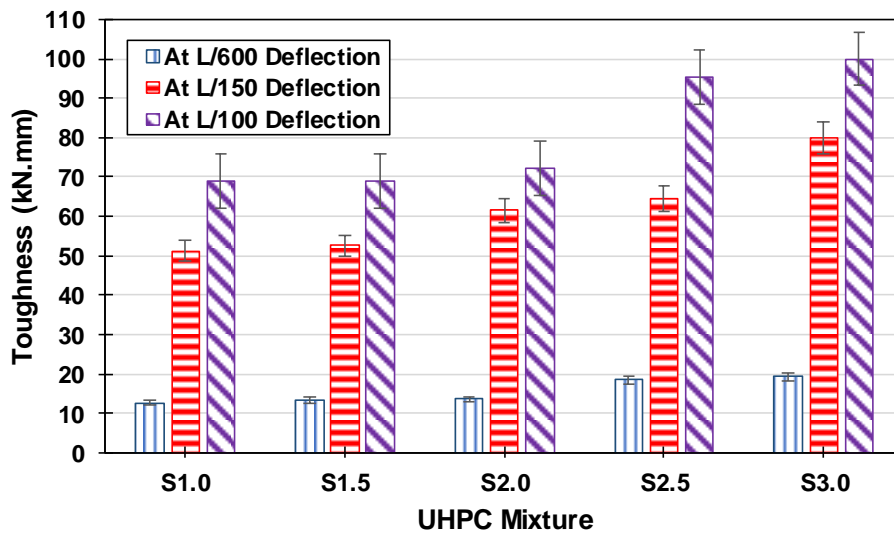
Figure 13. Comparison of the toughness calculated at the vertical deflections of L/600, L/150, and L/100 for the UHPC mixtures made with various dosages of straight microfibers

This increase, however, slowed down in the mixtures with a steel fiber dosage beyond 2.0%. Similarly, the toughness at the L/150 and L/100 deflections increased (up to 30% and 38%, respectively), highlighting the important role of fibers in bridging microcracks.

3.4.2. Effects of Fiber Type on Flexural Strength and Toughness

Further on the fiber dosage, the shape and size of the steel fibers are known to contribute to the flexural strength and toughness of UHPC mixtures. In this study, the flexural performance of the UHPC mixtures with two types of macrofibers, twisted wire and hooked, were evaluated separately and in combination with steel microfibers. For this purpose, the points associated with first cracking, peak load, and vertical deflection equal to L/600, L/150, and L/100, were extracted from the load-deflection curves. Figure 14(a) shows the load-deflection curves for the mixtures that contained twisted wire fibers.
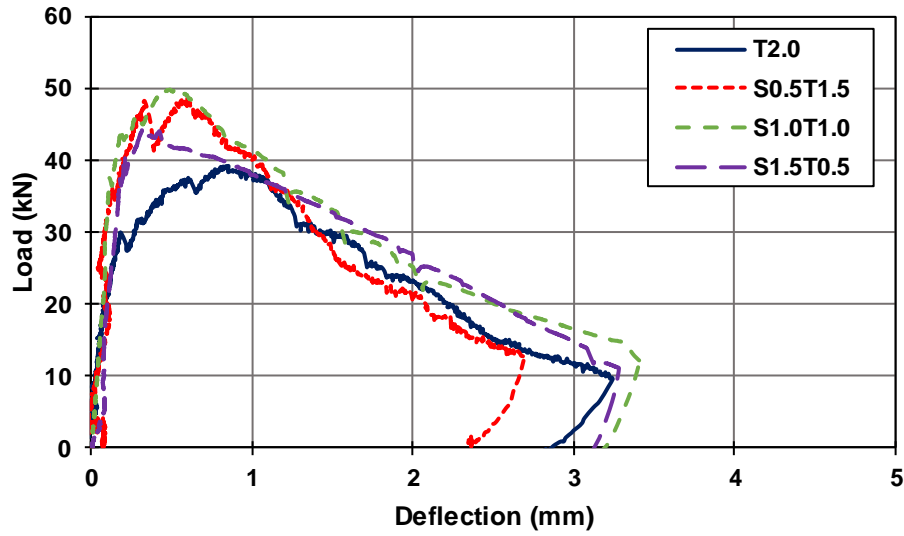
(a)
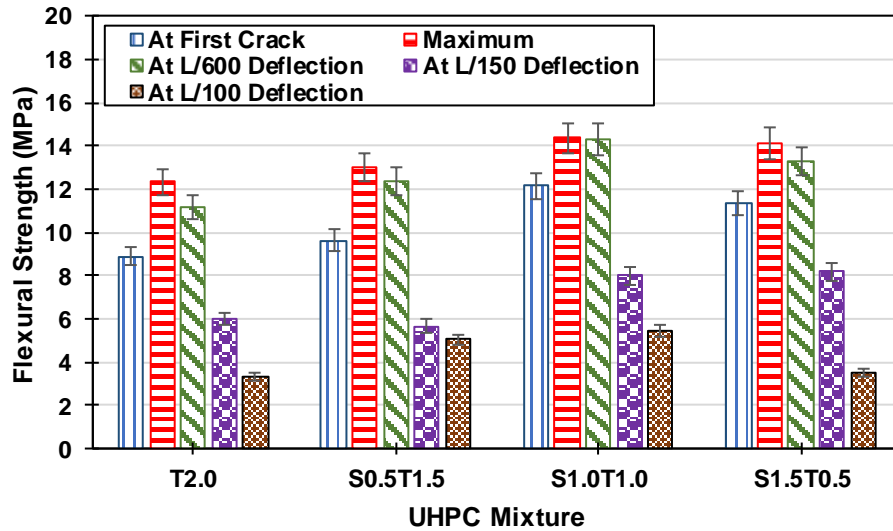
(b)

**Figure 14. (a) Load-deflection curves and (b) flexural strengths of the UHPC mixtures made with a combination of straight microfibers and twisted wire fibers**

A key characteristic of the load-deflection curves obtained for this set of UHPC mixtures is the notable drop in the load carrying capacity after the initiation of the first crack. All of the mixtures, however, experienced strain hardening, leading to a peak load higher than that recorded at the first crack. Such an observation highlights how the twisted wire fibers can contribute to bridging the initial cracks and improving the overall flexural capacity. In particular, this contribution originates from the twisted shape of the mixed fibers, which provide an additional bond with the concrete matrix, resisting the fiber pullout.

From the strain hardening obtained after the initial drop, it can be inferred that the twisted wire fibers start to get engaged as the applied load increases. The load associated with the first crack

and the peak load were both found to increase when increasing the straight microfiber dosage up to 1.0%. The highest peak load was recorded for the S1.0T1.0 mixture, while the S0.5T1.5 and S1.5T0.5 mixtures provided a slightly lower flexural capacity than the S1.0T1.0 mixture. Comparing the S1.0T1.0 to the S2.0 mixture, it was noted that the first cracking load and the peak load were 11% and 15% higher in the S1.0T1.0 mixture than the S2.0 mixture. This reflected the superior crack bridging capacity of the twisted wire fibers. The inclusion of twisted wire fibers at the dosages of 1.5% and 2.0%, however, reduced the first cracking load and the peak load below those obtained for the mixture with 2.0% straight microfiber. This was because of the reduction in the availability of microfibers to bridge the microcracks. Thus, the microcracks came together to form a macrocrack, which reduced the capacity to carry additional loads.

To understand the role of twisted wire fibers in controlling the crack widths during the post-cracking response, the residual strengths at the L/600, L/150, and L/100 deflections were also determined (previous Figure 14(b)). This figure shows that the residual strengths recorded at the target deflections follow the same trend with the highest values for the S1.0T1.0 mixture and the lowest values for the T2.0 mixture. In general, the straight microfibers were found to strengthen the concrete matrix and help with bridging the cracks, while the twisted wire fibers weakened the concrete matrix but provided superior crack bridging ability. Thus, the S1.0T1.0 mixture, which had a balanced combination of both fiber types, provided the best results.

For the mixtures that contained hooked fibers, Figure 15 shows all of the recorded load-deflection curves.

(a)

36
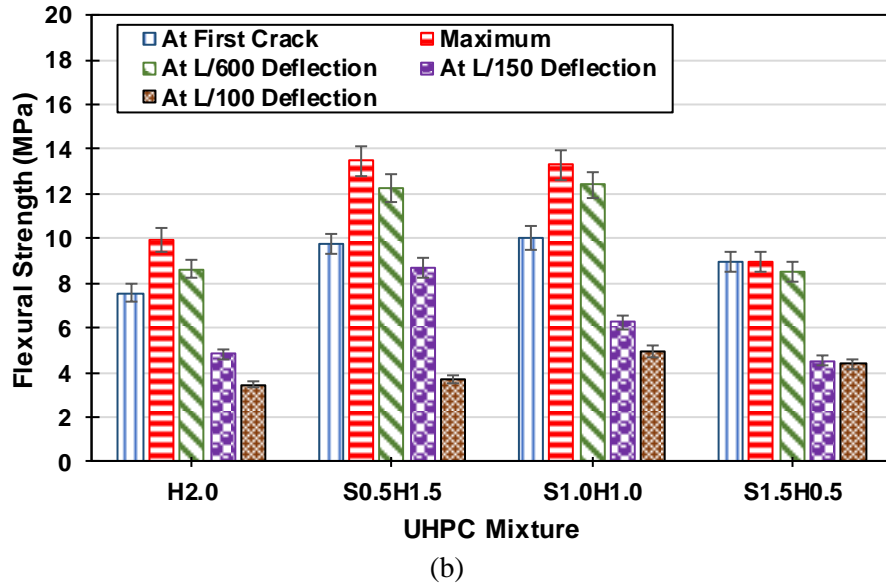
Figure 15. (a) Load-deflection curves and (b) flexural strengths of the UHPC mixtures made with a combination of straight microfibers and hooked fibers

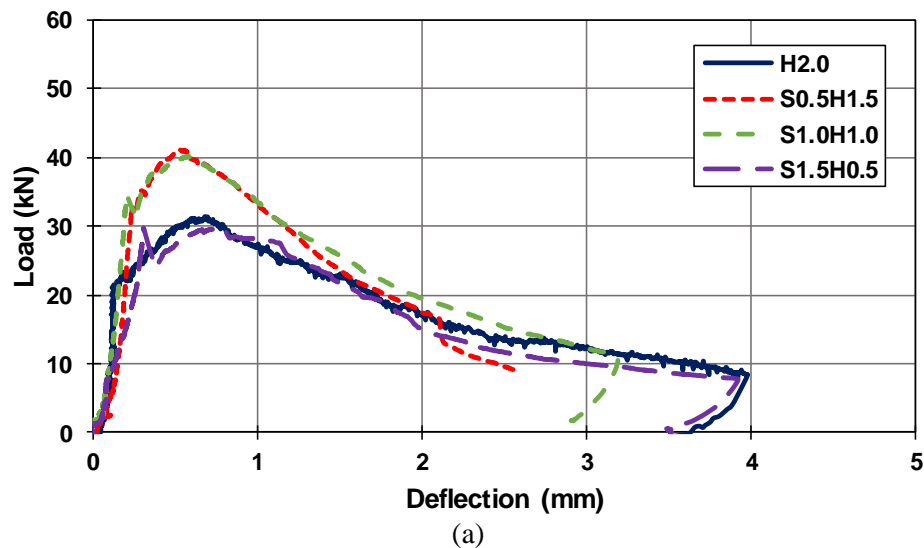The first cracking point is clearly reflected in the curves, followed by a small drop in the load and then a strain hardening region before the peak load is reached. The addition of hooked fibers to the UHPC mixtures was found to lower the load required to form the first cracks, compared to the UHPC mixture made with 2.0% straight microfiber. The peak load, however, was higher than that recorded for the S2.0 mixture. This highlighted the combined contribution of straight microfibers and hooked fibers to delaying crack formation.

The S0.5H1.5 mixture provided the highest flexural strength. The maximum strength was observed to decrease for the UHPC mixtures that contained a lower and a higher dosage of hooked fibers, although the S1.0H1.0 combination resulted in a strength very close to that obtained for the S0.5H1.5 combination. The S1.5H0.5 mixture resisted the same load at the first crack and at the peak. This further explained the crack bridging ability of the hooked fibers and the importance of their dosage.

The residual strength of the S0.5H1.5 mixture at the L/150 deflection is almost the same as that of the S2.0 mixture, while the other mixtures that contained hooked fibers provided lower residual strengths. This trend is reversed for the residual strengths at the L/100 deflection, in which the UHPC mixtures that contained hooked fibers provided a residual strength equal to or higher than that of the S2.0 mixture. This indicated the role of the hooked fibers to bridge the cracks at the later stages of loading, primarily because of their shape. The hook at the two ends of each fiber helps anchor the fiber to the concrete matrix, resisting the possible slippage of the fiber, even if the bond with the surrounding concrete is lost. This is in complete agreement with the findings reported by Park et al. (2012) and Meng and Khayat (2018).

A review of the results obtained for both twisted wire fibers and hooked fibers showed that the use of macrofibers increased the toughness of the UHPC mixtures. Figure 16 provides the

37

toughness for all of the mixtures that contained twisted wire and hooked fibers at the deflections of L/600, L/150, and L/100.
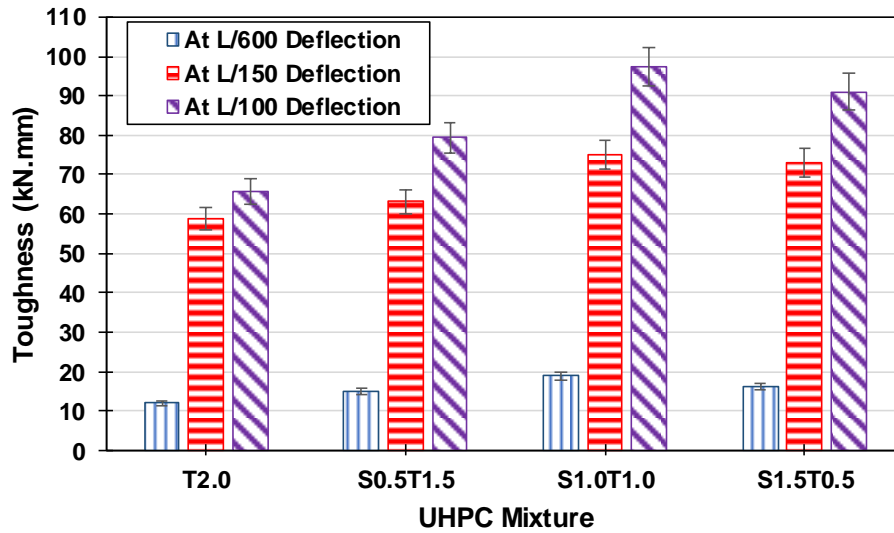
(a)
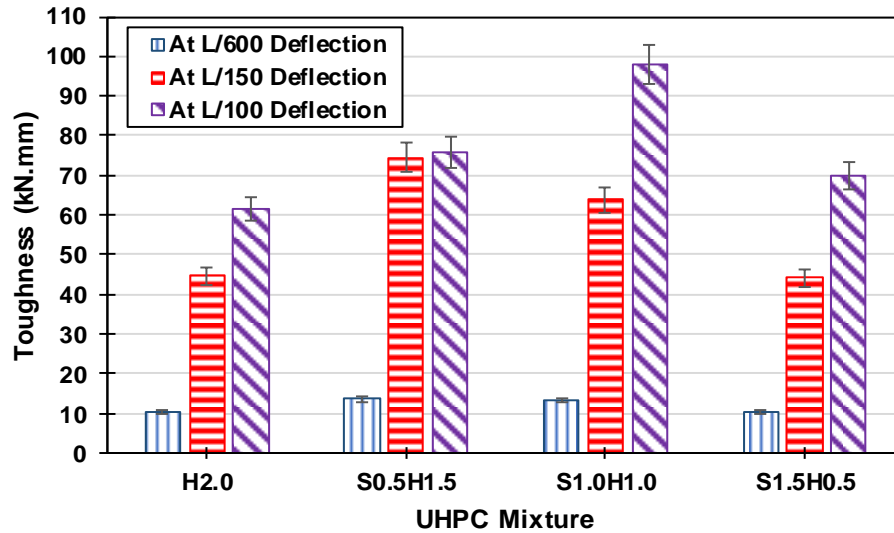
(b)

Figure 16. Comparison of toughness calculated at the vertical deflections of L/600, L/150, and L/100 for UHPC mixtures with a combination of (a) straight microfibers and twisted wire fibers and (b) straight microfibers and hooked fibers

For the mixtures with a hybrid of straight microfibers and twisted wire fibers, the toughness is highest in the S1.0T1.0 mixture and lowest in the T2.0 mixture. The toughness values calculated for the S0.5T1.5, S1.0T1.0, and S1.5T0.5 mixtures were consistently higher than those obtained for the S2.0 mixture and lower than those obtained for the T2.0 mixture at all three deflections. This highlighted the importance of wire fibers in limiting the crack width and increasing the energy absorption capacity of the UHPC mixtures.

The toughness results for the mixtures with a hybrid of straight microfibers and hooked fibers showed that the S0.5H1.5 mixture provided the best performance. Compared to the S2.0 mixture, the S0.5H1.5 mixture delivered a similar toughness at the L/600 deflection and an increase of 21% and 5% at the L/150 and L/100 deflections, respectively. A similar observation was made for the S1.0H1.0 mixture, in which the toughness values recorded at the L/150 and L/100 deflections exceeded those obtained for the S2.0 mixture. This reflected the crack bridging and energy absorption capacity of the hooked fibers.

3.5. Digital Image Correlation

The DIC technique was employed to use the series of images taken during the flexural tests for the purpose of evaluating the displacements and strains experienced by the UHPC beam specimens. The post processing of the DIC results was also performed to calculate the crack widths. A two-step preparation procedure was adopted in this part of the study.

In the initial step, the surfaces of the UHPC beam specimens were covered with a white paint and left to dry for three hours. In the second step, the dried white surfaces were sprayed with a black paint to make a pattern of black speckles on the surfaces. The specimens were then left to dry for another hour. Upon recording the entire loading process to capture all the stages of cracking, the obtained videos were split into a series of images. The images were processed using Ncorr, which is an open-source digital image correlation program developed in MATLAB. The program detected the positions of individual points, along with their displacements and strains. The displacement results were then processed to determine the crack width along the depth of each UHPC beam specimen.

The images obtained for the S2.0, T2.0, and H2.0 mixtures are presented in Figures 17 through 19 at six instances. The instances were selected at (a) vertical load of 15 kN, under which none of the UHPC mixtures began cracking, (b) first cracking load, (c) peak strength, (d) deflection of L/600, (e) deflection of L/150, and (f) deflection of L/100. Each instance shows the normal strain in the longitudinal direction to capture the crack formation and propagation along the length of the UHPC beam specimen.
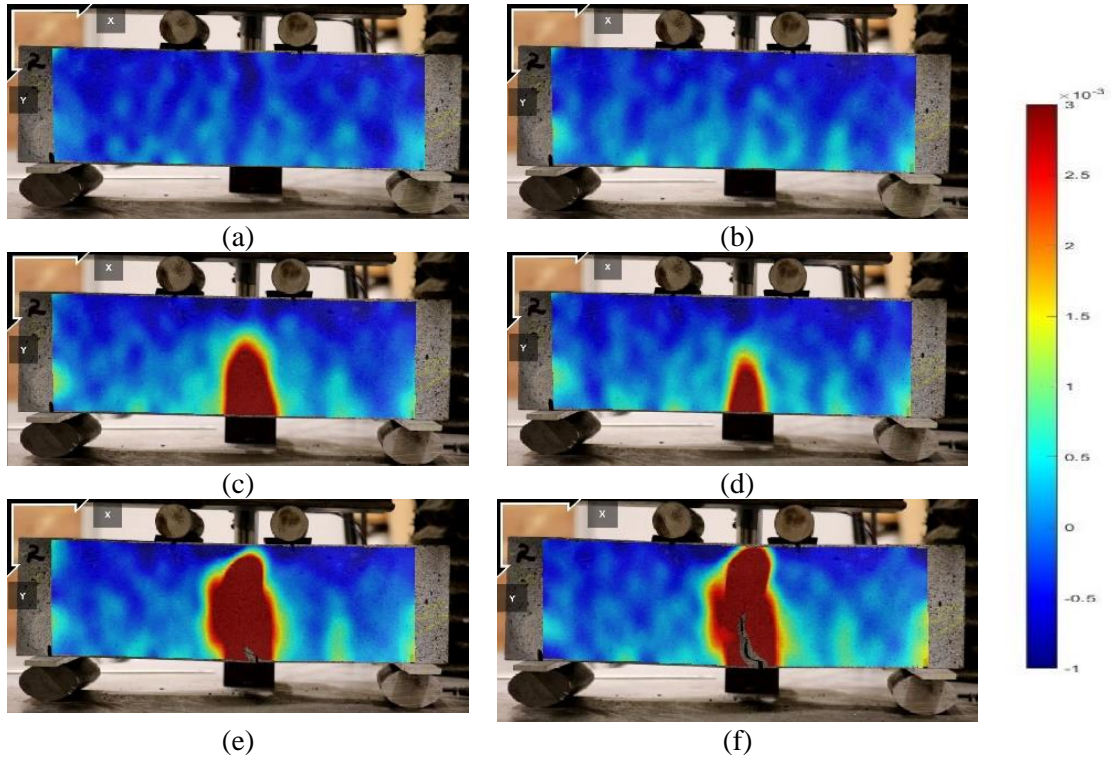
Figure 17. Longitudinal strain distribution obtained for the S2.0 mixture at (a) vertical load of 15 kN, (b) first cracking load, (c) peak load, (d) deflection of L/600, (e) deflection of L/150, and (f) deflection of L/100
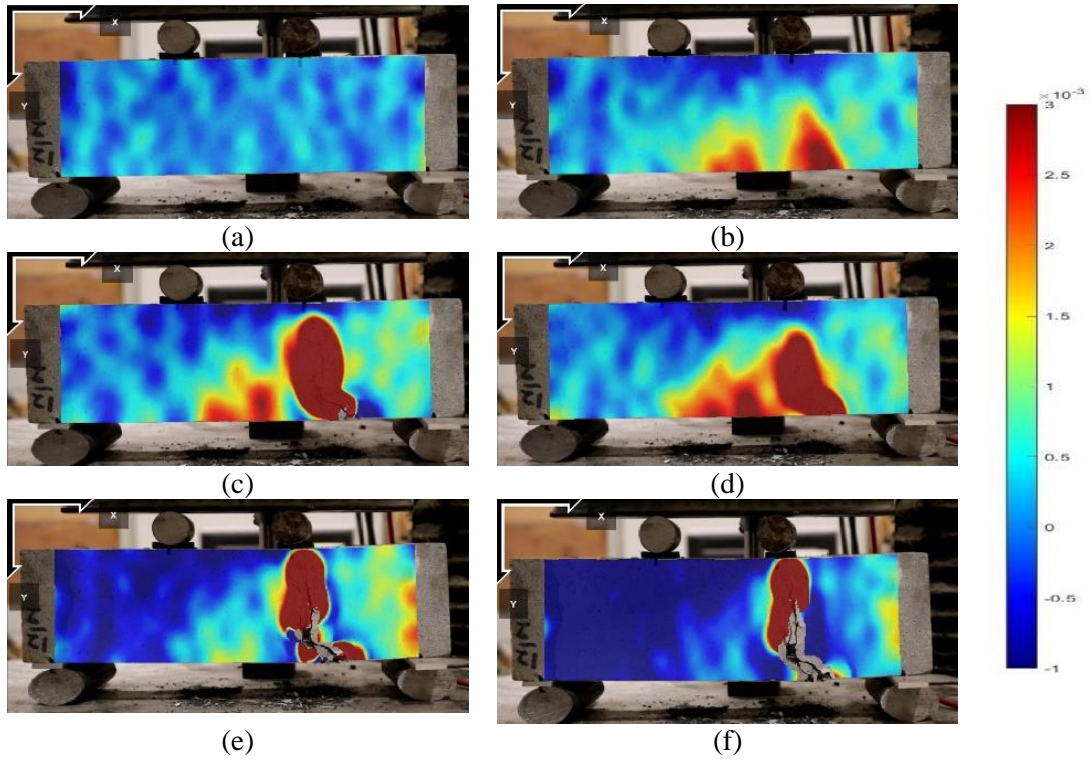
Figure 18. Longitudinal strain distribution obtained for the T2.0 mixture at (a) vertical load of 15 kN, (b) first cracking load, (c) peak load, (d) deflection of L/600, (e) deflection of L/150, and (f) deflection of L/100
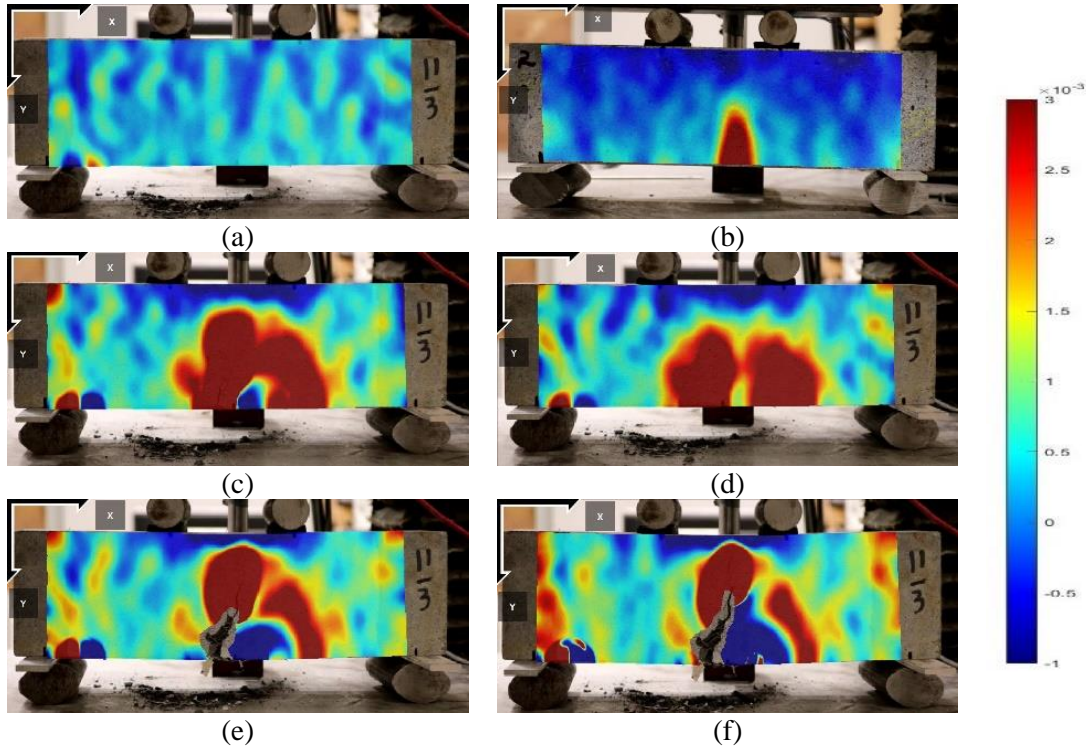
Figure 19. Longitudinal strain distribution obtained for the H2.0 mixture at (a) vertical load of 15 kN, (b) first cracking load, (c) peak load, (d) deflection of L/600, (e) deflection of L/150, and (f) deflection of L/100

Overall, the strains remained relatively low in the S2.0 mixture until the microcracks were observed. On the other hand, the T2.0 and H2.0 mixtures started experiencing relatively high strains even under the vertical load of 15 kN. A close observation of the strain distributions in the three tested mixtures showed that the S2.0 mixture underwent high strains only at one region, where the cracks also began to form. However, the T2.0 and H2.0 mixtures have multiple high strain regions, reflecting the possibility of multiple cracks and the ability of macrofibers to further distribute the loading demand in the UHPC beam specimens.

Referring to Figure 19(f), multiple cracks (and also spalling) can be noted in the T2.0 mixture under the vertical deflection of L/100. The cracks in the H2.0 mixture remained similar to those recorded in the T2.0 mixture, but they showed a wide opening once they started forming.

A comparison of the maximum crack widths obtained from DIC for the S2.0, T2.0, and H2.0 mixtures at the vertical deflections of L/150 and L/100 is presented in Figure 20.
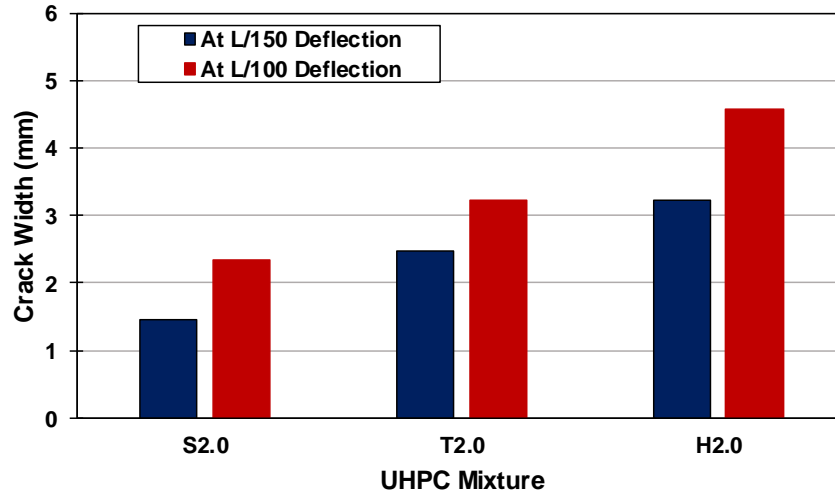
Figure 20. Comparison of maximum crack widths obtained from DIC for the S2.0, T2.0, and H2.0 mixtures under vertical deflections of L/150 and L/100

The comparison shows that the S2.0 mixture experienced the lowest crack width, while the H2.0 mixture underwent the greatest crack width for both deflections. This was an important observation, reflecting that, under the same vertical deflection, the straight microfibers provided better performance in controlling the crack width than the twisted wire and hooked macrofibers. The reported observation was completely in line with the results obtained for flexural strength, where the H2.0 mixture showed the lowest flexural strength, while the S2.0 mixture provided the greatest flexural strength. The results obtained for the crack width through the depth of the UHPC specimens further supported the reported findings, as the H2.0 mixture consistently had the widest cracks and the S2.0 mixture had the narrowest cracks at similar depths.

To quantify the extent of crack propagation in the tested UHPC beam specimens, the crack width profiles were determined throughout the depth of each specimen at the end of the loading process. Figure 21(a) presents the results for the UHPC mixtures with the five dosages of straight microfibers.

(a)

(b)

(c)
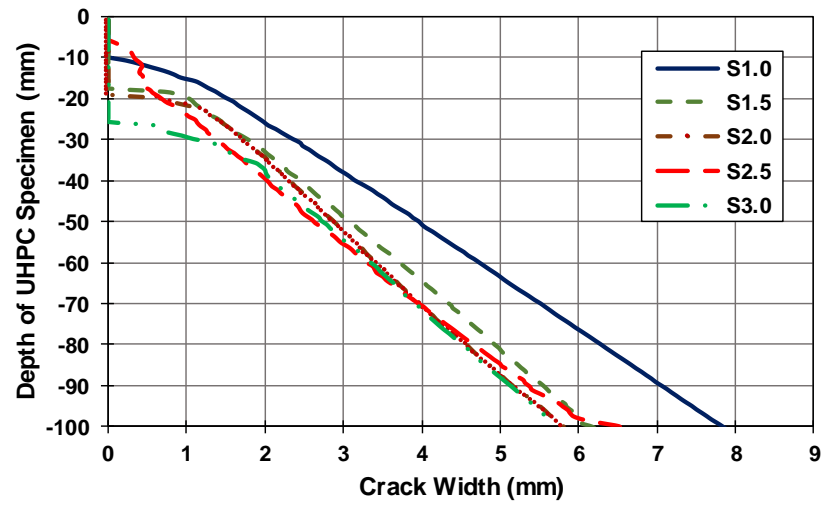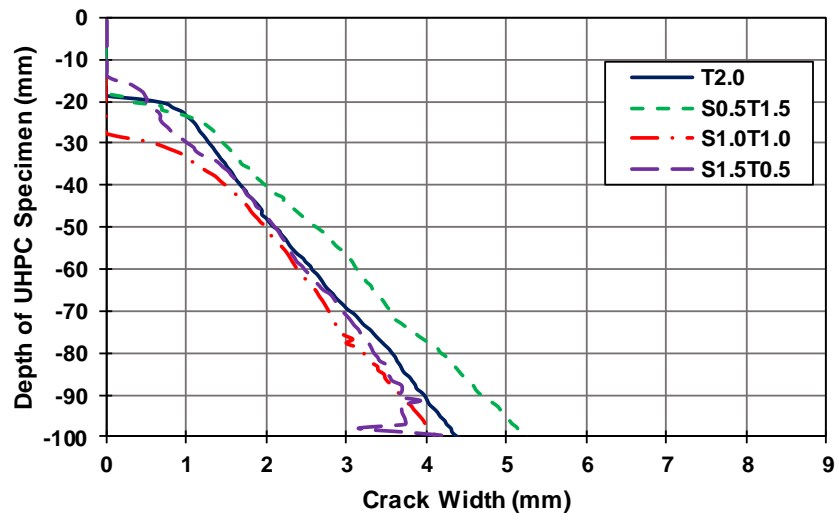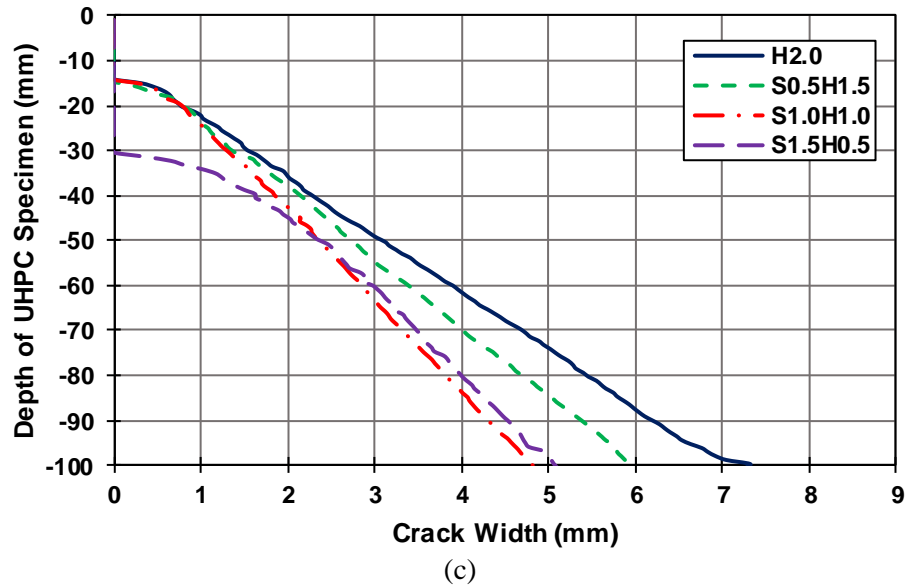
Figure 21. Comparison of crack width profiles for UHPC mixtures with (a) various dosages of straight microfibers, (b) combination of straight microfibers and twisted wire fibers, and (c) combination of straight microfibers and hooked fibers

Crack width was observed to decrease when increasing the steel fiber dosage. In the UHPC mixture with a steel fiber dosage of 3.0%, the crack was found to stop at 25 mm (1 in.) from the top surface. However, in the UHPC mixture with a steel fiber dosage of 1.0%, the crack extended until 10 mm (0.039 in.) from the top surface of the specimen. This clearly highlights the role of steel microfibers in limiting cracks.

The previous Figure 21(b) presents the crack width comparison for the UHPC mixtures that contained a combination of straight microfibers and twisted wire fibers. The comparison showed that the S1.0T1.0 mixture had the lowest crack width, while the S0.5T1.5 mixture experienced the largest crack width after the loading stopped. It can also be observed that the crack extension stopped at 30 mm (1.81 in.) and 20 mm (0.79 in.) from the top surface of the S1.0T1.0 and S0.5T1.5 mixtures, respectively.

The crack width along the depth was investigated also for the UHPC mixtures made with a combination of straight microfibers and hooked fibers. As reflected in the previous Figure 21(c), the S1.5H0.5 and S1.0H1.0 mixtures showed the narrowest crack widths, while the H2.0 mixture experienced the widest crack width. The crack extended until 15 mm (0.59 in.) from the top surface of the H2.0 mixture, while the S1.5H0.5 mixture was able to stop the crack at the depth of 31 mm from the top surface. A comparison of the crack widths obtained for the mixtures made only with steel microfibers and the mixtures made with a hybrid of micro- and macrofibers showed that all the latter mixtures experienced crack widths narrower than those recorded in the former mixtures. This highlights how a combination of micro- and macrofibers can deliver enhanced flexural properties without requiring an increase of the total dosage of steel fibers.

3.6. Main Findings

This study explored the effects of various dosages, shapes, and sizes of steel fibers on the flexural response characteristics of UHPC. The dosage of steel microfibers was varied from 1.0% to 3.0% (with increments of 0.5%). Two mixtures were prepared using two macrofibers, twisted wire and hooked, without any microfibers. Upon understanding the main characteristics of the UHPC mixtures made with either micro- or macrofibers, an additional six UHPC mixtures were prepared using various combinations of the micro- and macrofibers. The mixtures were tested for their workability, compressive strength, and flexural strength, while detailed DIC analyses were conducted in parallel. The following findings and conclusions were drawn from this study:

- The flow of the UHPC mixtures was found to be affected by changing the dosage of steel microfibers and the type of macrofibers used in the developed mixtures. To obtain a target flow of at least 200 mm (7.87 in.), the required amount of superplasticizer had to be increased when increasing the microfiber dosage. The increase in the use of superplasticizer exceeded 20% when the microfiber dosage changed from 1.0% to 3.0%. For the UHPC mixtures with macrofibers, the demand for the superplasticizer was the greatest for the mixtures with the hooked fibers, while the mixtures with the twisted wire fibers required the same amount of superplasticizer as that used in UHPC mixtures with microfibers. Overall, workability was found to be the best in UHPC mixtures with steel microfibers, followed by those with twisted wire fibers. The hooked fibers were found to be the most difficult fibers to mix.

- Compressive strengths after 7 and 28 days consistently increased when increasing the dosage of straight microfibers. In particular, an increase of 34% and 12% were observed in the 7-day and 28-day compressive strengths after an increase of straight microfibers from 1.0% to 3.0%, respectively. Investigations on the effects of fiber dosage on flexural strength and toughness of the developed UHPC mixtures indicated that increasing the dosage of steel microfibers helps with both pre- and post-cracking response, despite introducing potential workability issues. An increase of the microfiber dosage from 1.0% to 3.0% resulted in a 58% and 84% increase in the first cracking strength and maximum flexural strength, respectively. Similarly, the toughness at L/600, L/150, and L/100 increased by 53%, 56%, and 45%, respectively, when the microfiber dosage changed from 1.0% to 3.0%. The mixtures that contained only macrofibers (i.e., the T2.0 and H2.0 mixtures) resulted in the lowest flexural strengths and toughness among all of the UHPC mixtures tested. This was attributed to the fact that macrofibers weaken the concrete matrix, and, thus, adversely affect the strength and toughness properties.

- The combination of straight microfibers and twisted wire fibers resulted in the best first cracking strength and maximum flexural strength for the S1.0T1.0 and S1.5T0.5 mixtures. These mixtures also achieved higher residual strengths at the L/600, L/150, and L/100 deflections, compared to the S2.0 mixture. A similar trend was observed for toughness. The toughness values obtained for all of the mixtures with a hybrid of straight microfibers and twisted wire fibers were greater than those recorded in the mixtures with only microfibers.

This successfully captured the increased role of macrofibers in the post-cracking response of UHPC specimens.

- In the mixtures that contained hooked fibers, the S0.5H1.5 mixture provided the highest first cracking strength, maximum flexural strength, and toughness at the L/600, L/150, and L/100 deflections. The strength and toughness, however, dropped when the ratio of straight microfibers and hooked fibers was changed. Despite the reported drop, the toughness values obtained at the L/600, L/150, and L/100 deflections were still higher than those recorded for the S2.0 mixture. This highlighted how macrofibers contribute to the improvement of post-cracking flexural capacity, especially if a proper dosage is used.

- The DIC analyses provided original insight into the role of fibers to limit the cracks in the UHPC specimens. By measuring the strain and displacement distributions, both the widths and depths of the cracks were systematically quantified as a function of the applied load. The mixtures with a combination of micro- and macrofibers were found to provide a superior flexural response, characterized by narrow crack widths and limited propagation of cracks into the depth. This reflected the importance of utilizing both micro- and macrofibers in UHPC mixtures. While the microfibers were found to play an important role in delaying microcracks, thus strengthening the concrete matrix, macrofibers were determined to be critical in bridging macrocracks, thus improving the post-cracking flexural response of the UHPC specimens.

4. UHPC MADE WITH A HYBRID OF SYNTHETIC AND STEEL FIBERS

4.1. Introduction

UHPC has been considered a material of choice for a variety of structural engineering applications. Among UHPC's superior properties, flexural strength and ductility are known to primarily originate from the presence of steel fibers in the UHPC mixture. The inclusion of steel fibers, however, constitutes almost a third of the cost of UHPC products, while the availability of steel fibers has posed practical challenges. To address these issues, the use of synthetic polymer- and glass-based fibers, as a partial replacement of steel fibers, has been deemed promising. The advantages of such fibers include their light weight, cost-effectiveness, corrosion resistance, and production convenience. In addition, the use of synthetic fibers is largely popular for fiber-reinforced concrete (FRC) and engineered cementitious concrete (ECC) products, helping the concrete industry utilize the wealth of fundamental knowledge and practical experience accumulated to date toward using synthetic fibers in UHPC applications.

The use of synthetic fibers in UHPC is still a new topic and only limited literature is available on the effect of different types of fibers on the UHPC's fresh and hardened properties. Among the existing studies, polyethylene fibers were evaluated by Zhou et al. (2018) as a partial replacement for steel fibers in UHPC. The study found that increasing the percentage of polyethylene fibers results in a reduction in the compressive strength, but it can be helpful in improving the flexural strength and strain hardening properties of the mixtures.

In a study not related to UHPC, Ozsar et al. (2017) examined the distribution of a hybrid of high-density polyethylene (HDPE) and nylon fibers in self-compacting concrete (SCC). The study reported that, although the fiber addition did not have any pronounced effect on the compressive strength of the developed mixtures, the flexural strength properties, in both pre- and post-crack stages, were affected, depending on the type of polymer fiber employed. In particular, nylon fibers had a notable positive effect on the pre-crack stage compared to HDPE fibers.

Polypropylene (PP) fibers have been considered for UHPC, mainly because of their capability to serve as a sacrificial material during fire, as PP fibers have a melting point lower than that of steel fibers (Tahwia 2017). In a separate study conducted by Chen et al. (2020), it was confirmed that PP fibers melt earlier than steel fibers under high temperatures. This provided alternate channels that helped reduce the internal vapor pressure, and thus, maintained a residual strength, reducing the risk of structural failure under fire. Abid et al. (2019) and Hager et al. (2009) also found PP fibers effective in preventing the spalling of reactive powder and fiber reinforced concrete at high temperatures.

From the perspective of mechanical properties, PP fibers have shown great promise in FRC and ECC applications (Deb et al. 2018). For UHPC products, Christ et al. (2019) explored a hybrid use of PP and steel fibers. The total fiber dosage was kept at 3.0%. The prepared mixtures were tested for compressive and tensile strengths. The flexural strength tests were also carried out on relatively small beams with the dimensions of 44.5 mm×44.5 mm×160 mm (1.75×1.75×6.30

in.). The researchers found that the mixtures made with hybrid fibers provided a high load carrying capacity compared to the mixtures made with only PP fibers.

Smarzewski and Barnat-Hunek (2017) investigated the effect of a low dosage of PP fibers (less than 1.0%) mixed with steel fibers on UHPC's flexural properties. The test results showed that the addition of PP fibers reduced the compressive strength, but flexural strength remained almost the same in the mixtures that contained PP fibers only. However, the combination of PP and steel fibers greatly improved both flexural strength and the post-crack response of the developed UHPC mixtures. The 50/50 combination of PP and steel fibers showed the greatest increase in flexural strength (38%) as compared to that for the UHPC mixtures that had no fibers.

PVA fibers have received growing attention because of their light weight, high tensile strength, and low cost. Meng and Khayat (2018) investigated the use of PVA fibers, along with steel fibers, in UHPC. It was reported that the addition of PVA fibers by 0.5% required a 25% increase in the HRWR admixture, mainly because of the water absorption characteristics of this type of fiber. In this study, higher dosages of PVA fibers were also attempted but not pursued further because of the significant reduction in flow. A combination of PVA and steel fibers with the total fiber dosage of 2.0% was found to result in the maximum flexural properties.

Alkali-resistant (AR) glass fibers have been effectively incorporated into FRC products for structural engineering applications (Dopko et al. 2018, Karim and Shafei 2021). The use of AR glass fibers can also be promising for UHPC products, primarily because of their corrosion resistance and ability to bridge microcracks in the initial stages of cracking (Holubova et al. 2017). While there has been no study on the flexural behavior of UHPC mixtures made with AR glass fibers, the glass fibers have been considered for architectural UHPC panels (Chen and Challivard 2012, Tomas et al. 2015).

Carbon fibers are also finding their applications in UHPC products, especially in the form of nanotubes and microfibers. The carbon nanotubes have been explored mainly for conductive and electromagnetic shielding applications (Sbia et al. 2014, Lee et al. 2018, Jung et al. 2020). Meng and Khayat 2016 investigated the effects of carbon nano fillers (CNFs) in conjunction with steel fibers on the four-point bending behavior of a set of UHPC beams. A 0.3% addition of CNFs (with a length of 50 mm [2 in.] to 200 mm [8 in.]) resulted in a significant improvement in the flexural strength and toughness of the UHPC mixtures.

Sahmenko et al. (2015) studied a combination of carbon microfibers (with a length of 12 mm [0.5 in.]) and steel microfibers (with a length of 30 mm [1.18 in.]). Under a three-point bending test, the study reported that the addition of 2.0% carbon fibers improved the flexural strength by 28%, the addition of 2.0% steel fibers improved the flexural strength by 139%, and the addition of 1.0% carbon and 1.0% steel fibers improved the flexural strength by 189%, compared to the mixture that contained no fibers.

Despite the past studies on various synthetic fibers, there was a gap in the body of knowledge concerning how such fibers are compared in UHPC applications. This motivated this stage of the

project to perform a detailed investigation into a diverse set of synthetic fibers, focusing on their contributions to the flexural response of UHPC.

The synthetic fibers of choice included nylon, PP, PVA, AR glass, and carbon fibers. Despite variations in their lengths, the synthetic and steel fibers considered for the current study can all be categorized as straight fibers. For each fiber type, three mixture designs were developed, covering different combinations of synthetic and steel fiber dosages, including 0.5% steel with 1.5% synthetic, 1.0% steel with 1.0% synthetic, and 2.0% steel with 1.0% synthetic fibers.

Given that the addition of synthetic fibers can directly influence the UHPC's flow and strength properties, the research team performed the necessary tests to measure the flow, compressive strength, and flexural strength of the developed UHPC mixtures. The flexural test results were further supported by DIC analyses to further understand the flexural response of the UHPC mixtures that contained various types and dosages of fibers. The strain distribution and crack width data obtained from DIC was found especially helpful in providing a fundamental understanding of fiber contribution to various stages of loading.

The outcome of this effort provided a side-by-side comparison of the main flexural properties of the UHPC specimens made with various polymer- and glass-based fibers. This can greatly facilitate deciding on the fiber types that can partially replace steel fibers, to not only introduce cost-saving advantages but also address the issues associated with the possible shortage of steel fibers.

4.2. Materials, Testing Matrix, and Test Plan

The materials used for the mixtures investigated in this stage of the research were similar to those reported in Chapters 2 and 3. The materials included ordinary portland cement, regular sand, masonry sand, silica fume, and an HRWR admixture. The regular sand had the maximum size of less than 0.6 mm (0.0236 in.). As for fibers, in addition to steel fibers, five other types of fibers, nylon, PP, PVA, AR glass, and carbon, were considered (see Figure 22).

(a)   (b)

(c)   (d)

(e)   (f)
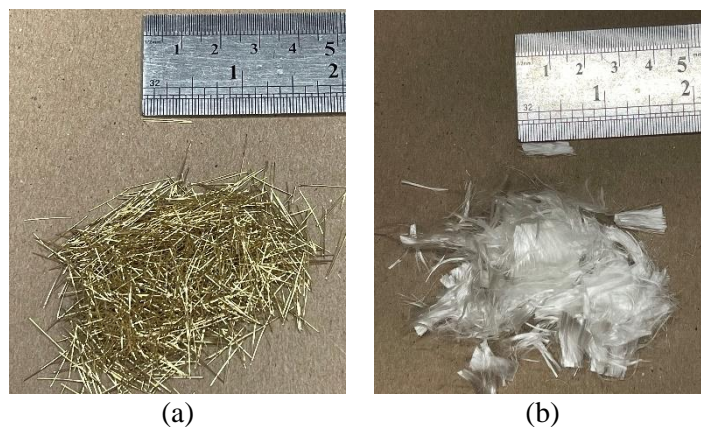
Figure 22. (a) Steel, (b) nylon, (c) PP, (d) PVA, (e) AR glass, and (f) carbon fibers

The properties of the selected fibers are provided in Table 9.

Table 9. Properties of synthetic and steel fibers investigated

Fiber	Length (mm (in.))	Diameter (mm (in.))	Tensile Strength (MPa (ksi))	% Elongation
Steel	13 (0.51)	0.20 (0.0079)	2,000 (290)	5–20
Nylon	13 (0.51)	0.009 (0.0004)	896 (130)	16–20
Polypropylene	6.5–13 (0.26–0.51)	0.34 (0.0134)	276 (40)	11
Polyvinyl Alcohol	12–18 (0.50–0.70)	0.20 (0.0079)	1,000–1,600 (145–232)	7
AR Glass	42 (1.65)	0.65 (0.026)	1,724 (250)	2.3
Carbon	12 (0.50)	0.0072 (0.0003)	4,137 (600)	1.0–2.1

The mixtures were prepared with a regular sand-to-cement ratio of 0.53, masonry sand-to-cement ratio of 0.47, silica fume-to-cement ratio of 0.14, and w/c ratio of 0.21. The provided ratios, which were determined from a set of preliminary investigations, were kept unchanged for all of

the tested mixtures. The amount of HRWR admixture, however, varied, depending on the type of fibers used (Table 10).

Table 10. Testing matrix with HRWR used for the mixes with different types of synthetic fiber

Mixture ID	HRWR Admixture	Steel	Nylon	PP	PVA	AR Glass	Carbon
S0.5N1.5	0.120	0.5	1.5				
S1.0N1.0	0.110	1.0	1.0				
S2.0N1.0	0.110	2.0	1.0				
S0.5P1.5	0.090	0.5		1.5			
S1.0P1.0	0.083	1.0		1.0			
S2.0P1.0	0.085	2.0		1.0			
S0.5V1.5	0.070	0.5			1.5		
S1.0V1.0	0.068	1.0			1.0		
S2.0V1.0	0.070	2.0			1.0		
S0.5G1.5	0.060	0.5				1.5	
S1.0G1.0	0.057	1.0				1.0	
S2.0G1.0	0.057	2.0				1.0	
S0.5C1.5	0.063	0.5					1.5
S1.0C1.0	0.061	1.0					1.0
S2.0C1.0	0.061	2.0					1.0

PP, PVA, and AR represent glass, carbon, and steel fibers, respectively
HRWR Admixture is presented as the HRWR-to-cement weight ratio, while the fibers are presented as the percentage of the concrete's total volume

Three mixtures were developed for each type of synthetic fiber, delivering a total of 15 UHPC mixtures made with a hybrid of steel and synthetic fibers. The proportioning of the mixtures is presented in the previous Table 10. It should be noted that the.

The developed UHPC mixtures contained various dosages of steel and synthetic fibers. The steel fiber dosages were 0.5%, 1.0%, and 2.0% of the total volume of the concrete, while the synthetic fiber dosages were 1.5%, 1.0%, and 1.0% in the corresponding mixtures, respectively. The maximum fiber content was maintained in the range of 2.0% to 3.0% because the fiber dosages beyond this range cause difficulties in attaining a good flow (Abbas et al. 2015, Alsalman et al. 2017, Teng et al. 2020, Ragalwar et al. 2020).

The UHPC mixtures were tested for flow, compressive strength, and flexural strength. The flow was measured using a flow table modified following ASTM C143 for mortar. The flow test was in accordance with the standard except for skipping the 25 drops of the table, as the developed mixtures were self-consolidating. The compressive strength was measured on 100×200 mm (4×8 in.) cylinders. The third-point loading test was performed on 100×100×400 mm (4×4×14 in.) beams, with a clear span length (L) of 300 mm (12 in.) in accordance with ASTM C1609. The

applied force was measured by using a load cell to obtain an accurate assessment of the loading demand. On the other hand, the deflection was measured by using a linear variable differential transformer (LVDT) at each beam's mid-span. Three samples were tested for each mixture and type of test. The flexural tests were paired with the DIC analyses of images obtained during the test to determine the strain distribution, initiation and propagation of cracks, and crack width profiles.

4.3. Flow and Workability

From the flow measurements, it was found that the flow of the UHPC mixtures is influenced depending on the fiber types used (Table 11).

Table 11. Results obtained for the flow and compressive strength properties

Mix ID	Flow (mm (in))	7-Day Strength (MPa (ksi))	28-Day Strength (MPa (ksi))
S0.5N1.5	165.1 (6.5)	82.2 (11.9)	83.5 (12.1)
S1.0N1.0	182.9 (7.2)	80.1 (11.6)	86.8 (12.6)
S2.0N1.0	177.8 (7.0)	80.1 (11.6)	88.8 (12.9)
S0.5P1.5	190.5 (7.5)	78.0 (11.3)	89.8 (13.0)
S1.0P1.0	203.2 (8.0)	71.3 (10.3)	87.1 (12.6)
S2.0P1.0	195.6 (7.7)	79.2 (11.5)	95.4 (13.8)
S0.5V1.5	210.8 (8.3)	62.8 (9.1)	78.1 (11.3)
S1.0V1.0	215.9 (8.5)	74.5 (10.8)	93.6 (13.6)
S2.0V1.0	209.6 (8.3)	78.7 (11.4)	108.1 (15.7)
s0.5G1.5	203.2 (8.0)	75.2 (10.9)	93.8 (13.6)
S1.0G1.0	213.4 (8.4)	102.5 (14.8)	106.6 (15.5)
S2.0G1.0	213.4 (8.4)	98.7 (14.3)	103.4 (15.0)
S0.5C1.5	191.8 (7.6)	79.8 (11.6)	83.5 (12.1)
S1.0C1.0	203.2 (8.0)	90.8 (13.2)	102.8 (14.9)
S2.0C1.0	200.7 (7.9)	107.8 (15.6)	121.6 (17.6)

The inclusion of the synthetic fibers considered all increased the amount of HRWR admixture required to achieve a flow of 200 mm (8 in.) in comparison to the mixtures made with only steel fibers. The mixtures that contained 0.5% and 1.0% synthetic fibers provided a flow very close to or greater than the target flow. The only exceptions were the mixtures made with the nylon fibers, which presented a challenge when it comes to mixing and workability, mainly because of the ability of nylon fibers to absorb water. The water absorption of nylon fibers has been reported to be as high as 3.0% (or more) by weight (Eltahir et al. 2015), resulting in a reduction of the water available for achieving an appropriate flow.

A comparison of the mixtures made with synthetic fibers indicated that the workability improves from nylon to PP, carbon, PVA, and AR glass fibers. This order can be explained by the water absorption capacity of individual fibers. While nylon fibers have the greatest water absorption capacity, the same capacity decreases to 0.3% in PP fibers and 0.1% to 1.0% in PVA fibers (Shafei et al. 2021, Tabtabaeian et al. 2017). Carbon and AR glass fibers have zero water absorption capacity. The mixtures made with a high dosage of synthetic fibers (i.e., 1.5% of nylon, PP, and carbon) provided a flow close to the target flow (with a margin of 9% to 18%).

4.4. Compressive Strength

The compressive strength was measured using the specimens cured for 7 and 28 days (previous Table 11).

Considering the 7-day compressive strength, the mixture with the highest dosage of nylon fibers (S0.5N1.5) provided the maximum compressive strength among the mixtures that contained nylon fibers. The mixtures with 1.0% nylon fibers (S1.0N1.0 and S2.0N1.0), however, had compressive strengths close to but lower than the S0.5N1.5 mixture. The 7-day compressive strengths in all three of the mixtures that contained PP fibers were lower than those obtained from the mixtures made with nylon fibers. This was explained based on the tensile strength of PP fibers, which is a third of that of nylon fibers. In particular, the compressive strength was lowest for the S1.0P1.0 mixture and highest for the S2.0P1.0 mixture. This trend was consistent with the findings provided in Smarzewski and Barnat-Hunek2017. In comparison to the UHPC mixture with no fibers, the cited study reports a reduction of 7% and 57% in the UHPC's compressive strength after the addition of 0.25% and 1.0% of PP fibers, respectively. Overall, the UHPC mixtures with PVA fibers resulted in the lowest compressive strengths at the age of 7 days. On the other hand, the mixtures with AR glass and carbon fibers provided the highest compressive strengths compared to the mixtures that contained nylon, PP, and PVA fibers.

The 28-day compressive strength consistently increased compared to the 7-day compressive strength. This increase was in the range of 2%–11%, 15%-22%, 24%–38%, 4%–24%, and 5%–13% for nylon, PP, PVA, AR glass, and carbon fibers, respectively. The lowest increase in compressive strength was observed for the S0.5N1.5 mixture. This can be explained by the water absorption characteristics of nylon fibers, which reduce the availability of free water required for the cement hydration reactions, adversely affecting strength development. The S2.0C1.0 mixture provided the highest 28-day compressive strength, followed by the S2.0V1.0, S2.0G1.0, S2.0P1.0, and S2.0N1.0 mixtures. The presented observations highlight that an optimum combination of synthetic and steel fibers is critical to achieve a satisfactory compressive strength, while benefiting from the advantages of synthetic fibers.

4.5. Flexural Strength

From the flexural tests, various response measures were obtained, processed, and compared. The most important measurement was the load-deflection relationship, which provided detailed insight into the pre- and post-cracking behavior of the UHPC mixes with various fiber types. In addition, the strength at the first crack, flexural strength at the peak load, and residual strengths

at the vertical deflections of L/600, L/150, and L/100 were determined by following the procedure provided by Kim et al. (2008, 2011). Figure 23(a) shows the load-deflection relationship in the UHPC mixtures that contain nylon, PP, and PVA fibers.

(a)

(b)
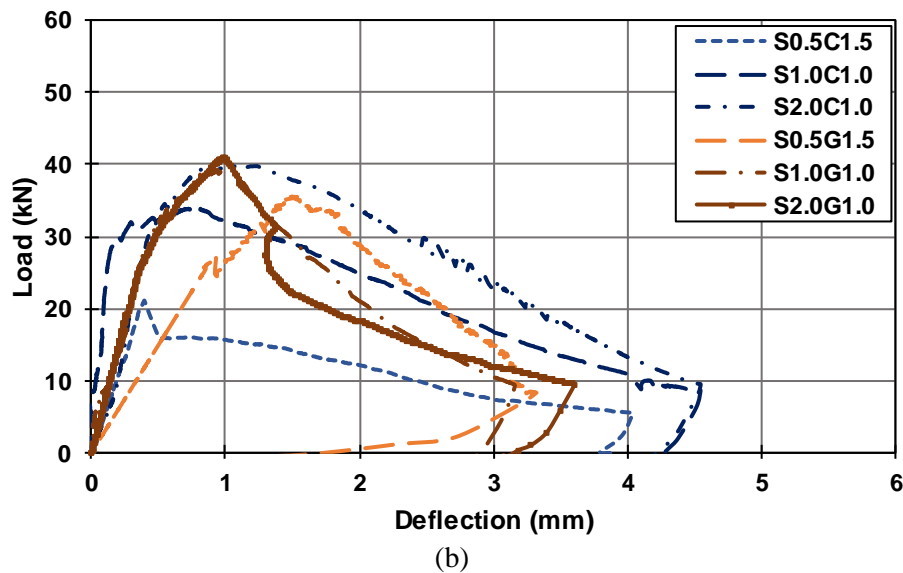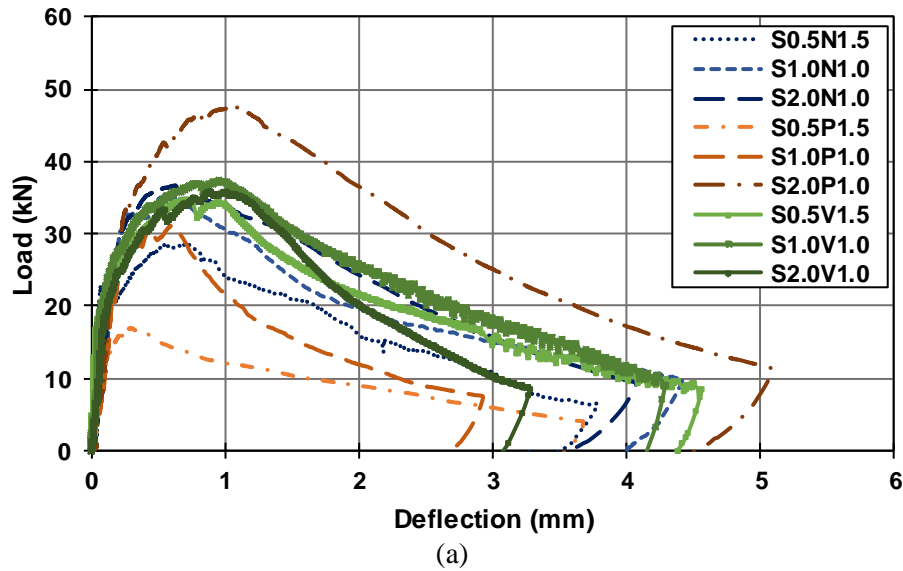
Figure 23. Load deflection curves for (a) UHPC mixtures with nylon, PP, and PVA fibers and (b) UHPC mixtures with AR glass and carbon fibers

Each load-deflection curve starts with a steep straight line, reflecting a high initial stiffness. The curve then becomes nonlinear until the first cracking point, presenting the degradation of the initial stiffness because of the formation of internal microcracks.

At the first cracking point, the load-deflection curve shows a drop in all of the tested mixtures. This drop is more noticeable in the mixtures that contain a higher dosage of synthetic fibers (i.e.,

1.5%). The mixtures are observed to have a smooth tension stiffening region after the first crack with a deflection capacity beyond L/100.

The load-deflection curves extracted from the UHPC specimens made with AR glass and carbon fibers are presented in Figure 23(b). The obtained curves show a visible drop in the load-carrying capacity at the first cracking point for both fiber types. The mixture made with a carbon fiber dosage of 1.5% does not show any strain hardening. This results in the same load magnitude for the first cracking and peak loads, owing to the brittleness of carbon fibers, which have the lowest elongation capacity, as presented in the previous Table 9.

In contrast, all of the other mixtures show a strain hardening region, which result in a peak load greater than the first cracking load. After the peak load, all of the tested mixtures are noted to provide a high deflection capacity with their deflections exceeding L/100.

Figure 24(a) presents the main flexural properties of the mixtures made with a hybrid of nylon and steel fibers.

(a)

(b)

(c)

(d)

(e)
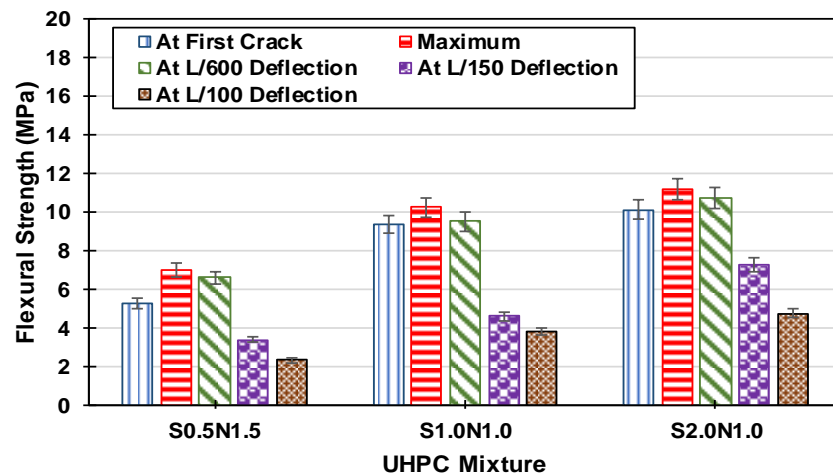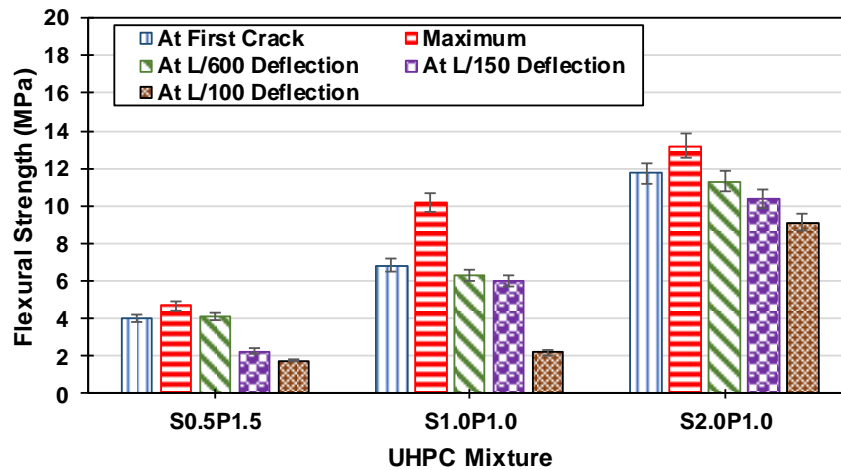
Figure 24. Comparison of first-crack strength, maximum strength, and residual strength at deflections of L/600, L/150, and L/100 in UHPC mixtures that contain (a) nylon, (b) PP, (c) PVA, (d) AR glass, and (e) carbon fibers

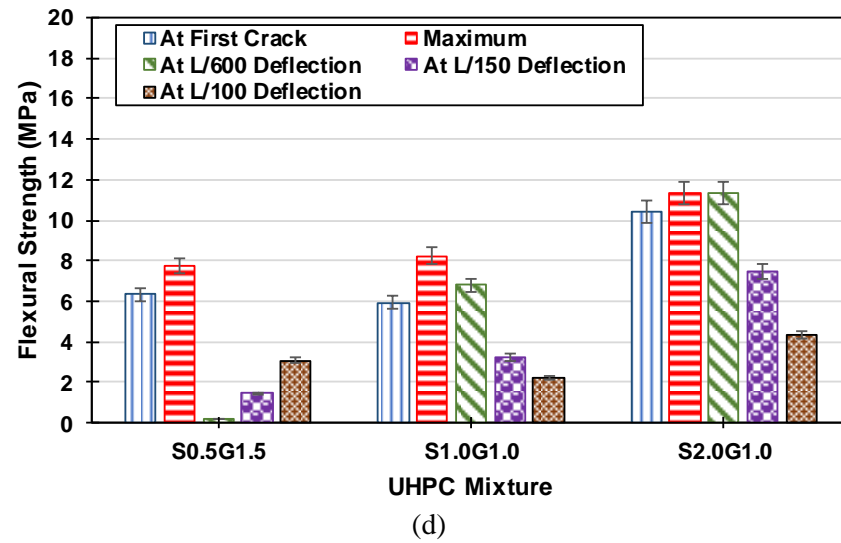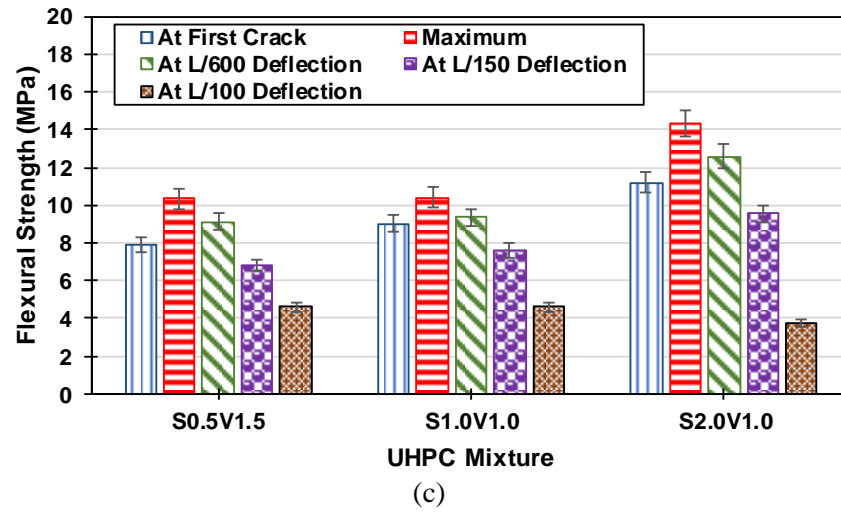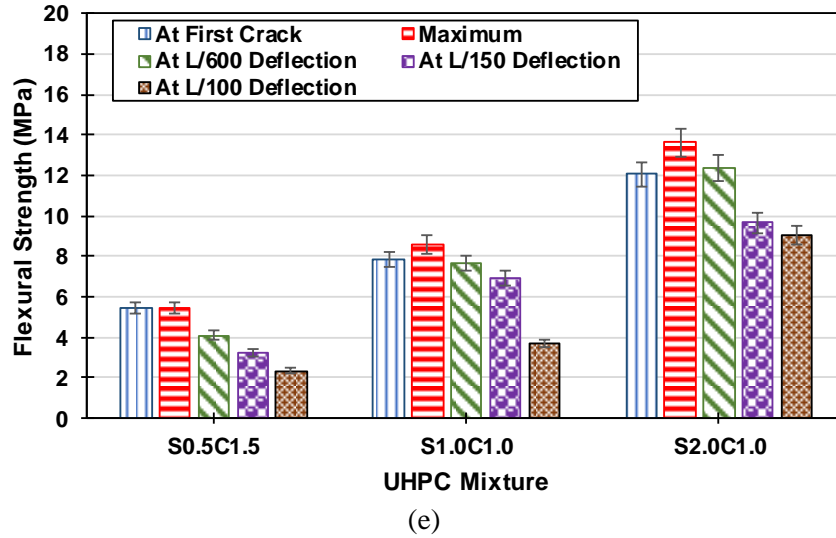The S0.5N1.5 mixture resulted in the lowest strengths, while the S2.0N1.0 mixture provided the highest strengths among the mixtures that contained nylon fibers. This was consistent with the compressive strength test results, in which the S0.5N1.5 and S2.0N1.0 mixtures provided the lowest and highest compressive strengths, respectively.

The flexural strength results for the mixtures made with a hybrid of PP and steel fibers are presented in the previous Figure 24(b). The results show that the combination of PP and steel fibers leads to improved flexural performance over the combination of nylon and steel fibers. After changing the fiber type from nylon to PP (with a similar dosage of 1.0% synthetic fibers and 2.0% steel fibers), an increase of 16% in first-crack strength, 33% in maximum flexural strength, and 5%, 43%, and 93% in residual strengths (at deflections of L/600, L/150, and L/100, respectively) is noted.

A similar increasing trend is observed when switching to the PVA fibers, as reflected in the previous Figure 24(c). This can be attributed to the high tensile strength of PVA fibers compared to nylon and PP fibers. Compared to the S0.5V.1.5 mixture, the S1.0V1.0 and S2.0V1.0 mixtures show a 13% and 16% increase in first-crack strength and 1% and 14% in maximum strength, respectively.

The UHPC mixtures made with AR glass and steel fibers show the lowest first-crack and maximum strengths for the mixtures with 1.0% steel and 1.0% synthetic fiber dosages. At the 1.5% dosage, however, the mixture with AR glass fibers provides the second greatest first-crack and maximum strength, following the UHPC mixture that contains PVA fibers. The residual strengths (at L/150 and L/100 deflections) recorded for the UHPC mixtures that contained AR glass fibers are found to be significantly lower than those obtained for the UHPC mixtures made with the other fiber types. This can be attributed to the length of AR glass fibers, which are

notably longer than the other fiber types considered. This is in line with the available literature, which indicates longer fibers result in larger microcracks (Hung et al. 2020).

Flexural strength properties were also evaluated for the mixtures prepared with carbon and steel fibers (previous Figures 24(d) and 24(e)). The UHPC mixture made with a high dosage of carbon fibers (1.5%) is found to provide flexural strength properties lower than all of the other mixtures, except for those made with PP fibers. At a 1.0% dosage of carbon and 2.0% dosage of steel fibers, the developed mixture offers the highest first-crack strength in comparison to all the mixtures, while the maximum strength remains lower than the mixtures made with PP and PVA fibers.

Reviewing the flexural response measures obtained for the mixtures with 1.5% synthetic fibers and 0.5% steel fibers, the S0.5V1.5 mixture shows the highest first-crack strength and maximum flexural strength, followed by the mixtures that contain AR glass and carbon fibers. On the other hand, the S0.5P1.5 mixture provides the lowest first-crack strength and maximum flexural strength.

The residual strengths at the deflections of L/600 and L/150 were also maximum for the S0.5V1.5 mixture and minimum for the S0.5G1.5 mixture. This observation highlights the fact that PVA fibers were the most effective fibers at the steel dosage of 0.5%.

The mixtures evaluated for 1.0% synthetic fibers and 1.0% steel fibers, however, indicate that the S1.0N1.0 and S1.0V1.0 mixtures provide the highest first-crack strength and maximum flexural strength, respectively, while the S1.0P1.0 mixture provides the lowest strength properties, consistent with the findings from the mixtures with 1.5% synthetic fibers and 0.5% steel fibers.

The maximum flexural strength is determined to be lowest for the S1.0G1.0 mixture. Similarly, the residual strengths at the deflections of L/600, L/150, and L/100 are found to be minimum for the S1.0P1.0 mixture.

Overall, the S1.0V1.0 mixture is found to provide the best flexural performance at all five of the strength points. When increasing the total fiber content from 2.0% to 3.0%, however, the rank of contribution of synthetic fibers changes, as the highest first-crack strength and maximum flexural strength are reported for the S2.0C1.0 mixture. From the review of the residual strengths at the deflections of L/600, L/150, and L/100, the S2.0C1.0 and S2.0P1.0 mixtures show the best performance overall.

4.6. Toughness

The role of fibers is known to become further evident in the post-cracking response of flexural specimens. This originates from the capability of fibers to bridge the cracks and provide strain hardening and/or tension stiffening after the maximum flexural strength is exceeded. To properly quantify the energy absorption capacity of the mixtures made with different fiber combinations, toughness was calculated for all of the developed mixtures at the deflections of L/600 and L/150

according to ASTM C1609. An additional deflection of L/100 was also considered, following the recommendation made by Kim et al. 2008, 2011. From Figure 25(a), the toughness of the UHPC mixtures with nylon and steel fibers improved as the dosage of steel fibers was increased from 0.5% to 2.0%.

(a)

(b)

(c)

(d)

61

(e)
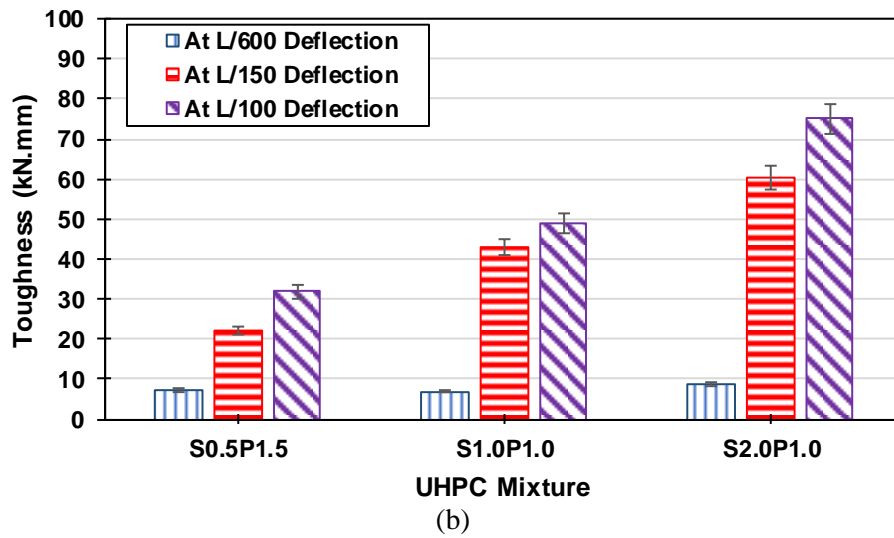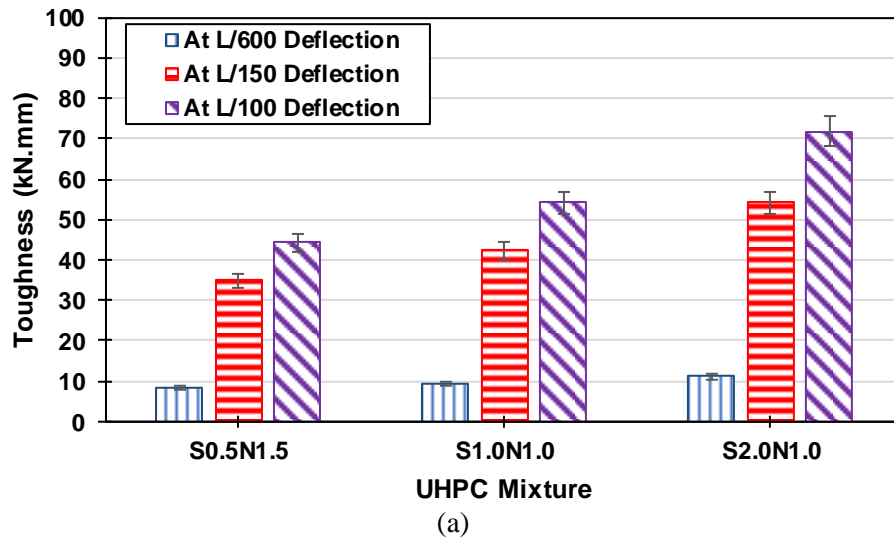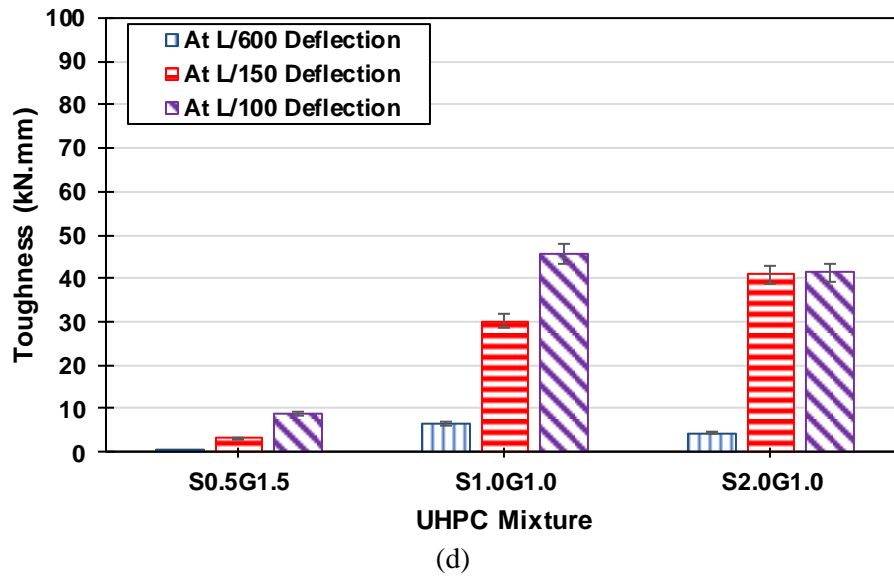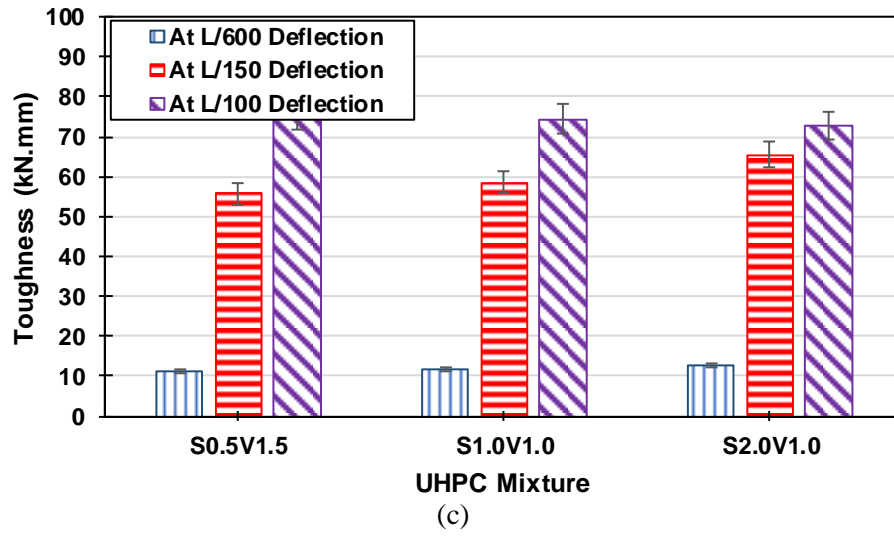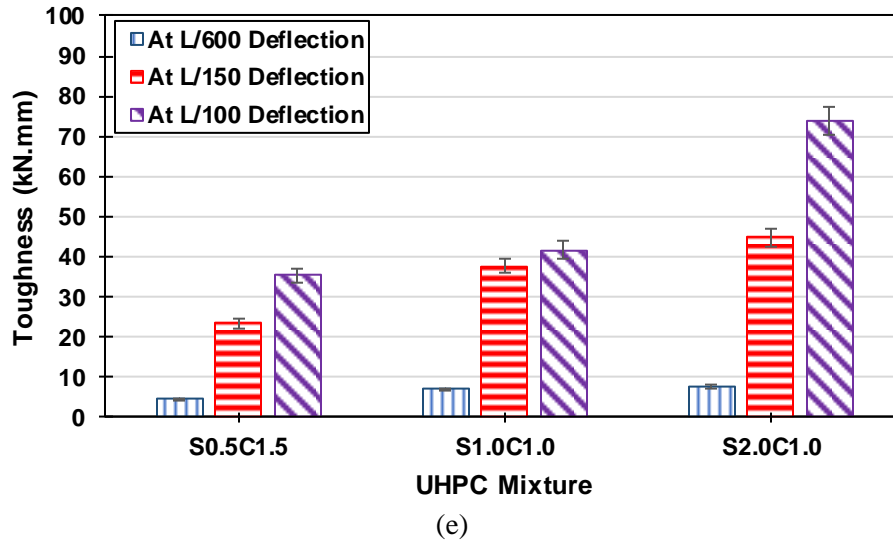
Figure 25. Comparison of toughness calculated at vertical deflections of L/600, L/150, and L/100 for UHPC mixtures with (a) nylon, (b) PP, (c) PVA, (d) AR glass, and (e) carbon fibers

This led to a total increase of 34%, 56%, and 63% in the toughness recorded at the deflections of L/600, L/150, and L/100, respectively.

The toughness for the mixtures that contained PP and steel fibers are presented in the previous Figure 25(b). When increasing the steel fiber dosage from 0.5% to 2.0%, the toughness recorded at the deflections of L/600, L/150, and L/100 were found to increase by 18%, 172%, and 136%, respectively. In general, however, the toughness recorded for this group of mixtures was lower than that for the mixtures that contained nylon and steel fibers.

The mixtures with a hybrid of PVA and steel fibers showed superior post-cracking behavior (previous Figure 25(c)). This was reflected in their toughness, which exceeded 10, 55, and 70 kN.mm under the vertical deflections of L/600, L/150, and L/100, respectively. The role of PVA fibers was further increased as the recorded toughness did not significantly change with the steel fiber dosage, in contrast to the mixtures that contained nylon and PP fibers.

On the other hand, the UHPC mixtures with AR glass and steel fibers showed the lowest toughness values at all of the dosages tested (previous Figure 25(d)). This was mainly because AR glass fibers were long in comparison to the other fiber types, and thus, the size of the microcracks became proportionally large (Hung et al. 2020)

Finally, the mixtures with a hybrid of carbon and steel fibers showed toughness values in the same range as those with PP and steel fibers. As reflected in the previous Figure 25(e), increasing the steel fiber dosage from 0.5% to 2.0% improved the toughness at the deflections of L/600, L/150, and L/100 by 70%, 92%, and 110%, respectively.

Overall, the mixtures that contained 1.5% synthetic fibers and 0.5% steel fibers showed the lowest toughness. This can be attributed to the relatively low tensile strength of synthetic fibers in comparison to steel fibers and the relatively large quantity of water reducer used in those mixtures. From a side by side comparison of all of the mixtures, the S0.5V1.5 mixture showed the highest toughness, followed by the S0.5N1.5 mixture. On the other hand, the S1.5G0.5 mixture showed the lowest toughness at all three of the deflections considered.

Among the mixtures with 1.0% synthetic and 1.0% steel fibers, the S1.0V1.0 mixture showed the highest toughness, while the S1.0G1.0 mixture had the lowest toughness. Finally, among the mixtures with a total fiber dosage of 3.0% (1.0% synthetic and 2.0% steel fibers), the S2.0P1.0 and S2.0G1.0 mixtures showed the highest and lowest toughness, respectively. At the 3.0% fiber dosage, the toughness values recorded at the L/100 deflection were within less than 5% of each other for the S2.0P1.0, S2.0V1.0, S2.0C1.0, and S2.0N1.0 mixtures. This highlights the role of steel fibers in UHPC mixture design.

4.7. Equivalent Flexural Strength Ratio

To further characterize the flexural performance of the developed UHPC mixtures, the equivalent flexural strength ratio, $R_{T,n}^{D}$, is calculated in accordance with ASTM C1609 (Nayyar et al. 2014, Rashiddadash et al. 2014, Liu et al. 2019):

$$R_{T,n}^{D} = \frac{n T_{n}^{D}}{f_{p} b h^{2}} \tag{5}$$

where n is the deflection ratio corresponding to the toughness measured (e.g., 150 at the deflection of L/150), T_{n}^{D} is the toughness measured at the deflection of L/n, f_{p} is the peak flexural strength, and b and h are the cross-sectional dimensions of the flexural specimen. The obtained ratio provides a normalized equivalent flexural strength to measure the relative strength maintained after cracking at the deflection of interest.

For example, $R_{T,150}^{D}$ is determined to be 61% for the S2.0P1.0 mixture. This reflects that an average post-peak strength of 61% is maintained at the L/150 deflection. The equivalent flexural strength ratios calculated at the L/150 and L/100 deflections are presented in Figure 26.

(a)

(b)
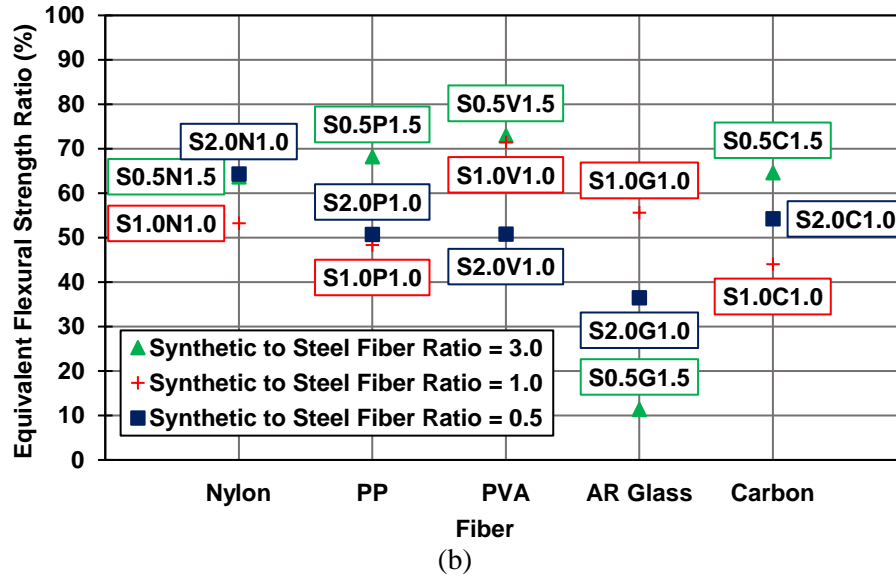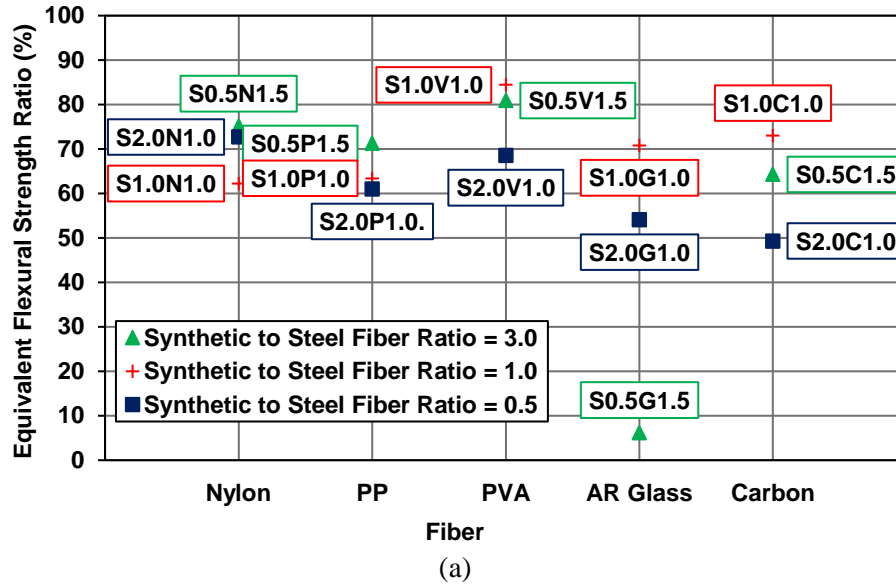
Figure 26. Equivalent flexural strength ratios at vertical deflections of (a) L/150 and (b) L/100

This figure summarizes the ratios obtained for the UHPC mixtures with 1.5% synthetic and 0.5% steel fibers (synthetic to steel fiber ratio of 3.0), 1.0% synthetic and 1.0% steel fibers (synthetic to steel fiber ratio of 1.0), and 1.0% synthetic and 2.0% steel fibers (synthetic to steel fiber ratio of 0.5).

As shown in Figure 26(a), the $R^D_{T,150}$ values of the mixtures with nylon and steel fibers were maximum for the S0.5N1.5 mixture and minimum for the S1.0N1.0 mixture. The mixtures with PP and steel fibers, however, have lower $R^D_{T,150}$ values in comparison to the mixtures that contained nylon and steel fibers. The S0.5P1.5 and S2.0P1.0 mixtures resulted in the maximum and minimum $R^D_{T,150}$, respectively. The UHPC mixtures with PVA and steel fibers delivered the

highest $R^D_{T,150}$ among all the mixtures tested. And, specifically, this was maximum in the S1.0V1.0 mixture. On the other hand, the mixtures with AR glass and steel fibers had the lowest $R^D_{T,150}$ among all of the mixtures tested. And, specifically, this was minimum in the S0.5G1.5 mixture. Following the mixtures that contained PVA and nylon fibers, the mixtures with carbon fibers showed the highest $R^D_{T,150}$ overall. This was maximum and minimum in the S1.0C1.0 and S2.0C1.0 mixtures, respectively.

Similar to $R^D_{T,150}$, the values obtained for $R^D_{T,100}$ are presented in Figure 26(b). This figure shows that, with a synthetic to steel fiber ratio of 3.0, the UHPC mixtures made with PVA, PP, and carbon fibers have the highest $R^D_{T,100}$. On the other hand, the $R^D_{T,100}$ was lowest in the mixtures that contained nylon, PP, and carbon fibers with a synthetic to steel fiber ratio of 1.0. With a synthetic to steel fiber ratio of 0.5, $R^D_{T,100}$ was minimized for the UHPC mixtures with PVA and carbon fibers.

From the previous Figures 26(a) and 26(b), it is noted that $R^D_{T,150}$ and $R^D_{T,100}$ can be the same for two different fiber types used in different dosages. This is an important point from the design perspective, as it reflects how an expected toughness (or post-cracking strength) can be achieved with an informed selection of various fiber types and dosages. Further review of the results obtained for $R^D_{T,150}$ and $R^D_{T,100}$ also shows that a high steel fiber dosage does not necessarily improve the post-cracking strength. This can be confirmed in the mixtures made with a synthetic to steel fiber ratio of 0.5 (i.e., 1.0% synthetic and 2.0% steel fibers), as presented in the previous Figures 26(a) and 26(b). The provided assessment is completely consistent with the findings of Liu et al. 2019, which reported that a fiber dosage above 2.0% does not significantly affect the flexural behavior of hybrid fiber reinforced concrete.

Furthermore, $R^D_{T,100}$ is found to be the highest for the UHPC mixtures that contain a high dosage of synthetic fibers (with a synthetic to steel fiber ratio of 3.0). This highlights that the inclusion of synthetic fibers keeps the post-cracking strength close to the maximum flexural strength, especially in mixtures with a high synthetic to steel fiber ratio.

4.8. Digital Image Correlation

DIC analyses were employed to review the series of images taken during flexural tests for the purpose of evaluating the displacements and strains experienced by the UHPC beam specimens under the vertical load. Post processing of the DIC results was also performed to estimate crack widths. To achieve this goal, a two-step specimen preparation process was adopted.

In the first step, the surfaces of the UHPC beam specimens were covered with a white paint and left to dry for three hours. In the second step, the dried white surfaces were sprayed with a black paint to make a pattern of black speckles on the surfaces. The specimens were then left to dry for another hour. Upon recording the entire loading process to capture all the stages of cracking, the obtained videos were split into a series of images. The images were processed using Ncorr, which is an open-source digital image correlation program developed in MATLAB. The program

detected the positions of individual points, along with their displacements and strains. The displacement results were then processed to determine the crack width along the depth of each UHPC beam specimen.

Focusing on the displacements and strains in the longitudinal direction of the UHPC beams, the crack formation and propagation were characterized along the length and depth of each beam specimen. Figures 27 and 28 present the longitudinal strain distribution in the S2.0P1.0 and S2.0C1.0 mixtures, respectively.
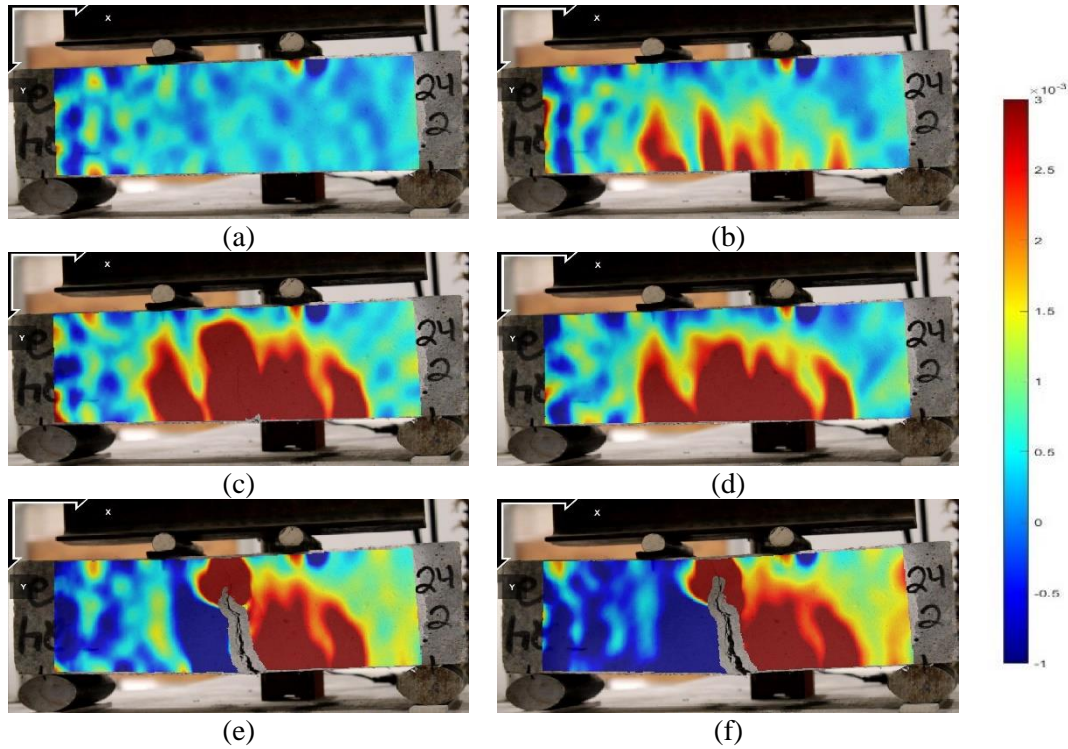
Figure 27. Longitudinal strain distribution obtained for S2.0P1.0 mixture at (a) vertical load of 20 kN, (b) first cracking load, (c) peak load, (d) deflection of L/600, (e) deflection of L/150, and (f) deflection of L/100
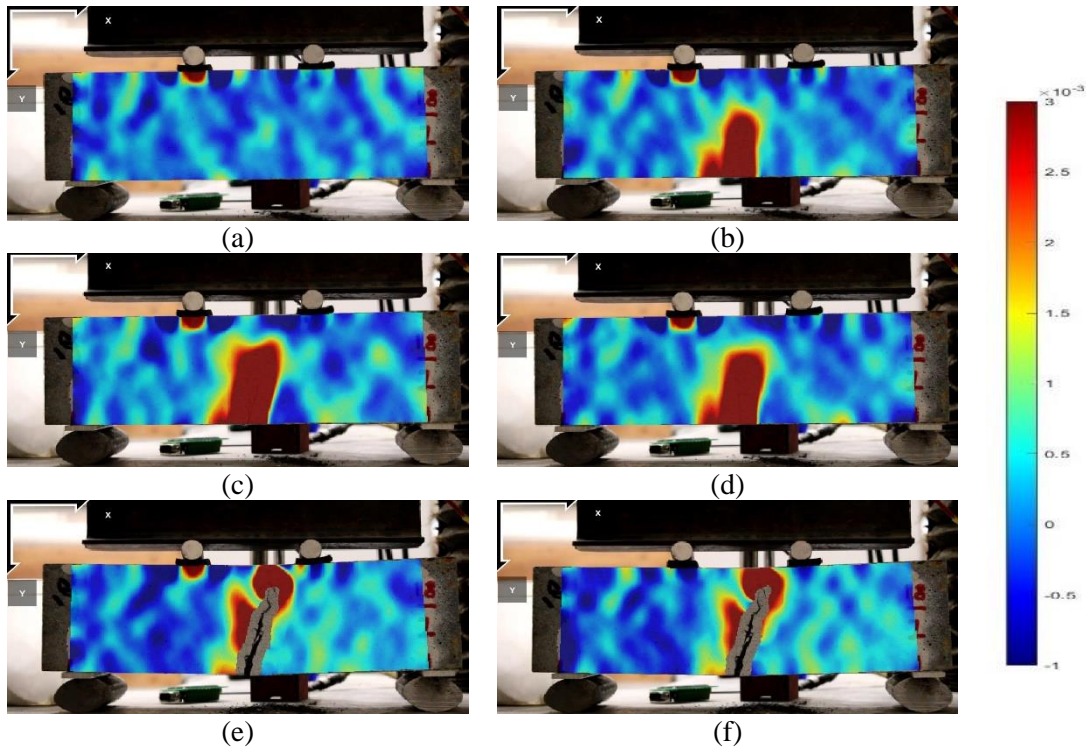
Figure 28. Longitudinal strain distribution obtained for S2.0C1.0 mixture at (a) vertical load of 20 kN, (b) first cracking load, (c) peak load, (d) deflection of L/600, (e) deflection of L/150, and (f) deflection of L/100

These two mixtures were selected because the UHPC mixtures made with PP and steel fibers experienced the narrowest crack widths, while the UHPC mixtures with carbon and steel fibers had the widest crack widths. For a side by side comparison, six different stages were considered: (a) vertical load of 20 kN, (b) first-crack load, (c) maximum strength, (d) deflection of L/600, (e) deflection of L/150, and (f) deflection of L/100.

The strains were found to be low in both mixtures under the vertical load 20 kN. At the first crack, the S2.0P1.0 mixture showed multiple high strain locations, while the high strain locations were limited to one region in the S2.0C1.0 mixture. The strains were further distributed in the UHPC mixture with PP and steel fibers, reflecting the potential for multiple cracks. This was completely in line with the fact that mixtures that contain fibers with a higher elongation capacity can benefit from a more uniform strain/stress distribution.

Figure 29 presents the longitudinal strain distribution for the mixtures with 1.0 synthetic and 2.0% steel fibers at the end of the loading process.
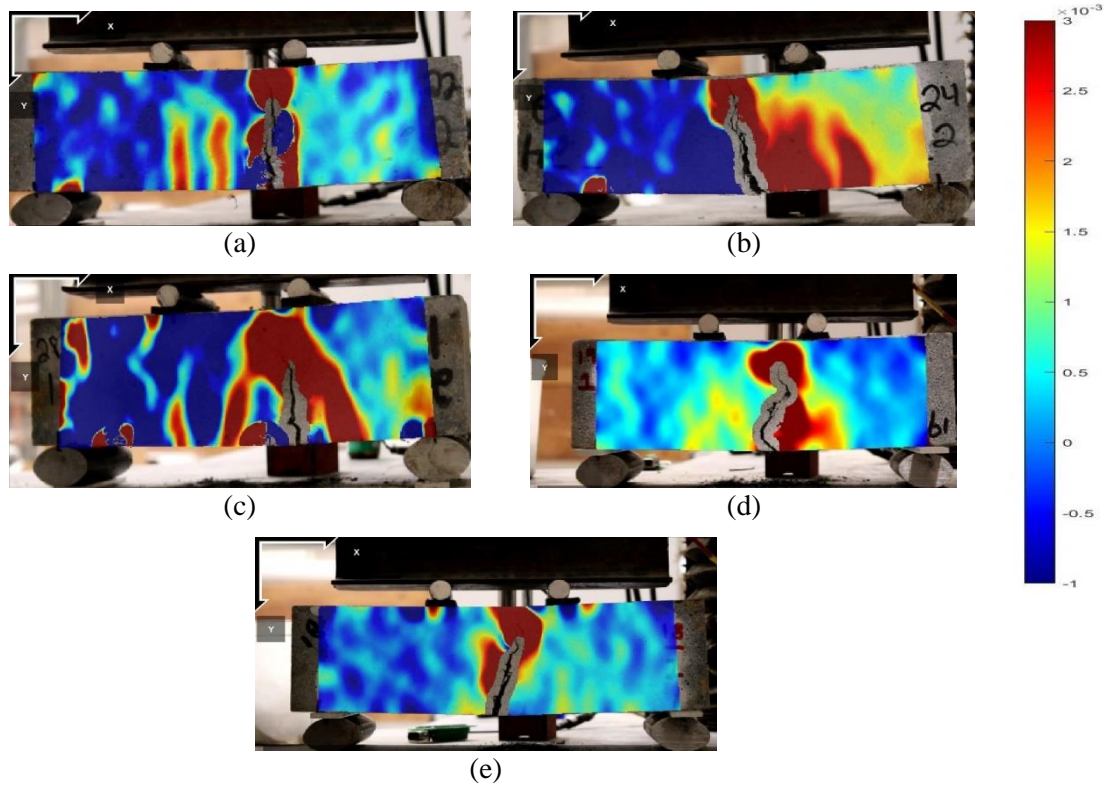
Figure 29. Longitudinal strain distribution obtained at end of loading for (a) S2.0N1.0, (b) S2.0P1.0, (c) S2.0V1.0, (d) S2.0G1.0, and (e) S2.0C1.0 mixtures

It can be seen that the S2.0N1.0, S2.0P1.0, and S2.0V1.0 mixtures exhibited the potential for multiple cracks. This is consistent with the literature, which reports that FRC with PVA fibers can experience two to three cracks under flexure (Kim et al. 2011). On the other hand, the S2.0G1.0 and S2.0C1.0 mixtures had only one major crack, while their maximum strains were also along the same crack line. This observation suggests that nylon, PP, and PVA fibers were more effective in strengthening the concrete matrix, and, thus, distributing the strains to a larger region. This can be attributed to the elongation capability of these three fibers, which is significantly greater than that of AR glass and carbon fibers, as reflected in the previous Table 9.

In particular, the response noted for the mixtures that contain PP fibers is consistent with Smarzewski and Barnat-Hunek 2017, which report that most PP fibers are stretched to failure rather than being pulled out of the cementitious matrix.

The obtained images were utilized further to determine the crack width along the depth of the UHPC specimens at the end of the loading process. The crack width for the UHPC mixtures with nylon and steel fibers showed that the S0.5N1.5 and S1.0N1.0 mixtures had the maximum and minimum crack widths, respectively, although the extension of cracks into their depths was almost the same. A common observation was that the crack widths did not consistently change along the depths, reflecting the ability of nylon fibers to control the crack (Figure 30(a)).

(a)

(b)

(c)

69
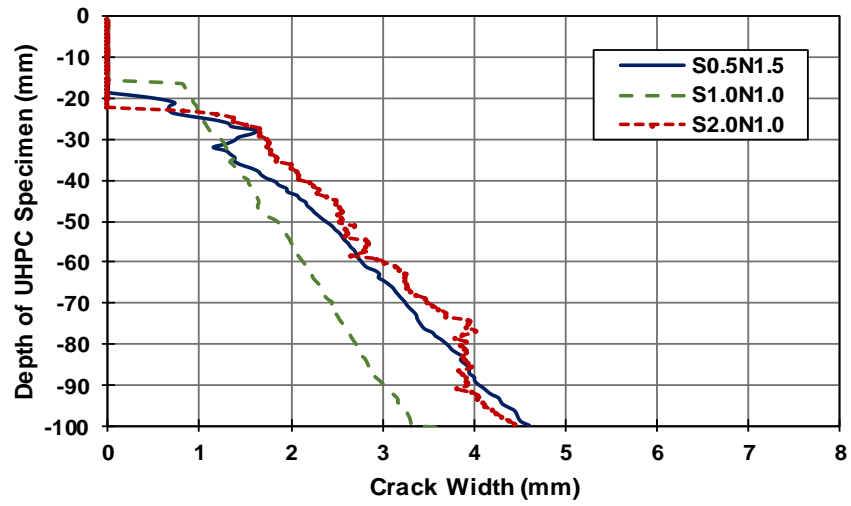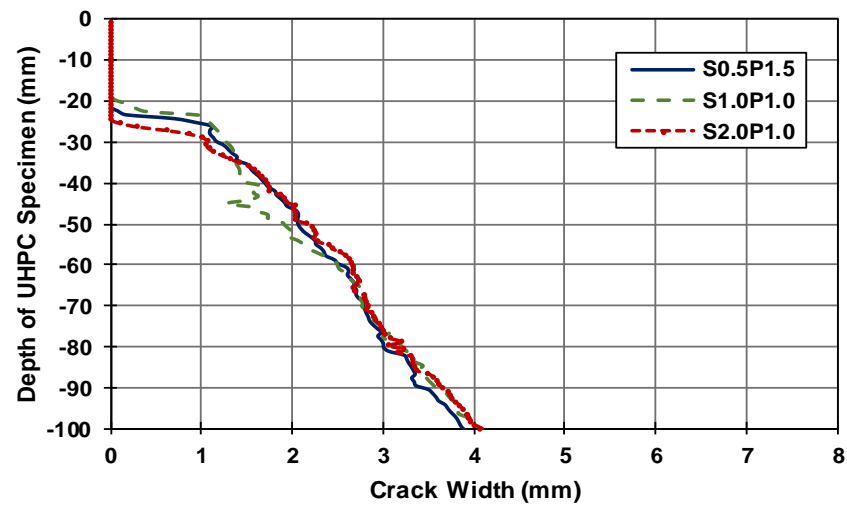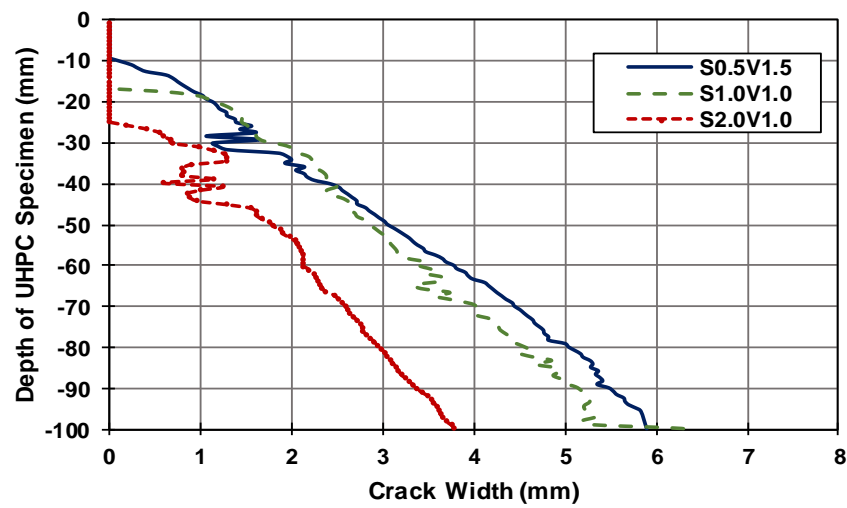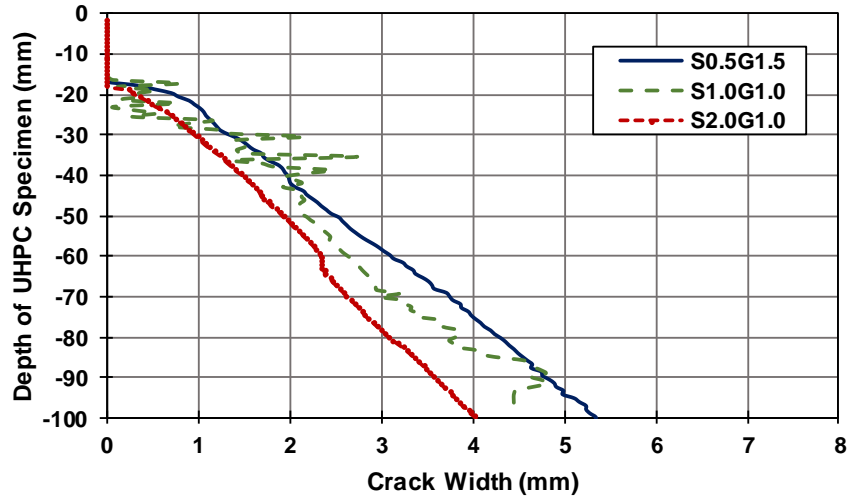
(d)
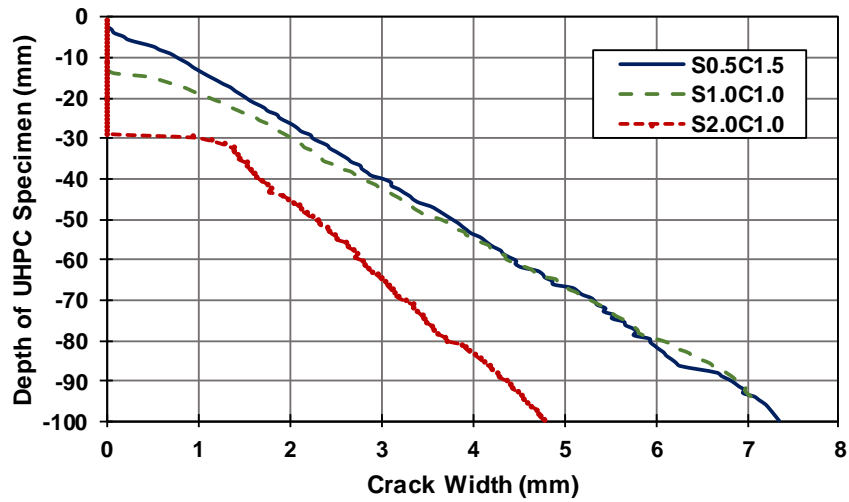
(e)

Figure 30. Crack width along the depth of UHPC specimen for mixtures that contain (a) nylon, (b) PP, (c) PVA, (d) AR glass, and (e) carbon fibers

The UHPC mixtures that contained PP and steel fibers experienced almost the same crack widths. However, the penetration of the cracks into their depths was slightly less than that for the mixtures that contained nylon and steel fibers (previous Figure 30(b)). Among the mixtures with a hybrid of PVA and steel fibers, the S2.0V1.0 mixture had the narrowest crack width along the depth, while the S0.5V1.5 mixture had the widest crack width (previous Figure 30(c)). The crack extension along the depth was also minimum for the S2.0V1.0 mixture and maximum for the S0.5V1.5 mixture. This can be explained considering that a higher number of fibers are available to bridge the cracks in the S2.0V1.0 mixture than in the S0.5V1.5 mixture.

A similar trend was observed in the mixtures that contained AR glass and steel fibers, where the S2.0G1.0 mixture showed the minimum crack width, while the S0.5G1.5 mixture had the maximum crack width over the depth (previous Figure 30(d)).

From the previous Figure 30(e), which was developed for the UHPC mixtures that contained a hybrid of carbon and steel fibers, the S2.0C1.0 mixture showed the minimum crack width, while the S0.5C1.5 mixture had the maximum crack width, exceeding 7 mm (0.28 in.). The S1.0C1.0 and S0.5C1.5 mixtures showed almost the same maximum crack widths. The crack was found to almost fully penetrate into the S0.5C1.5 mixture, while the S2.0C1.0 mixture was able to limit the crack at the depth of 30 mm (1.18 in.). This reflects the fact that, once the concrete matrix starts degrading, carbon fibers become ineffective, mainly because they are pulled out of the concrete matrix prior to rupturing.

A side by side comparison of the crack width profiles shows that, among the mixtures with 1.5% synthetic and 0.5% steel fibers, the S0.5P1.5 mixture experienced the narrowest cracks, followed by the S0.5N1.5, S0.5G1.5, and S0.5V1.5 mixtures. On the other hand, the S0.5C1.5 mixture experienced the widest crack.

In the UHPC mixtures with 1.0% synthetic and 1.0% steel fibers, the S1.0N1.0 mixture had the minimum crack width, followed by the S1.0P1.0, S1.0G1.0, and S1.0V1.0 mixtures. On the other hand, the S1.0C1.0 mixture had the maximum crack width.

Finally, for the mixtures with 1.0% synthetic and 2.0% steel fibers, the S2.0V1.0 mixture had the narrowest crack, followed by the S20.P1.0, S2.0G1.0, and S2.0N1.0 mixtures. On the other hand, the S2.0C1.0 mixture had the widest crack width.

From the data obtained for crack widths, it can be inferred that an increase in the steel fiber dosage results in control of crack propagation. In addition, the inclusion of synthetic fibers that have a relatively low tensile strength (e.g., nylon, PP, and PVA fibers) can result in small crack widths, as most of the mixed fibers continue to elongate under an increasing load and deflection instead of being prematurely pulled out of the concrete matrix.

4.9. Main Findings

The flexural response characteristics of UHPC greatly depend on the type and dosage of fibers included in the mixture. In the absence of any holistic investigations in the literature, this study evaluated the flexural performance of UHPC mixtures made with five different synthetic fibers: nylon, PP, PVA, AR glass, and carbon. The scope of this investigation covered workability, compressive strength, and flexural strength of several combinations of synthetic and steel fibers. The following conclusions were drawn from the experimental tests that were conducted and the supporting DIC analyses.

- The workability of the developed UHPC mixtures varied based on the type and dosage of synthetic fibers. The mixtures with nylon fibers demanded the highest HRWR admixture and still fell short of reaching the target flow. This was attributed to the ability of nylon fibers to absorb water. On the other hand, the mixtures that contained AR glass fibers needed the least amount of the HRWR admixture and provided the best flow. Overall, the mixtures that contained PVA and AR glass fibers were able to successfully meet the workability

71

requirements without any agglomeration of fibers.

- The compressive strength of the UHPC mixtures with a hybrid of synthetic and steel fibers varied with the dosage and type of synthetic fiber. The compressive strength was greatest for the combination with 1.0% synthetic and 2.0% steel fibers, while a drop in the total fiber content, and in particular in the steel fiber dosage, adversely affected compressive strength. Among the mixtures with 1.5% synthetic and 0.5% steel fibers and those with 1.0% synthetic and 1.0% steel fibers, the mixtures that contained AR glass and steel fibers provided maximum compressive strengths. This was mainly because of two factors: first, AR glass fibers were long (compared to the other fiber types considered), which helped with effectively bridging the cracks, and, second, the mixtures that contained AR glass fibers required a low dosage of water reducer. For the UHPC mixtures made with 1.0% synthetic and 2.0% steel fibers, the mixture that had carbon and steel fibers delivered the greatest strength, while the mixture made with nylon and steel fibers provided the lowest strength. The low compressive strength in the UHPC mixtures that contained nylon fibers was attributed to the high dosage of water reducer that needed to be added.

- Based on the load-deflection curves, flexural strength properties were evaluated at five distinct points. In the mixtures with 1.5% synthetic and 0.5% steel fibers, the PVA fibers resulted in the highest first-crack strength, maximum strength, and residual strengths at L/600, L/150, and L/100 deflections, while the PP fibers resulted in the lowest strength properties at the corresponding points. At the dosage of 1.0% synthetic and 1.0% steel fibers, nylon fibers resulted in the maximum first-crack strength, followed by PVA fibers, while AR glass fibers provided the minimum first-crack strength. The maximum strength and all the residual strengths were highest for the mixtures that contained PVA fibers, followed by nylon and PP fibers. At the dosage of 1.0% synthetic and 2.0% steel fibers, the S2.0P1.0 and S2.0V1.0 mixtures delivered the highest first-crack and maximum strengths. On the other hand, the mixtures made with PVA, PP, and carbon fibers delivered similar residual strengths at the L/150 deflection.

- Toughness was evaluated at three deflection points: L/600, L/150, and L/100. At the dosage of 1.5% synthetic and 0.5% steel fibers, the toughness was highest for the mixtures made with PVA fibers, followed by nylon and PP fibers. On the other hand, the mixtures that contained AR glass fibers had the minimum toughness. For the mixtures with the dosage of 1.0% synthetic and 1.0% steel fibers, PVA fibers consistently resulted in highest toughness, followed by nylon and PP fibers. Similarly, with the dosage of 1.0% synthetic and 2.0% steel fibers, the toughness at the L/600 deflection was highest for the mixtures made with PVA fibers, followed by nylon, and then PP fibers. However, the toughness at the L/100 deflection was found to remain in a margin of 4% for the mixtures made with PP, PVA, nylon, and carbon fibers. This was attributed to the fact that the main contribution to toughness originates from steel fibers, especially in large vertical deflections. The overall trend also suggested that the fibers with a relatively high elongation capacity and a relatively low tensile strength (PVA, nylon, and PP fibers) resulted in a higher toughness than the other fibers (carbon and AR glass fibers). This can be further explained by the fact that the fibers

with a high elongation capacity and a low tensile strength tend to continue resisting the applied load until failure instead of experiencing a pullout.

- Equivalent flexural strength ratios were calculated to provide a measure of average post-cracking strength available up to a deflection point relative to peak flexural strength. The mixtures with PVA fibers had the highest $R_{T,150}^{D}$, followed by those with nylon, PP, and carbon fibers. Similarly, for $R_{T,100}^{D}$, the mixture with PVA fibers delivered the highest ratios, followed by those with PP, carbon, and nylon fibers. Overall, the mixtures with a higher synthetic to steel fiber ratio provided larger equivalent flexural strength ratios. This highlighted the ability of synthetic fibers to maintain post-cracking strength, especially under large deflections. The DIC analyses further helped with understanding the crack formation, propagation, and distribution in the investigated UHPC mixtures. The obtained images showed that nylon, PP, and PVA fibers resulted in a better strain/stress distribution in comparison to carbon and AR glass fibers. In particular, the mixtures made with PP fibers had the narrowest crack widths, followed by those with nylon, PVA, and AR glass fibers, while the crack widths were the widest in mixtures that contained carbon fibers. This observation can be explained, noting that crack width increases when experiencing brittleness while increasing the fiber's tensile strength.

5. SUMMARY AND RECOMMENDATIONS

UHPC is known not only for its high strength but its superior durability. This report details the efforts made to improve all of these factors in a non-proprietary UHPC mix. The initial efforts focused on the development of a base mixture utilizing widely available materials. The efforts resulted in a mixture with a third the cost of the proprietary UHPC mixes with a promise to provide comparable strength and durability.

The base mix was further improved by changing the ratio of different constituents to that of the cement: the sand to cement ratio, the silica fume to cement ratio, and the w/c ratio. Further efforts were made to look at the effect of different types of constituents, as in two different types of silica fume and two different gradations of sand that were explored. A set of mixes were obtained from these efforts.

Selected mixtures were further investigated for transport properties, volume stability, and freeze-thaw resistance. These investigations were key for the use of non-proprietary UHPC in bridges, since they are usually exposed and vulnerable to changing weather conditions and other environmental factors. The results obtained were compared to the properties of two proprietary mixtures. All of the non-proprietary mixes showed great promise in all key aspects for which they were tested.

One of the main properties that makes UHPC desirable is its tensile strength and relatively ductile post-cracking behavior, which results in increased durability and tighter crack widths. The high tensile strength and ductile behavior is attained by incorporating steel fibers in the UHPC. Although the steel fiber provides invaluable properties to the UHPC mixture, it also contributes significantly to the high price of UHPC. Bearing in mind the importance of steel fibers in UHPC mixes, a set of mixtures were prepared by varying the steel fiber dosage. The effect of steel fibers on workability, flexural strength, and toughness was explored.

Furthermore, two other types of steel fibers, i.e., hooked fibers and twisted wire fibers, were investigated in combination with straight steel fibers to obtain an optimum combination for the desired flexural strength and toughness. For the straight steel fibers, the higher dosage resulted in better desired results but also resulted in reduced workability and a higher demand for super plasticizer.

Among the combination of mixtures tested, the combination S1.0H1.0, S0.5H1.5, S1.0W1.0, and S1.5W0.5 resulted in comparable first cracking strength and peak strength. The corresponding toughness values for these mixes also showed comparable results to 2% straight steel fibers. This suggests that an optimal combination of straight steel fibers and other types of fiber varies depending on the fiber type(s) available.

From the mixes explored, it was found that mixes with steel and wire fibers worked best when the straight steel content was 1% or higher, while, for hooked fibers, the combination had better

results with a straight steel dosage less than 1%. It should be noted, however, that both steel hooked fiber and wire fiber performed poorly when used without any straight steel fibers.

The efforts were further expanded to explore less expensive synthetic fibers as partial or full replacement for steel fibers in UHPC mixes. Although the synthetic fibers resulted in some difficulty in mixing and workability, the results showed improved flexural strength and ductility. Five types of synthetic fibers—nylon, PP, PVA, AR glass, and carbon—were tested, in combination with steel fibers.

The workability of AR glass fibers was the best followed by PVA fibers, then PP fibers, then carbon, and lastly nylon fibers. Nylon fibers present particularly greater challenges because of their high absorption property. The results for flexural testing and toughness showed that the PVA fibers deliver greater promise even in lower steel dosages followed by nylon fibers and PP fibers, respectively.

This report provides a set of non-proprietary mixture design recommendations that can be prepared with widely available materials. The report also provides comprehensive insight into the role of and contribution of various fiber alternatives. A trade off may need to be made depending on the type of application.

REFERENCES

Abbas S., A. M. Soliman, and M. L. Mehdi. 2015. Exploring Mechanical and Durability Properties of Ultra-High Performance Concrete Incorporating Various Steel Fiber Lengths and Dosages. *Construction and Building Materials*, Vol. 75, pp. 429–441.

Alsalman, A., C. N. Dang, and W. M. Hale. 2017. Development of Ultra-High Performance Concrete with Locally Available Materials. *Construction and Building Materials*, Vol. 133, pp. 133–145.

Abid, M., X. Hou, W. Zheng, and R. R. Hussain. 2019. Effect of Fibers on High-Temperature Mechanical Behavior and Microstructure of Reactive Powder Concrete. *Materials*, Vol. 12, No. 329, pp.1–30.

Andreasen, A. H. M. and J. Andersen. 1930. On the Relationship Between Grain Gradation and Space in Products made from Loose Grains (with Some Experiments) (Über die Beziehung zwischen Kornabstufung und Zwischenraum in Produkten aus losen Körnern [mit einigen Experimenten]). *Colloid & Polymer Science/Colloid Journal*, Vol. 50, No. 3, pp. 217–228.

Arora, A., Y. M. Yao, B. Mobasher, and N. Neithalath. 2019. Fundamental Insights into the Compressive and Flexural Response of Binder-and Aggregate-Optimized Ultrahigh Performance Concrete (UHPC). *Cement Concrete Composites*, Vol. 98, pp. 1–13.

Bao, Y., M. Valipour, W. Meng, K. Khayat, and G. Chen. 2017. Distributed Fiber Optic Sensorenhanced Detection and Prediction of Shrinkage-Induced Delamination of Ultrahigh-Performance Concrete Bonded over an Existing Concrete Substrate. *Smart Materials and Structures*, Vol. 26, No. 8, 085009.

Berry, M., R. Snidarich, and C. Wood. 2017. *Development of Non-Proprietary Ultra-High Performance Concrete.* Western Transportation Institute, Montana State University, Bozeman, MT.

Borges, P. H. R, L. F. Fonseca, V. A. Nunes; T. H. Panzera, and C. C. Martuscelli. 2014. Andreasen Particle Packing Method on the Development of Geopolymer Concrete for Civil Engineering. *Journal of Materials in Civil Engineering*, Vol. 26, No. 4, pp. 692–697.

Brouwers, H. J. H. 2006. Particle-Size Distribution and Packing Fraction of Geometric Random Packings. *Physical Review E*, 031309, pp. 1–14.

Brouwers, H. J. H and H. J. Radix. 2005. Self-Compacting Concrete: Theoretical and Experimental Study. *Cement and Concrete Research*, Vol. 35, No. 11, pp. 2116–2136.

Chan, Y. W. and S. H. Chu. 2004. Effect of Silica Fume on Steel Fiber Bond Characteristics in Reactive Powder Concrete. *Cement and Concrete Research*, Vol. 34, No. 7, pp. 1167–1172.

Chen, J. and G. Chanvillard. 2012. UHPC Composites Based on Glass Fibers with High Fluidity, Ductility, and Durability. *Proceedings of Hipermat, 3rd International Symposium on UHPC and Nanotechnology for High Performance Construction Materials*, March 7–9, Kassel, Germany.

Chen, H. J., Y. L. Yu, and C. W. Tang. 2020. Mechanical Properties of Ultra-High Performance Concrete Before and After Exposure to High Temperatures. *Materials*, Vol. 13, No. 770, pp. 1–17.

Chen, S., R. Zhang, L. J. Jia, J. Y. Wang, and P. Gu. 2018. Structural Behavior of UHPC Filled Steel Tube Columns under Axial Loading. *Thin-Walled Structures*, Vol. 130, pp. 550–563.

Christ, R., F. Pacheco, H. Ehrenbring, U. Quinino, M. Mancio, Y. Munoz, and B. Tutikan. 2019. Study of Mechanical Behavior of Ultra-High Performance Concrete (UHPC) Reinforced with Hybrid Fibers and with Reduced Cement Consumption. *Construction Engineering Magazine*, Vol. 34, No. 2, pp. 159–168.

Deb, S., N. Mitra, S. B. Majumder, and S. Maitra. 2018. Improvement in Tensile and Flexural Ductility with the Addition of Different Types of Polypropylene Fibers in Cementitious Composites. *Construction and Building Materials*, Vol. 180, pp. 405–411.

De Larrard, F. and T. Sedran. 1994. Optimization of Ultra-High-Performance Concrete by the Use of a Packing Model. *Cement and Concrete Research*, Vol. 24, No. 6, pp. 997–1009.

Dong Y. 2018. Performance Assessment and Design of Ultra-High Performance Concrete (UHPC) Structures Incorporating Life-Cycle Cost and Environmental Impacts. *Construction and Building Materials*, Vol. 167, pp. 414–425.

Dopko, M., M. Najimi, B. Shafei, X. Wang, P. Taylor, and B. M. Phares. 2018. Flexural Performance Evaluation of Fiber Reinforced Concrete Incorporating Multiple Macro-Synthetic Carbon Fibers. *Transportation Research Record: Journal of the Transportation Research Board*, Vol. 2672, No. 27, pp. 1–12.

Eltahir, Y. A., H. A. M. Saeed, Y. Xia, H. Yong, aand W. Yimin. 2015. Mechanical Properties, Moisture Absorption, and Dyeability of Polyamide 5,6 Fibers. *Journal of the Textile Institute*, Vol. 107, No. 2, pp. 208–214.

El-Tawil, S., M. Alkaysi, A. E. Naaman, W. Hansen, and Z. Liu. 2016. *Characterization and Application of a Non Proprietary Ultra High Performance Concrete for Highway Bridges.* University of Michigan, Ann Arbor, MI.

Fuller, W. B and S. E. Thomson. 1907. The Laws of Proportioning Concrete. *Transactions of the American Society of Civil Engineers*, Vol. 59, No. 2.

Funk, J. E. and D. R. Dinger. 1994. *Predictive Process Control of Crowded Particulate Suspensions Applied to Ceramic Manufacturing.* Kluwer Academic Publishers, Boston, MA.

Ghafari, E., H. Costa, and E. Júlio. 2015. Statistical Mixture Design Approach for Eco-Efficient UHPC. *Cement and Concrete Composites*, Vol. 55, pp. 17–25.

Graybeal, B. 2014. T*ech Note: Design and Construction of Field Cast UHPC Connections.* FHWA-HRT-14-084. Federal Highway Administration, Turner-Fairbank Highway Research Center, Mclean, VA.

Gu, C.P., G. Ye, and W. Sun. 2015. Ultrahigh Performance Concrete-Properties, Applications and Perspectives. *Science China Technological Sciences*, Vol. 58, No. 4, pp. 587–599.

Hager, I., K. Mroz, and T. Tracz. 2009. Contributions of Polypropylene Fibers Melting to Permeability Change in Heated Concrete-The Fiber Amount and Length Effect. *Material Science and Engineering*, Vol. 706, 012009, pp. 1–6.

Hannawi, K., H. Bian, W. Prince-Agbodjan, and B. Raghavan. 2016. Effect of Different Types of Fibers on the Microstructure and the Mechanical Behavior of Ultra-High Performance Fiber-Reinforced Concretes. *Composites Part B: Engineering*, Vol. 86, pp. 214–220.

Holubova, B., H. Hradecka, M. Netusilova, T. Gavenda, and A. Helebrant. 2017. Corrosion of Glass Fibres in Ultra-High Performance Concrete and Normal Strength Concrete. *Ceramics-SIlikaty*, Vol. 61, No. 4, pp. 319–326.

Hunger, M. 2010. An Integral Design Concept for Ecological Self-Compacting Concrete. PhD dissertation. Eindhoven University of Technology, Eindhoven, the Netherlands.

Hung, C. C., Y. T. Cheng, and C. H. Yen. 2020. Workability, Fiber Distribution, and Mechanical Properties of UHPC with Hooked End Steel Macro-Fibers. *Construction and Building Materials*, Vol. 260, 119944, pp. 1–12.

Jung, M., Y. S. Lee, S. G. Hong, and J. Moon. 2020. Carbon Nanotubes (CNTs) in Ultra-High Performance Concrete (UHPC): Dispersion, Mechanical Properties, and Electromagnetic Interference (EMI) Shielding Effectiveness (SE). *Cement and Concrete Research*, Vol. 131, 106017, pp. 1–15.

Karim, R. and B. Shafei. 2021. Performance of Fiber-Reinforced Concrete Link Slabs with Embedded Steel and GFRP Rebars. *Engineering Structures*, Vol. 229, 111590, pp. 1–12.

Kim, D. J., A. E. Naaman, and S. El-Tawil. 2008. Comparative Flexural Behavior of Four Fiber Reinforced Cementitious Composites. *Cement and Concrete Composites*, Vol. 30, No. 10, pp. 917–928.

Kim, D. J., H. S. Park, S. G. Ryu, and T. K. Koh. 2011. Comparative Flexural Behavior of Hybrid Ultra High Performance Concrete with Different Macro Fibers. *Construction and Building Materials*, Vol. 25, pp. 4144–4155.

Koh, K.T, G. S. Ryu, S. T. Kang, J. J. Park, and S. W. Kim. 2011. Shrinkage Properties of Ultra High Performance Concrete (UHPC). *Advanced Science Letters*, Vol. 4, No. 3, pp. 948–952.

Larsen, I. L. and R. T. Thorstensen. 2020. The Influence of Steel Fibers on Compressive and Tensile Strength of Ultra-High Performance Concrete: A Review. *Construction and Building Materials*, Vol. 256, 119459, pp. 1–15.

Lee, S. H., S. Kim, and D. Y. Yoo. 2018. Hybrid Effects of Steel Fiber and Carbon Nanotube on Self Sensing Capability of Ultra-High Performance Concrete. *Construction and Building Materials*, Vol. 185, pp. 530–544.

Liu, F., W. Ding, and Y. Qiao. 2019. Experimental Investigation on the Flexural Behavior of Hybrid Steel-PVA Fiber Reinforced Concrete Containing Fly Ash and Slag Powder. *Construction and Building Materials*, Vol. 228, 116707, pp. 1–13.

Ma, R., L. Guo, S. Ye, W. Sun, and J. Liu. 2019. Influence of Hybrid Fiber Reinforcement on Mechanical Properties and Autogenous Shrinkage of an Ecological UHPFRCC. *Journal of Material in Civil Engineering*, Vol. 31, No. 5, 04019032, pp. 1–8.

Mazloom, M, A. A.Ramezanianpour, and J. J.Brooks. 2004. Effect of Silica Fume on Mechanical Properties of High-Strength Concrete. *Cement and Concrete Composites*, Vol. 26, No. 4, pp. 347–357.

Mechterine, V., L. Dudziak, and S. Hempel. 2009. Internal Curing to Reduce Cracking Potential of Ultra High Performance Concrete by Means of Super Absorbent Polymers. *Proceedings of 2nd International RILEM Workshop on Concrete Durability and Service Life Planing*, pp. 31–38.

Meng, W. and M. K. Khayat. 2016. Mechanical Properties of Ultra-High-Performance Concrete Enhanced with Graphite Nanoplatelets and Carbon Nanofibers. *Composites Part B*, Vol. 107, pp. 113–122

——. 2018. Effect of Hybrid Fibers on Fresh Properties, Mechanical Properties, and Autogenous Shrinkage of Cost Effective UHPC. *Journal of Material in Civil Engineering*, Vol. 30, No. 4, 04018030, pp. 1–8.

Milan, R., B. Tomas, B. Jiri, and N. Sarka. 2016. Impact of Steel Fibers on Workability and Properties of UHPC. *Solid State Phenomenon*, Vol. 249, pp. 57–61.

Mobasher, B, A. Arora, M. Aguayo, F. Kianmofrad, Y. Yao, and N. Neithalath. 2019. *Developing Ultra High-Performance Concrete Mix Design for Arizona Bridge Element Connections.* Arizona State University, Tempe, AZ.

Najimi, M., N. Ghafoori, and M. Sharbaf. 2018. Alkali-Activated Natural Pozzolan/Slag Mortars: A Parametric Study. *Construction and Building Materials*, Vol. 164, pp. 625–643.

Nayyar, S. K., R. Gettu, and S. Krishan. 2014. Characterisation of the Toughness of Fiber Reinforced Concrete-Revisited in the Indian Context. *The Indian Concrete Journal*, pp. 8–22.

Ozsar, D. S., F. Ozalp, H. D. Yilmaz, and B. Akcay. 2017. Effects of Nylon Fiber and Concrete Strength on Shrinkage and Fracture Behavior of Fiber Reinforced Concrete. *Strain Hardening Cement-Based Composites*, pp. 188–194.

Park, S. H, D. J. Kim, G. S. Ryu, and K. T. Koh. 2012. Tensile Behavior of Ultra-High Performance Hybrid Fiber Reinforced Concrete. *Cement and Concrete Composites*, Vol. 34, No. 2, pp. 172–184.

Park, J.-J., D.-Y. Yoo, G.-J. Park, and S.-W. Kim. 2017. Feasibility of Reducing the Fiber Content in Ultra-High-Performance Fiber-Reinforced Concrete Under Flexure. *Materials*, Vol. 10, No. 118.

Ragalwar, K., W. F. Heard, B. A. Williams, D. Kumar, and R. Ranade. 2020. On Enhancing the Behavior of Ultra-High Performance Concrete through Multi-Scale Reinforcement. *Cement and Concrete Composites*, Vol. 105, 103422, pp. 1–16.

Rashiddadash, P., A. A. Ramezanianpour, and M. Mahdikhani. 2014. Experimental Investigation on Flexural Toughness of Hybrid Fiber Reinforced Concrete (HFRC) Containing Metakaolin and Pumice. *Construction and Building Materials*, Vol. 51, pp. 313–320.

Richard, P. and M. Cheyrezy. 1995. Composition of Reactive Powder Concretes. *Cement and Concrete Research*, Vol. 25, No. 7, pp. 1–11.

Russell, H. G. and B. A. Graybeal. 2013. *Ultra-High Performance Concrete: A State-of-the-Art Report for the Bridge Community*. FHWA-HRT-13-060. Federal Highway Administration, Turner-Fairbank Highway Research Center, McLean, VA.

Sahmenko, G., A. Krasnikovs, A. Lukasenoks, and M. Eiduks. 2015. *Ultra High Performance Concrete Reinforced with Short Steel and Carbon Fibers*. Proceedings of the 10th International Scientific and Practical Conference. Vol. 1, pp. 193–199.

Sbia, L. A., A. Peyvandi,, P. Soroushian, J. Lu, and A. M. Balachandra. 2014. Enhancement of Ultrahigh Performance Concrete Material Properties with Carbon Nanofiber. *Advances in Civil Engineering*, Vol. 2014, 854729, pp. 1–10.

Shafei, B., M. Kazemian, M. Dopko, and M. Najimi. 2021. State-of-the-Art Review of Capabilities and Limitations of Polymers and Glass Fibers Used for Fiber-Reinforced Concrete. *Materials*, Vol. 14, No. 409, pp. 1–44.

Shi, C., Z. Wu, J. Xiao, D. Wang, Z. Huang, and Z. Fang. 2015. A Review on Ultra High Performance Concrete: Part I. Raw Materials and Mix Design. *Construction and Building Materials*, Vol. 101, pp. 741–751.

Shihada, S. and M. Arafa. 2010. Effects of Silica Fume, Ultrafine, and Mixing Sequences on Properties of Ultra High Performance Concrete. *Asian Journal of Materials Science*, Vol. 2, No. 3, pp. 137–146.

Shehab El-Din, K. H, A. H. Mohammed, M. A. Khater, and S. Ahmed. 2016. *Effect of Steel Fibers on Behavior of Ultra High Performance Concrete*. First Internation Interactive Symposium on UHPC, Des Moines, IA.

Smarzewski, P. and D. Barnat-Hunek. 2017. Property Assessment of Hybrid Fiber-Reinforced Ultra-High Performance Concrete. *International Journal of Civil Engineering*, Vol. 16, pp. 593–606.

Soliman, N. A. and A. Tagnit-Hamou. 2017a. Using Glass Sand as an Alternative for Quartz Sand in UHPC. *Construction and Building Materials*, Vol. 145, pp. 243–252.

——. 2017b. Partial Substitution of Silica Fume with Fine Glass Powder in UHPC: Filling the Micro Gap. *Construction and Building Materials*, Vol. 139, pp. 374–383.

Tabatabaeian, M., A. Khaloo, A. Joshaghani, and E. Hajibandeh. 2017. Experimental Investigation on Effects of Hybrid Fibers on Rheological, Mechanical, and Durability Properties of High-Strength SCC. *Construction and Building Materials*, Vol. 147, pp. 497–509.

Tahwia, A. M. 2017. Performance of Ultra-High Performance Fiber Reinforced Concrete at High Temperatures. *International Journal of Engineering and Innovative Technology*, Vol. 6, No. 10, pp. 1–7.

Teng, L., W. Meng, and M. K. Khayat. 2020. Rheology Control of Ultra-High Performance Concrete Made with Different Fiber Contents. *Cement and Concrete Research*, Vol. 138, 106222, pp. 1–18.

Tomas, B., T. Petr, V. Miroslav, B. Petr, and S. Nenadalova. 2015. Experimental Tests of White UHPC Plates Reinforced by PVA Fibers and Textile Glass Reinforcement. *Advance Materials Research*, Vol. 1125, pp. 83–88.

Wille, K. and C. Boisvert-Cotulio. 2015. Material Efficiency in the Design of Ultra-High Performance Concrete. *Construction and Building Materials*, Vol. 86, pp. 33–43.

Wille K., A. E. Naaman, S. El-Tawil, and G. J. Parra-Montesinos. 2012. Ultra-High Performance Concrete and Fiber Reinforced Concrete: Achieving Strength and Ductility without Heat Curing. *Materials and Structures Construction*, Vol. 45, No. 3, pp. 309–324.

Yoo, D.-Y. and N. Banthia. 2016. Mechanical Properties of Ultra-High-Performance Fiber-Reinforced Concrete: A Review. *Cement and Concrete Composites*, Vol. 73, pp. 267–280.

Yoo, D.-Y. and Y.-S. Yoon. 2015. Structural Performance of Ultra-High-Performance Concrete Beams with Different Steel Fibers. *Engineering Structures*, Vol. 102, pp. 409–423.

Yoo, D.Y., J. J. Park, S. W. Kim, and Y. S. Yoon. 2014. Influence of Reinforcing Bar Type on Autogenous Shrinkage Stress and Bond Behavior of Ultra High Performance Concrete. *Cement and Concrete Research*, Vol. 48, pp. 150-161.

Yoo, D. Y, M. J. Kim, S.W. Kim, and J. J. Park. 2017. Development of Cost Effective Ultra High Performance Fiber-Reinforced Concrete using Single and Hybrid Steel Fibers. *Construction and Building Materials*, Vol. 150, pp. 383–394.

Yu, R., P. Spiesz, and H. J. H. Brouwers. 2014. Mix Design and Properties Assessment of Ultra-High Performance Fibre Reinforced Concrete (UHPFRC). *Cement and Concrete Research*, Vol. 56, pp. 29–39.

Zhang, M. H., C. T. Tam, and M. P. Leow. 2003. Effect of Water-to-Cementitious Materials Ratio and Silica Fume on the Autogenous Shrinkage of Concrete. *Cement and Concrete Research*, Vol. 33, No. 10, pp. 1687–1694.

Zhou, Y., B. Xi, K. Yu, L. Sui, and F. Xing. 2018. Mechanical Properties of Hybrid Ultra-High Performance Engineered Cementitious Composites Incorporating Steel and Polyethylene Fibers. *Materials*, Vol. 11, No. 8, 1448, pp. 1–21.

Zou, X. X. and J. Q. Wang. 2018. Experimental Study on Joints and Flexural Behavior of FRP Truss-UHPC Hybrid Bridge. *Composite Structures*, Vol. 203, pp. 414–424.

THE INSTITUTE FOR TRANSPORTATION IS THE FOCAL POINT FOR TRANSPORTATION AT IOWA STATE UNIVERSITY.

InTrans centers and programs perform transportation research and provide technology transfer services for government agencies and private companies;

InTrans contributes to Iowa State University and the College of Engineering's educational programs for transportation students and provides K–12 outreach; and

InTrans conducts local, regional, and national transportation services and continuing education programs.

INSTITUTE FOR TRANSPORTATION

IOWA STATE UNIVERSITY

Visit **InTrans.iastate.edu** for color pdfs of this and other research reports.